**Distribution Agreement**

In presenting this thesis or dissertation as a partial fulfillment of the requirements for an advanced degree from Emory University, I hereby grant to Emory University and its agents the non-exclusive license to archive, make accessible, and display my thesis or dissertation in whole or in part in all forms of media, now or hereafter known, including display on the world wide web. I understand that I may select some access restrictions as part of the online submission of this thesis or dissertation. I retain all ownership rights to the copyright of the thesis or dissertation. I also retain the right to use in future works (such as articles or books) all or part of this thesis or dissertation.

_____

Shawn Patrick Alter

**Impaired vesicular storage of norepinephrine and serotonin in Parkinson's disease-related pathogenesis**

By

Shawn Patrick Alter
Doctor of Philosophy

Graduate Division of Biological and Biomedical Sciences
Molecular and Systems Pharmacology

_____
Gary W. Miller, Ph.D.
Advisor

_____
Yoland Smith, Ph.D.
Committee Member

_____
Mike Iuvone, Ph.D.
Committee Member

_____
David Weinshenker, Ph.D.
Committee Member

Accepted:

_____
Lisa A. Tedesco, Ph.D.
Dean of the James T. Laney School of Graduate Studies

_____
Date

# Impaired vesicular storage of norepinephrine and serotonin in Parkinson's disease-related pathogenesis

By

Shawn Patrick Alter
B.A., Case Western Reserve University, 2009

Advisor: Gary Wright Miller, PhD

An abstract of

a dissertation submitted to the Faculty of the Laney Graduate School of Emory University
in partial fulfillment of the requirements for the degree of
Doctor or Philosophy

Molecular and Systems Pharmacology Program
Graduate Division of Biological and Biomedical Sciences
2015

## Abstract

The vesicular monoamine transporter 2 is essential for the storage and release of dopamine, norepinephrine, and serotonin. While the etiology of Parkinson's disease remains obscure, it is known that vesicular monoamine function is disrupted in Parkinson's disease, and these neurotransmitter systems degenerate or are disrupted. In addition to the profound motor symptoms of PD, patients also experience a host of nonmotor symptoms, including psychiatric and autonomic disturbances. I hypothesized that disrupting vesicular storage of norepinephrine and serotonin would lead to dysfunction and degeneration of the respective neuronal systems. Using histological, pharmacological, and behavioral analyses, I assessed the integrity of the noradrenergic and serotonergic systems of mice with drastically reduced expression of VMAT2. In addition to nigrostriatal degeneration, VMAT2 deficient mice undergo severe and progressive loss of the norepinephrine-producing cells of the locus ceruleus, as well as reductions in noradrenergic innervation of the brain. We also assessed neurochemical innervation of the hearts of VMAT2 deficient mice and observed drastic reductions in norepinephrine and reduced expression of the norepinephrine transporter, which is consistent with the pathology of orthostatic hypotension in Parkinson's disease. Despite preservation of the dorsal raphe and efferent innervation, VMAT2 deficient mice exhibited neurochemical depletion of serotonin that resulted in aberrant response to serotonergic agonists. Collectively, these data indicate that reduced vesicular monoamine function wreaks havoc on the noradrenergic and serotonergic systems, causing general monoamine depletion, degeneration of the locus ceruleus, and disruptions in serotonergic function, all of which can drive the nonmotor symptoms of Parkinson's disease.

# Impaired vesicular storage of norepinephrine and serotonin in Parkinson's disease-related pathogenesis

By

Shawn Patrick Alter
B.A., Case Western Reserve University, 2009

Advisor: Gary Wright Miller, PhD

A dissertation submitted to the Faculty of the Laney Graduate School of Emory University
in partial fulfillment of the requirements for the degree of
Doctor or Philosophy

Molecular and Systems Pharmacology Program
Graduate Division of Biological and Biomedical Sciences
2015

**Acknowledgments**

This document is the product of six years of training and research with amazing mentors, teachers, colleagues, and friends. As my mentor and advisor, Gary provided timely guidance, strategic insight, and unwavering support as I navigated the challenges and opportunities of my doctoral training. I could not have asked for a better leader. The members of the Miller and Caudle Laboratories were more than my colleagues; rather, they became my dearest of friends. I was fortunate to have an extremely supportive and dedicated committee; David, Mike, and Yoland provided great advice and propelled my training and development as a scientist. In my training as a pharmacologist, I had the privilege of studying in an excellent training program, and I thank the faculty of the Molecular and Systems Pharmacology Program for their commitment to training young scientists. As a researcher interested in therapeutics for neurological disease, I was also fortunate to receive excellent training opportunities in neurology through the Department of Neurology's Translational Training Program and through opportunities provided by the faculty of Emory's Morris K. Udall Center for Parkinson's Disease Research.

**CONTENTS**

## LIST OF FIGURES

## LIST OF TABLES

# CHAPTER 1

## Introduction and Background:

## Vesicular Integrity and Parkinson's disease

**This majority of this chapter has been published as:**

Alter, S.P., Lenzi, G.M., Bernstein, A.I., Miller, G.W., 2013. Vesicular integrity in Parkinson's disease. Current Neurology and Neuroscience Reports 13, 362.

**Abstract**

The defining motor characteristics of Parkinson's disease (PD) are mediated by the neurotransmitter dopamine (DA). Dopamine molecules spend most of their lifespan stored in intracellular vesicles awaiting release and very little time in the extracellular space or the cytosol. Without proper packaging of transmitter and trafficking of vesicles to the active zone, dopamine neurotransmission cannot occur. In the cytosol, dopamine is readily oxidized; excessive cytosolic dopamine oxidation may be pathogenic to nigral neurons in PD. Thus, factors that disrupt vesicular function may impair signaling and increase the vulnerability of dopamine neurons. This review outlines the many mechanisms by which disruption of vesicular function may contribute to the pathogenesis of PD. From direct inhibition of dopamine transport into vesicles by pharmacological or toxicological agents to alterations in vesicle trafficking by PD-related gene products, variations in the proper compartmentalization of dopamine can wreak havoc on a functional dopamine pathway. Findings from patient populations, imaging studies, transgenic models, and mechanistic studies will be presented to document the relationship between impaired vesicular function and vulnerability of the nigrostriatal dopamine system. Given the deleterious effects of impaired vesicular function, strategies aimed at enhancing vesicular function may be beneficial in the treatment of PD.

## Introduction

The disease James Parkinson first described in 1817 as the *Shaking Palsy* and which now bears his name, Parkinson's disease (PD), is the second most common neurodegenerative disorder. It is defined by its motor symptoms, tremor, rigidity, bradykinesia, but is, in fact, multifaceted and is associated with nonmotor symptoms as well, including autonomic, cognitive, and neuropsychiatric disturbances. The motor symptoms of PD are in all likelihood primarily attributed to deficits in synaptic dopamine transmission, while the nonmotor symptoms may involve other neurotransmitters. PD pathology is characterized by deposition of α-synuclein-positive Lewy bodies in susceptible neurons and neuronal degeneration. However, Lewy pathology and neurodegeneration do not follow the same pattern of progression. Lewy bodies are, early on, deposited in the dorsal motor nucleus of the brainstem and spread in an ascending manner throughout the nervous system, but neurodegeneration is limited to specific areas. The dopaminergic neurons of the substantia nigra pars compacta (SNpc), which innervate the dorsal striatum, are preferentially destroyed in the course of the disease. Notably, cell loss is also observed in the locus ceruleus, in sympathetic neurons of the peripheral nervous system (releasing norepinephrine), and the dorsal raphe (releasing serotonin) (Greenfield and Bosanquet, 1953; Halliday et al., 1990).

The key role for vesicular function in PD was first hinted at over 50 years ago. In 1952, reserpine, an alkaloid isolated from the Indian snakeroot *Rauwolfia serpentine,* was introduced to Western medicine and widely prescribed for its antihypertensive and antipsychotic properties. Despite the beneficial effects of reserpine, side effects include depression, gastric dysmotility, and extrapyramidal symptoms, "resembling a complete

Parkinson Syndrome" (Richman and Tyhurst, 1955). While the molecular target of reserpine would not be identified for decades, investigators noted that reserpine depleted dopamine in biological tissue and caused parkinsonism in rats (Brodie et al., 1955; Pletscher et al., 1955). Arvid Carlsson found that administration of the dopamine precursor, L-3,4-dihydroxyphenylalanine (levodopa), rescued the Parkinsonian phenotype in rats (Carlsson et al., 1957). Soon after, Ehringer and Hornykiewicz discovered that striatal dopamine deficiency was responsible for Parkinsonian motor deficits (Ehringer and Hornykiewicz, 1960) and in 1961, Birkmayer and Hornykiewicz intravenously administered levodopa to a PD patient for the first time with marked success (Birkmayer and Hornykiewicz, 1961). An oral form of levodopa was approved for the treatment of PD in 1970.

Storage of neurotransmitters relies on the function of synaptic vesicles; disrupting vesicular function results in decreased release and increased cytoplasmic neurotransmitter, which is toxic to neurons. The toxicity of cytoplasmic dopamine, in particular, has been studied extensively and results from oxidative stress stemming from excessive autoxidation and enzymatic deamination. Similar mechanisms of toxicity have been studied in the norepinephrine system, and to a lesser extent, the serotonin system. For the purpose of this review, we will focus on the function of synaptic dopamine vesicles and ways they are disrupted in PD. We will both review evidence that defective vesicular function may be a determinant of PD pathogenesis and examine clinical indices of vesicular function and their potential as biomarkers for disease progression.

**Synaptic Vesicle Function**

Vesicles consist of spherical lipid bilayers and a vast array of proteins that mediate their various functions. Combined biochemical and genomic approaches have led to the identification of dozens of integral vesicular proteins involved in these activities, as well as biomolecules that are transiently associated with vesicles throughout their lifecycle (Blondeau et al., 2004; Coughenour et al., 2004; Morciano et al., 2005; Burre et al., 2006; Takamori et al., 2006). The composition and size of synaptic vesicles vary with respect to their neuronal phenotype and cargo (Liu and Edwards, 1997). Synaptic vesicles transport and store a variety of neurotransmitters including acetylcholine, amino acids (including GABA and glycine which are inhibitory and glutamate which is excitatory), biogenic amines (including DA, NE, and serotonin), and neuropeptides. By concentrating neurotransmitters into discrete packages for subsequent release, synaptic vesicles are essential for neurotransmission. The vast majority of neurotransmitters within a neuron are found stored within vesicles. As such, vesicles must sequester transmitters against a concentration gradient, using specialized transporters. Within monoaminergic neurons, the type II vesicular monoamine transporter (VMAT2; *SLC18A2*) preferentially transports one cytosolic monoamine into the vesicle in exchange for release of two protons into the cytosol (Edwards, 2007). This process is dependent on an electrochemical gradient generated by the vacuolar ATPase, which transports protons into the vesicle, acidifying the vesicle lumen and providing substrate for antiport by VMAT2 (Chaudhry et al., 2008).

Formed in the Golgi apparatus, vesicles are transported to the synaptic terminal via transient interactions between cytoskeletal and vesicular proteins (Hannah et al.,

1999). At the synaptic terminal, vesicles exist in distinct pools of various stages in the vesicle cycle; movement between these pools is dynamically regulated by vesicular proteins that respond to neuronal activity (Sudhof, 2004). A subset of vesicles, comprising the readily releasable pool (RRP), dock at the active zone of the presynaptic membrane awaiting calcium influx. Calcium induces vesicles to fuse with the presynaptic membrane and release their contents by exocytic release (see Figure 1-1A). Closely associated with the RRP is the larger reserve pool, and collectively these make up the recycling pool. Most distal to the terminal is the resting pool (Segovia et al., 2010). From electrophysiological and morphological observations in cultured hippocampal neurons, investigators have estimated that there are 6-8 vesicles in the RRP, 17-20 in the reserve pool, and 180 in the much larger resting pool (Schikorski and Stevens, 1997; Murthy and Stevens, 1999; Pyle et al., 2000; Südhof, 2000). Docking of RRP vesicles is mediated by interactions between vesicular and plasmalemmal proteins of the SNARE complex (Rizo and Sudhof, 2012). Synaptotagmins are calcium-sensing proteins that initiate membrane fusion during exocytosis (Maximov and Sudhof, 2005; Pang et al., 2006). With prolonged stimulation, vesicles in the reserve pool are recruited to the RRP. Vesicles fused to the plasma membrane have several possible fates, including reuse by so-called "kiss-and-stay" (immediate reuse) and "kiss-and-run" (trafficking to the reserve pool) mechanisms (Barker et al., 1972; Ceccarelli and Hurlbut, 1980; Sudhof, 2004). Vesicle components remaining in the plasma membrane are recycled or degraded by endosomes.

Proteins, such as LRRK2 and α-synuclein, which are implicated in PD, may disrupt vesicular trafficking and function. Mutations in the *LRRK2* gene (encoding the

leucine-rich repeat kinase 2), account for the highest proportion of genetic cases of PD (Paisan-Ruiz et al., 2008). LRRK2 has a functional kinase domain with a multitude of cellular phospho-targets that may alter vesicular activities. Additionally, the circularized beta-propeller structure of the WD-40 domains in LRRK2 has been shown to interact with cytoskeletal and vesicular proteins. Mutations in LRRK2 may disrupt vesicular trafficking and endosomal recycling of vesicular proteins (see Figure 1-3E) (Belluzzi et al., 2012).

The physiological role of α-synuclein (encoded by *SNCA*) remains elusive, though its genetic and pathological role in PD is well established (Polymeropoulos et al., 1997; Kruger et al., 1998; Singleton et al., 2003). Monomeric α-synuclein has been shown to reversibly bind and adjoin vesicle membranes (Davidson et al., 1998). Based on this and its presynaptic localization, it is hypothesized that its endogenous function is to regulate vesicular trafficking between the active zone and cytoplasmic pools. Combining transgenic models of α-synuclein overexpression and deletion, Scott and Roy observed that α-synuclein regulates the size of the recycling pool in cultured hippocampal neurons because overexpression decreased the recycling pool size and deletion increased the size of the recycling pool enhancing intersynaptic vesicular trafficking (Scott and Roy, 2012). Rats overexpressing human α-synuclein have reduced dopamine vesicle density and correlative reductions in motor activity (Gaugler et al., 2012). In the context of pathogenesis, fibrilization of α-synuclein forms the primary structural component of Lewy bodies, and toxic α-synuclein protofibrils form as intermediates in the fibrilization process (Caughey and Lansbury, 2003). Oxidized dopamine covalently binds α-synuclein, stabilizing these protofibril intermediates (Conway et al., 2001); for a

biophysical review of this subject, see (Rochet et al., 2004). *In vitro*, oligomeric α-synuclein can also disrupt SNARE complex formation (Choi et al., 2013). Furthermore, α-synuclein protofibrils have been shown to permeabilize vesicle membranes, which would leak vesicular dopamine into the cytoplasm and ablate the vesicle electrochemical gradient (Volles and Lansbury, 2002). These processes may synergistically interact in PD (see Figure 1-3D) and, in part, explain the vulnerability of dopamine neurons in PD.

**Monoaminergic Brain Regions affected in Parkinson's disease**

Since the identification nigral degeneration and Lewy bodies as pathogenetic events in PD, extensive neuropathological studies have revealed the disease's extensive reach and progressive staging throughout the nervous system (Braak et al., 2003). Braak's staging of Lewy Pathology has informed our understanding of the topographical progression of Lewy body formation and those neurons that are susceptible to its deposition. While Lewy pathology spreads abundantly throughout the brain and peripheral nervous system, not all affected neurons are lost in PD. Dopamine, norepinephrine, and serotonin neurons are especially vulnerable to neurodegeneration (Greenfield and Bosanquet, 1953; Paulus and Jellinger, 1991; Zarow et al., 2003), a curiosity which has inspired interest in monoamine toxicity in Parkinson's disease.

Of the brain regions affected in PD, the SNpc is the most intensely studied. The pathologist Edouard Brissaud first hypothesized that its degeneration was the key pathological event in PD in 1893. Pathologically, this event was readily recognized in the loss of pigment (neuromelanin) occurring within the cerebral peduncles of PD brains. Ehringer and Hornykiewicz (1960) later demonstrated that the consequent loss in striatal

dopamine correlated with the profound motor effects of the disease. In the 1980s, a sensational report revealed that MPTP—an unfortunate product of misguided garage chemistry—selectively lesioned the SNpc of drug addicts and caused Parkinsonism overnight (Langston et al., 1983). This discovery launched successive decades of research into understanding the vulnerability of the SNpc in PD. The MPTP model of Parkinsonism enabled the pioneering work that led to the field's current understanding of the neurocircuitry of basal ganglia in motor control (Wichmann and DeLong, 1996), and has guided the rationale of neuroprotective therapeutic research for PD.

An enigmatic feature of PD is the preservation of the dopaminergic ventral tegmental area (VTA). Dopaminergic neurons in the VTA are resistant to both Parkinsonian and MPTP–induced neurotoxicity (LaVoie and Hastings, 1999). This contrast in neuronal vulnerability has fueled numerous hypotheses into its differential vulnerability, under the tantalizing notion that identifying a key phenotypic difference may hold the key to neuroprotection in PD. A driver of the mesolimbic reward pathway, the VTA projects to the nucleus accumbens in the ventral striatum. Other phenotypic differences include its relative expression of monoamine transporters, intraneuronal calcium dynamics, electrophysiological activity. A thorough review by Surmeier and Sulzer discusses these determinants at length and demonstrates that myriad factors contribute to the differential vulnerability of neurons lost in PD, though none can be singly implicated (Sulzer and Surmeier, 2012).

While nigral degeneration is the most extensively studied feature in the progression of PD pathology, there is also a strong appreciation for pathology in the locus ceruleus (LC), located within the pons. The LC is the main source of norepinephrine in

the central nervous system. Like the nigra, the LC also exhibits neuromelanin-derived pigment. LC loss in PD was first described by Greenfield and Bosanquet in 1953, though they noted that it was less preferentially affected in contrast to the SNpc. Pathological staging in post mortem PD cases would later reveal that Lewy deposition in the LC precedes that of the SNpc (Braak et al., 2003; Del Tredici and Braak, 2012), and that noradrenergic degeneration correlated with cognitive psychiatric deficits in PD (Halliday et al., 1990; Paulus and Jellinger, 1991). Other accounts of LC pathology have described its degeneration as more severe than that of the SNpc (Zarow et al., 2003). As in the SNpc, MPTP lesions also destroy noradrenergic neurons in the LC of animals, but to a lesser extent (Hallman et al., 1985; Forno et al., 1986). Understanding why both of these catecholaminergic nuclei—the SNpc and LC—are both susceptible to Parkinsonian neurodegeneration represents a critical challenge in understanding neuronal vulnerability in PD.

The scientists who described reserpine's effects on striatal DA also acknowledged its disruption of neuronal serotonin (or 5-hydroxytryptamine, 5-HT) (Shore et al., 1957), leading Birkemayer and Hornykiewicz to investigate and describe its deficits in PD brains (Bernheimer et al., 1961). Distinct 5-HT neuronal pathology was not well characterized until the 1990s, at which point it was observed that the raphe nuclei (obscurus and median) also degenerate in PD (Halliday, Li, et al., 1990). However, unlike the substantia nigra, pathology in the raphe nuclei is variable, and does not correlate well with disease progression. A recent pathological report revealed that PD patients exhibit loss of striatal 5-HT, but maintain normal levels of striatal SERT expression in the striatum and exhibit no loss of TPH2+ neurons in the dorsal raphe

nucleus (Cheshire, 2015). Disruptions in serotonergic signaling likely underlie neuropsychiatric symptoms of PD (Kostic et al., 1987; Fahn, 2003), with as many as 35% of PD patients are diagnosed with comorbid depression (Aarsland et al., 2012). Despite consistent neurochemical disruption, serotonergic innervation is often preserved through the later stages of Parkinson's disease (Bédard et al., 2011). Persistence of serotonin neurons in regions of catecholaminergic degeneration is hypothesized to contribute to levodopa-induced dyskinesia (which will be discussed in chapter 4) (Navailles et al., 2011; Politis et al., 2011). It is worth noting that serotonin terminals are sensitive to MPTP toxicity, though 5-HT cell bodies appear to be resilient to this challenge, as well as serotonin-selective toxicants including MDMA and 5,7-DHT (Baumgarten and Lachenmayer, 2004).

**Cytoplasmic monoamine toxicity and VMAT2**

Features common to DA, NE, and 5-HT neurons are their expression of monoamine synthesizing, metabolizing, and transport proteins (plasmalemmal monoamine transporters and VMAT2) (Figures 1-1 and 1-2). DA and NE are synthesized from their common amino acid precursor, tyrosine. From tyrosine, tyrosine hydroxylase (TH) synthesizes L-DOPA, which is in turn decarboxylated by L-amino acid decarboxylase (AADC) to form DA. VMAT2 then transports DA into synaptic vesicles; within the vesicles of noradrenergic neurons, dopamine-β-hydroxylase hydroxylates DA to form NE. 5-HT neurons utilize a similar biosynthetic pathway to DA, in which the amino acid tryptophan is converted to form 5-hydroxytryptophan by tryptophan hydroxylase 2 (TPH2). TPH2 is the neuronal isoform of the TPH family, while TPH1 is

expressed in endocrine tissues and is involved in the biosynthesis of peripheral 5-HT, as well as other indoleamines including melatonin. The transport activity of VMAT2 is essential to monoamine storage and synaptic release, while its disruption results in increased breakdown of monoamines in the cytosol. As we will discuss, excessive cytosolic breakdown of monoamines can be neurotoxic.

Despite the essential role of dopamine, it is neurotoxic if vesicular storage is disrupted. Under normal conditions, low levels of dopamine are present in the cytosol following synthesis from DOPA, plasmalemmal transport by the dopamine transporter (DAT), and vesicular leak (Eisenhofer et al., 2004b). Cytosolic dopamine is metabolized by enzymatic deamination or autoxidation, producing reactive, harmful products. Efficient transport of dopamine by VMAT2 prevents accumulation of these toxic byproducts. Prior to this dissertation, less was known about the toxicities of cytosolic NE and 5-HT, thus providing the impetus for the aims of this dissertation.

To place the concept of cytosolic DA toxicity in the context of PD pathology, one hypothesis of the differential vulnerability between SNpc and VTA neurons is that relatively increased expression of the dopamine transporter (DAT) over expression of VMAT2 (DAT:VMAT2) correlates with vulnerability to Parkinsonian and MPTP toxicity. Dopamine terminals within the nucleus accumbens express lower ratios of DAT:VMAT2 than those in the putamen (Miller et al., 1999). This ratio is predictive of the MPTP toxicity in the striata of MPTP monkeys and is more exaggerated in Parkinson's disease (Miller et al., 1999; Kanaan et al., 2008).

Enzymatic deamination of dopamine occurs at the mitochondrion by monoamine oxidase (MAO) forming the aldehyde intermediate DOPAL, as well as $H_2O_2$ (Eisenhofer

et al., 2004a). DOPAL is reactive, and it readily forms adducts to cytosolic proteins. Alternatively, it may autoxidize, generating reactive oxygen species (Burke et al., 2004). The toxicity of DOPAL has been shown to oligomerize α-synuclein *in vitro* (Rees et al., 2009) and has been shown to cause neurodegeneration in mice (Wey et al., 2012). Relative DOPAL formation is elevated in the striata of postmortem PD brains (Goldstein, Sullivan, et al., 2011). Intraneuronally, DOPAL is preferentially detoxified by aldehyde dehydrogenase to form DOPAC (Eisenhofer et al., 2004a).

MAO also oxidatively converts cytosolic NE and 5-HT to the respective aldehyde metabolites, DOPEGAL and 5-HIAL. Both of these molecules have been demonstrated to oligomerize synuclein *in vitro* (Burke et al., 2004; Jinsmaa et al., 2015), but their chemical instability precludes further mechanistic study or detection *in situ* (David Goldstein, personal communication). DOPEGAL is detoxified by aldose reductase to form dihydroxyphenyl glycol (DHPG), while 5-HIAL is detoxified by aldehyde dehydrogenase to 5-hydroxyindoleacetic acid (5-HIAA).

Aside from enzymatic deamination, cytosolic DA and NE also break down by autoxidation, which occurs readily in the alkaline environment of the cytosol,. Autoxidation is particularly deleterious because it yields a reactive dopamine quinone, as well as superoxide, hydrogen peroxide, and a hydroxyl radical. Furthermore, the dopamine quinone itself is highly reactive and forms cysteinyl adducts (Graham et al., 1978), disrupting the function of target proteins and potentially DNA (Zahid et al., 2011). Another fate of autoxidized catecholamines is the formation of neuromelanin, the dark pigment that gives the SNpc its color. Notably, neuromelanin is also present in the LC, where oxidation of dopamine and NE also occurs. Neuromelanin forms in acidic

lysosomal compartments that contain VMAT2 and are capable of monoamine transport. Within the confines of these organelles, dopamine and norepinephrine quinones polymerize, forming neuromelanin (Sulzer and Zecca, 1999). 5-HT also autoxidizes to form tryptamine dione (Crino et al., 1989), but there is insufficient evidence that this byproduct contributes to serotonergic toxicity *in vivo*.

Numerous studies have shown that unregulated cytosolic dopamine is neurotoxic (Graham et al., 1978; Benshachar et al., 1995; Hastings et al., 1996; Asanuma et al., 2003). Mice expressing DAT on non-dopaminergic forebrain neurons that lack VMAT2 are able to take up dopamine but lack the machinery to properly store or metabolize it; these mice exhibit motor deficits and profound neurodegeneration, accompanied by markers of increased dopamine oxidation (Chen et al., 2008). Additionally, transgenic mice with altered expression of VMAT2 have illustrated how crucial vesicular storage of dopamine is to the integrity of the nigrostriatal system. Vesicular function is essential and VMAT2 knockout mice die soon after birth (Wang et al., 1997). Heterozygotes develop normally, but have increased sensitivity to amphetamine-induced locomotion, susceptibility to 1-methyl-4-phenyl-1,2,3,6-tetrahydropyridine (MPTP) toxicity (Takahashi et al., 1997; Fumagalli et al., 1999). VMAT2 hypomorph mice (~5% wild-type VMAT2 expression; VMAT2LO) have emerged as a mouse model of PD (Mooslehner et al., 2001; Caudle et al., 2007; Taylor et al., 2014). These mice develop normally, but undergo progressive nigrostriatal degeneration, α-synuclein accumulation, as well as motor and nonmotor symptoms of PD. They also show markers of oxidative stress, including cysteinyl-catechol adducts. Notably, neurodegeneration occurs only when these mice express α-synuclein (Manning-Bog et al., 2007; Ulusoy et al., 2012).

VMAT2LO mice exhibit L-DOPA-correctable motor deficits, including reduced stride-length and locomotor activity, as well as nonmotor symptoms of PD, including anosmia, gastric dysmotility, and depressive and anxiety-like behaviors (Caudle et al., 2007; Taylor et al., 2009). In contrast, PACAP38, a neuropeptide shown to increase VMAT2 expression, attenuates methamphetamine-induced neurotoxicity in mice, reduces markers of oxidative stress and neuroinflammation, and suggests that increased VMAT2 protects against oxidative stress (Guillot et al., 2008).

In addition to VMAT2's protective role against cytoplasmic dopamine toxicity, it also plays an important role in neuroprotection against exogenous toxicants that may damage dopamine neurons, including MPTP (Chaudhry et al., 2008; Guillot and Miller, 2009). After crossing the blood-brain barrier, MPTP is metabolized by glial monoamine oxidase to form the toxic metabolite, MPP+, which is then transported into neurons by the plasmalemmal monoamine transporters (Langston et al., 1983). MPP+ causes neurotoxicity by inhibiting mitochondrial respiration and triggering cell death. MPP+ is also a substrate for VMAT2 and can be sequestered away from sites of action. VMAT2 was initially cloned for its ability to confer resistance to MPP+ toxicity and is evolutionarily related to bacterial toxin extruding antiporters (TEXANS) (Liu et al., 1992; Eiden and Weihe, 2011). MPP+ autoradiography studies have revealed that MPP+ is sequestered in the monoaminergic nuclei throughout the brain, including the SN, VTA, LC, and DR (Speciale et al., 1998). It is conceivable that VMAT2 expression may modulate the effects of other exogenous toxicants involved in PD pathogenesis (Takahashi et al., 1997; Miller, 1999).

**Pharmacologic blockade of VMAT2**

Carlsson and colleagues' observation that reserpine induced a parkinsonian phenotype that was correctable with levodopa was a launching point for pharmacotherapy in PD. Subsequent experimentation revealed that the effects of reserpine were akin to sympathectomy, in that reserpinized subjects were still responsive to the inotropic and pressor effects of direct-acting sympathomimetics or adrenergic receptor agonists (directly acting sympathomimetics, e.g., norepinephrine, epinephrine, neosynephrine), but abolished the effects of indirectly acting sympathomimetics including the phenethylamines, amphetamine, ephedrine, and tyramine (Bertler et al., 1957; Burn and Rand, 1958). It was later realized that reserpine and the aforementioned indirectly acting sympathomimetics all function by inhibiting VMAT2 (Figure 1-3B).

Amphetamine (AMPH) and the substituted AMPH derivative methamphetamine (METH) are catecholamine releasers in the peripheral and central nervous systems. The rewarding effect of striatal dopamine release is largely responsible for the abuse potential of this class of drugs. When abused, AMPH and METH are capable of exerting profound dopaminergic toxicity (Yamamoto et al., 2010). AMPH and METH share the same mechanism of action and similar pharmacokinetic and pharmacodynamic properties (Melega et al., 1995; Sulzer, 2011a). AMPH and METH mediate dopamine release by competing for vesicular uptake of dopamine by VMAT2. Additionally, they are weak bases and may disrupt the electrochemical gradient of the vesicle by accepting free lumenal protons (Chaudhry et al., 2008). The increased level of cytosolic dopamine facilitates non-exocytic dopamine release into the synaptic terminal by efflux via the dopamine transporter (Sulzer, 2011b).

Administration of METH in animals causes striatal denervation, including loss of dopamine transporter expression, gliosis, and autophagic vacuolization (Wagner et al., 1980; Larsen et al., 2002; Yamamoto et al., 2010). In rats, this pathology is associated with cysteinyl dopamine adducts, suggesting that dopamine oxidation is indeed involved in METH toxicity (LaVoie and Hastings, 1999). This toxicity is relevant in humans; striatal dopamine transporter loss in METH-treated baboons is comparable to losses in human METH users who reported using similar doses of METH (Villemagne et al., 1998). METH-induced striatal DAT loss in humans is not as severe as losses observed in PD, but it has been shown to persist in patients three years after quitting, suggesting long-term damage that may sensitize one to PD (McCann et al., 1998). Recently, a retrospective statewide study in California found that patients admitted to the hospital for an AMPH or METH related incident were significantly more likely to develop PD than matched patient controls admitted for appendicitis (hazard ratio=1.75) (Callaghan et al., 2012). In contrast, the same study showed that patients admitted to the hospital for cocaine-related incidents did not have an increased likelihood of developing PD. Because cocaine inhibits DAT and also increases dopamine levels in the synaptic cleft, these findings support the notion that PD risk may stem from cytosolic dopamine toxicity. In support of this notion, VMAT2 expression inversely correlates with METH-induced toxicity in dopamine neurons (Guillot et al., 2008).

**Toxicological blockade of VMAT2**

Epidemiological evidence supporting an environmental connection to PD is compelling (Tanner, 1990; Semchuk et al., 1991, 1992; Priyadarshi et al., 2000, 2001;

Ritz and Costello, 2006; Steenland et al., 2006). Several classes of compounds have been associated with PD pathology, especially halogenated persistent organic pollutants (POPs) (Hatcher et al., 2008; Caudle et al., 2012). Halogenated POPs represent a broad class of environmental toxicants that include organochlorine insecticides, polychlorinated biphenyls (PCBs), and brominated flame retardants. Higher levels of many organochlorines and PCBs have been reported in postmortem brain tissue and serum of PD patients (Fleming et al., 1994; Corrigan et al., 1998, 2000; Weisskopf et al., 2010; Hatcher-Martin et al., 2012) and epidemiological studies have linked the compounds to PD (Elbaz et al., 2009). Mechanistic studies into these compounds suggest that many exert selective toxicity to dopaminergic neurons, inhibit synaptosomal and vesicular uptake, and cause oxidative stress (Miller et al., 1999; Bemis and Seegal, 2004; Fonnum et al., 2006)]. Taken together, these data suggest that many compounds epidemiologically linked to PD act by impairing vesicular function and increasing oxidative stress.

**Genetic variability of SLC18A2 in PD**

Given the role of VMAT2 in regulating cytosolic dopamine toxicity, mutations affecting the function or expression of the transporter (see Figure 1-3C) might be expected to affect susceptibility to PD. Genetic mutations in the coding region of *SLC18A2* are extremely rare, reflecting the essential nature of VMAT2 function. A recent report identified a crippling movement disorder in members of a consanguineous Saudi Arabian family carrying a recessive mutation in the coding region *SLC18A2* resulting in a P387L substitution in the fifth luminal loop of VMAT2 (Rilstone et al., 2013). Affected individuals developed infantile-onset parkinsonism, severe cognitive

impairment, mood disturbance, and autonomic dysfunction. Heterozygote parents were unaffected by the disorder, but were clinically depressed, consistent with a reduction in brain monoamines. The homozygous patients exhibited reductions in CSF and urinary monoamines, but increased monoamine metabolites. The investigators found that P387L mutation virtually abolished VMAT2 function in transfected cells. Treatment with the dopamine receptor agonist pramiprexole dramatically improved symptoms in all patients, though efficacy appeared to correlate inversely with age. Other coding mutations have been identified in humans, though they are very rare and have not been associated with neurological outcomes (Glatt et al., 2001; Burman et al., 2004).

While *SLC18A2* has very little variability in the coding regions, the gene has a large and highly polymorphic promoter sequence (17.4kb) (Lin et al., 2010). This high variability results in many low frequency haplotypes and renders genetic risk assessment difficult. Thus, studies of *SLC18A2* haplotype and PD risk have been inconclusive (Lill et al., 2012). However, analyses of the functional consequences of promoter polymorphisms have provided useful information. Glatt and colleagues screened the most prevalent promoter haplotypes in an American population and identified those that increased transcriptional activity of *SLC18A2 in vitro* (Glatt et al., 2006). Collectively, gain-of-function haplotypes were found to be protective against risk of PD in women; the effect was particularly robust in women homozygous for gain-of-function haplotypes (odds ratio=0.37). In a more recent study in Italy, investigators identified two SNPs within the promoter that conferred protection against PD, presumably by increasing VMAT2 expression (Brighina et al., 2013). The variability of the *SLC18A2* promoter

suggests that epigenetic influences may contribute to variable VMAT2 expression within populations.

**VMAT2 imaging in PD**

Positron emission tomography (PET) ligands of striatal dopamine terminal markers have been used to monitor the progression of PD and response to therapeutic treatments. VMAT2 has emerged as a reliable marker of striatal innervation in PD (Frey et al., 1996; Miller et al., 1999; Bohnen et al., 2006). Previously, high-affinity radioligands for DAT and the fluorinated DOPA analog, $^{18}$F-DOPA, were utilized for PET scans, but their binding substrates were found to modulated by levodopa and dopamine agonists. Changes in DAT binding by β-CIT in response to pramipexole (increased binding) and levadopa (reduced binding) had been mistakenly ascribed to changes in striatal innervation, when in fact DAT membrane expression is modified by these therapies (Hauser et al., 2000; Albin et al., 2002). $^{18}$F-DOPA PET signal, meanwhile, does not reliably correlate with striatal innervation because expression of AADC, for which $^{18}$F-DOPA is a substrate, increases in response to neuronal damage (Kish et al., 1995; Damier et al., 1999; Tedroff et al., 1999). In contrast to DAT, VMAT2 expression is not modified by the PD therapeutics LEVODOPA or selegiline (Kilbourn et al., 1996). Bohnen and colleagues demonstrated that striatal C11-dihydrotetrabenazine binding correlated reliably to clinically rated (UPDRS) motor deficits in PD patients (Bohnen et al., 2006). Another VMAT2 radioligand, F-18-AV-133 (a tetrabenazine derivative), is also being used to study nigrostriatal degeneration (Okamura et al., 2010; Chao et al., 2012). While VMAT2 radioligand binding

conveniently correlates to nigrostriatal denervation, it does not provide direct evidence of vesicular function or VMAT2 activity.

**VMAT2 as a peripheral biomarker of PD**

Studies examining VMAT2 in the human periphery may provide insight into how to measure central VMAT2 activity in PD. VMAT2 mediates the storage and release of norepinephrine in postganglionic neurons of the sympathetic nervous system. Sympathetic denervation commonly occurs in PD; orthostatic hypotension is a comorbid feature, affecting 30% of PD patients (Velseboer et al., 2011; Jain and Goldstein, 2012). *In vivo* imaging of sympathetic denervation in PD patients is accomplished with radiolabeled ligands for both the norepinephrine transporter (expressed at the plasma membrane of sympathetic neurons) and VMAT2 (Orimo et al., 1999, 2012; Li et al., 2002; Tijero et al., 2010). Sympathetic denervation may occur prior to the onset of motor symptoms of PD, with noradrenergic denervation of the heart paralleling the dopaminergic denervation of the striatum (Orimo et al., 2007; Goldstein et al., 2012).

Goldstein and colleagues generated an *in vivo* index of vesicular activity by pairing analysis of myocardial $^{18}$F-DA uptake and arterial $^{18}$F-DOPAC formation in patients (Goldstein et al., 2011). $^{18}$F-DA uptake is dependent on the presence of intact noradrenergic terminals, and MAO metabolism of $^{18}$F-DA to $^{18}$F-DOPAC is in competition with vesicular uptake (Eisenhofer et al., 1989). Thus, one can determine both the extent of cardiac noradrenergic innervation (by PET imaging) and the relative uptake activity in vesicles (by measuring relative 18F-DOPAC formation) with these combined methods. Goldstein and colleagues performed this analysis in patient cohorts including

those with PD with orthostatic hypotension, pure autonomic failure (a Lewy body disease featuring orthostatic hypotension without parkinsonism), multiple systems atrophy (a non-Lewy body synucleinopathy that clinically resembles PD), and healthy controls. The authors concluded that myocardial vesicular function was impaired only in patients with Lewy body diseases (PD with orthostatic hypotension and in pure autonomic failure), consistent with the effects of pathogenic α-synuclein in disrupting vesicular function (Lotharius and Brundin, 2002; Rochet et al., 2004).

VMAT2 is also present in platelets and may serve as a peripheral biomarker of monoaminergic vesicular function. Platelets express proteins involved in the storage and metabolism of serotonin, including the serotonin transporter (SERT), VMAT2, and monoamine oxidase. These blood cells have been used as models of serotonin neurons (Pletscher, 1988). Profiles of imipramine binding to platelet SERT have been used as peripheral biomarkers of SERT-binding in the brain (Paul et al., 1981; Yubero-Lahoz et al., 2013). Similarly, platelet VMAT2 levels may serve as a peripheral biomarker of central VMAT2 expression. Alterations in VMAT2 dihydrotetrabenazine binding in platelets have been linked to cases of depression, juvenile behavior disorders, and schizophrenia (Zucker et al., 2001; Toren et al., 2005; Zalsman et al., 2011). Platelet *SLC18A2* mRNA levels may also be predictive of PD. In 39 PD patients versus 39 healthy control subjects, the relative quantity of *SLC18A2* mRNA in platelets was decreased by 23% in the PD patients (Sala et al., 2010). Therefore, assessing platelet expression of VMAT2 may provide a future biomarker of PD risk.

**Summary**

We have summarized ways in which alterations in vesicular storage of dopamine influences neuronal viability and susceptibility to neurodegeneration in PD. All disruptions of vesicular storage discussed have the overall effect of increasing cytosolic dopamine. In sporadic PD, it is likely that a combination of genetic and epigenetic factors decrease levels of functional VMAT2 and in addition environmental exposure to compounds that alter vesicular function converge with these to affect vesicular integrity and levels of cytosolic dopamine. Therefore, measuring uptake in human patients may provide a more reliable measure of PD risk. Furthermore, interventions aimed at increasing vesicular function may be beneficial in the treatment of PD and may even be neuroprotective. These warrant a closer look in controlled trials.

To this point in time, there has been appreciation of vesicular function in nigrostriatal degeneration in PD, and appreciation of the other monoaminergic nuclei affected in PD. However, there has been no compelling connection between disrupted vesicular function and Parkinsonian pathology of the noradrenergic and serotonergic neurotransmitter systems. This dissertation will explore the effects of reduced vesicular function on the viability and function of these neurotransmitter systems.

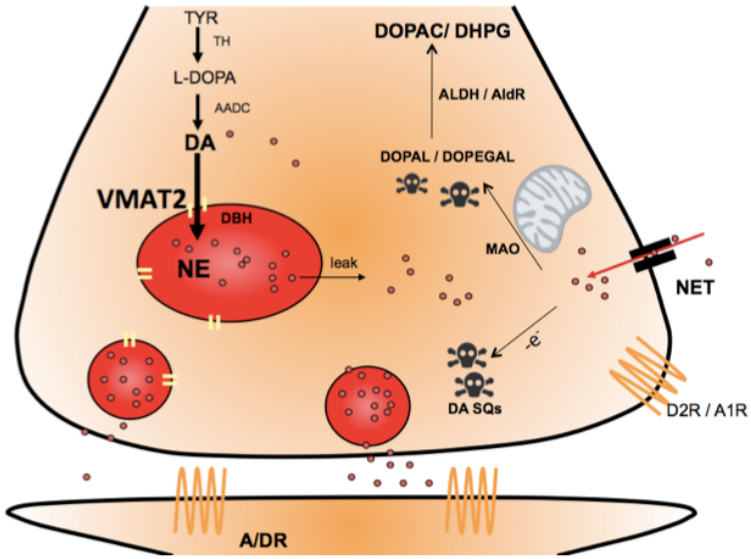


Dopamine and Norepinephrine

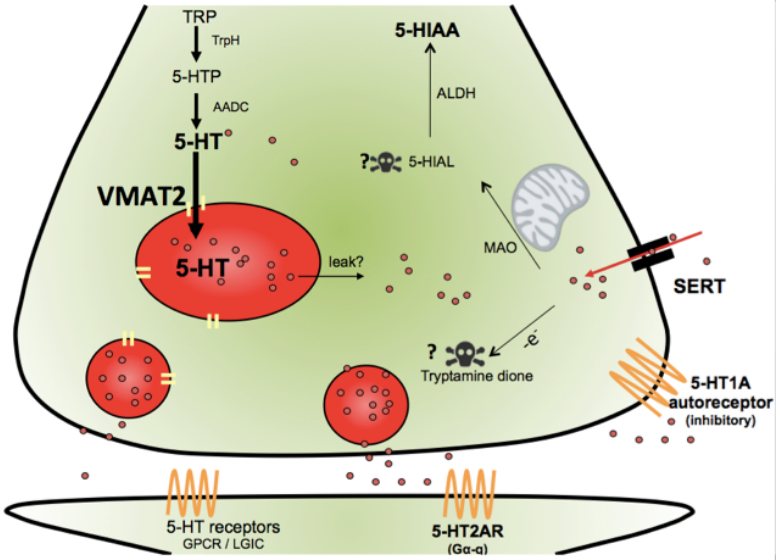


Serotonin

**Figure 1-1. Biosynthesis, transport, and catabolism of monoamines.**

Dopamine, norepinephrine, and serotonin neurons utilize amino acids to produce their cognate neurotransmitters. **Left.** In dopamine neurons tyrosine hydroxylase (TH) converts l-tyrosine (TYR) to levadopa (L-DOPA). L-amino acid decarboxylase converts L-DOPA to dopamine (DA), which is then sequestered into synaptic vesicles by VMAT2. In noradrenergic neurons, dopamine-β-hydroxylase converts DA to norepinephrine (NE). Following synaptic release or vesicular leak, catecholamines autoxidize to form semiquinone (SQ) intermediates, or are enzymatically deaminated by monoamine oxidase (MAO) to form reactive aldehyde intermediates: DA is deaminated to DOPAL, NE is deaminated to DOPEGAL. DOPAL and DOPEGAL are detoxified by aldehyde dehydrogenase and aldose reductase, respectively to form didydroxyphenylacetic acid (DOPAC) and dihydroxyphenylglycol (DHPG). **Right.** Serotonin metabolism occurs similarly, with several key distinctions. The amino acid tryptophan (TRP) is hydroxylated by tryptophan hydroxylase (TPH2, high homology to TH) to form 5-hydroxytrypotphan (5-HTP). Like L-DOPA, 5-HTP is decarboxylated by AADC, yielding the serotonin (5-hydroxytryptamine, 5-HT). 5-HT transport, release, and breakdown occur by the same mechanisms as DA and NE. MAO metabolizes 5-HT to 5-5-hydroxyindolealdehyde (5-HIAL), which ALDH converts to hydroxyindoleacetic acid (5-HIAA).

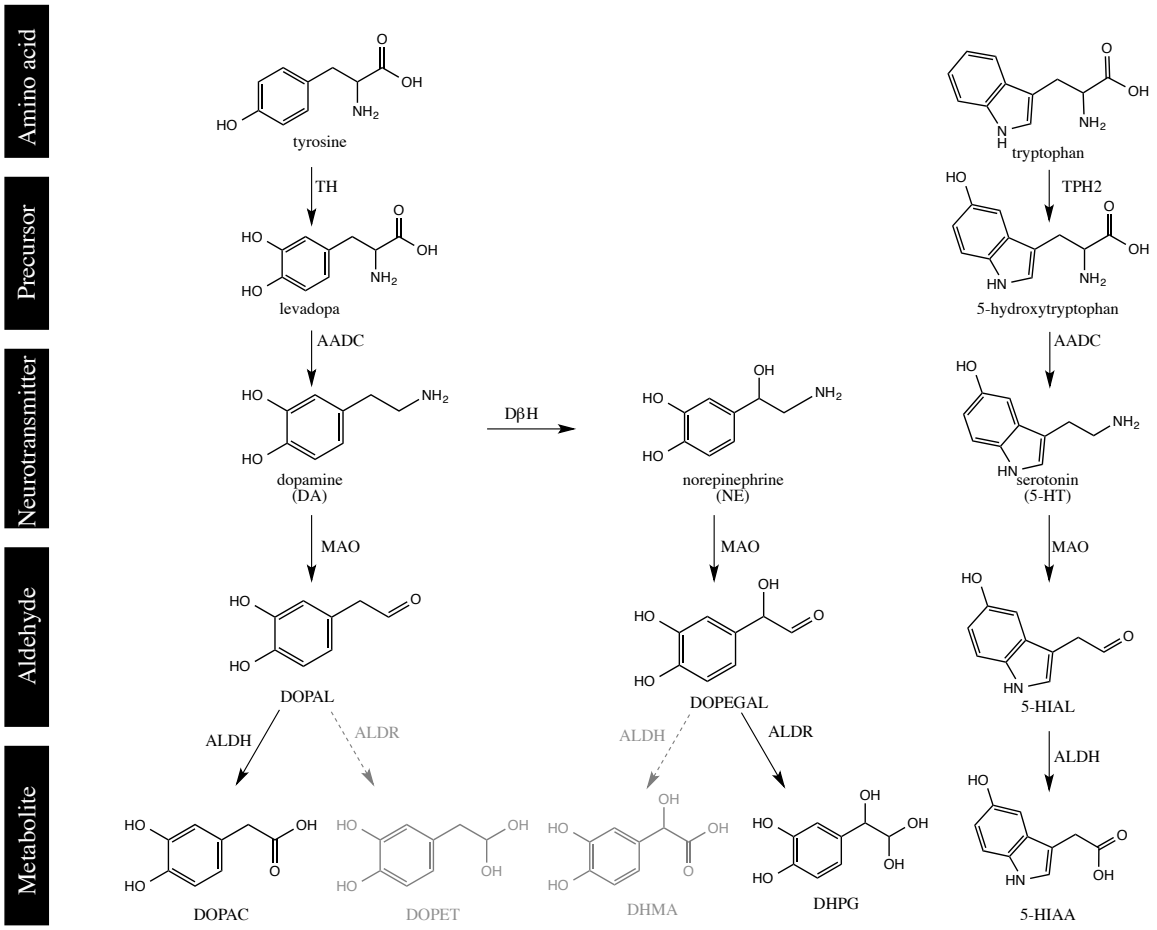
Amino acid
Precursor
Neurotransmitter
Aldehyde
Metabolite
tyrosine
TH
levadopa
AADC
dopamine
(DA)
DβH
norepinephrine
(NE)
MAO
DOPAL
DOPEGAL
ALDH
ALDR
DOPAC
DOPET
DHMA
DHPG
tryptophan
TPH2
5-hydroxytryptophan
AADC
serotonin
(5-HT)
MAO
5-HIAL
ALDH
5-HIAA

**Figure 1-2. Neuronal pathways for the biosynthesis and metabolic breakdown of monoamines.** Structural depiction of the synthesis and metabolic breakdown pathways in Figure 1-1.

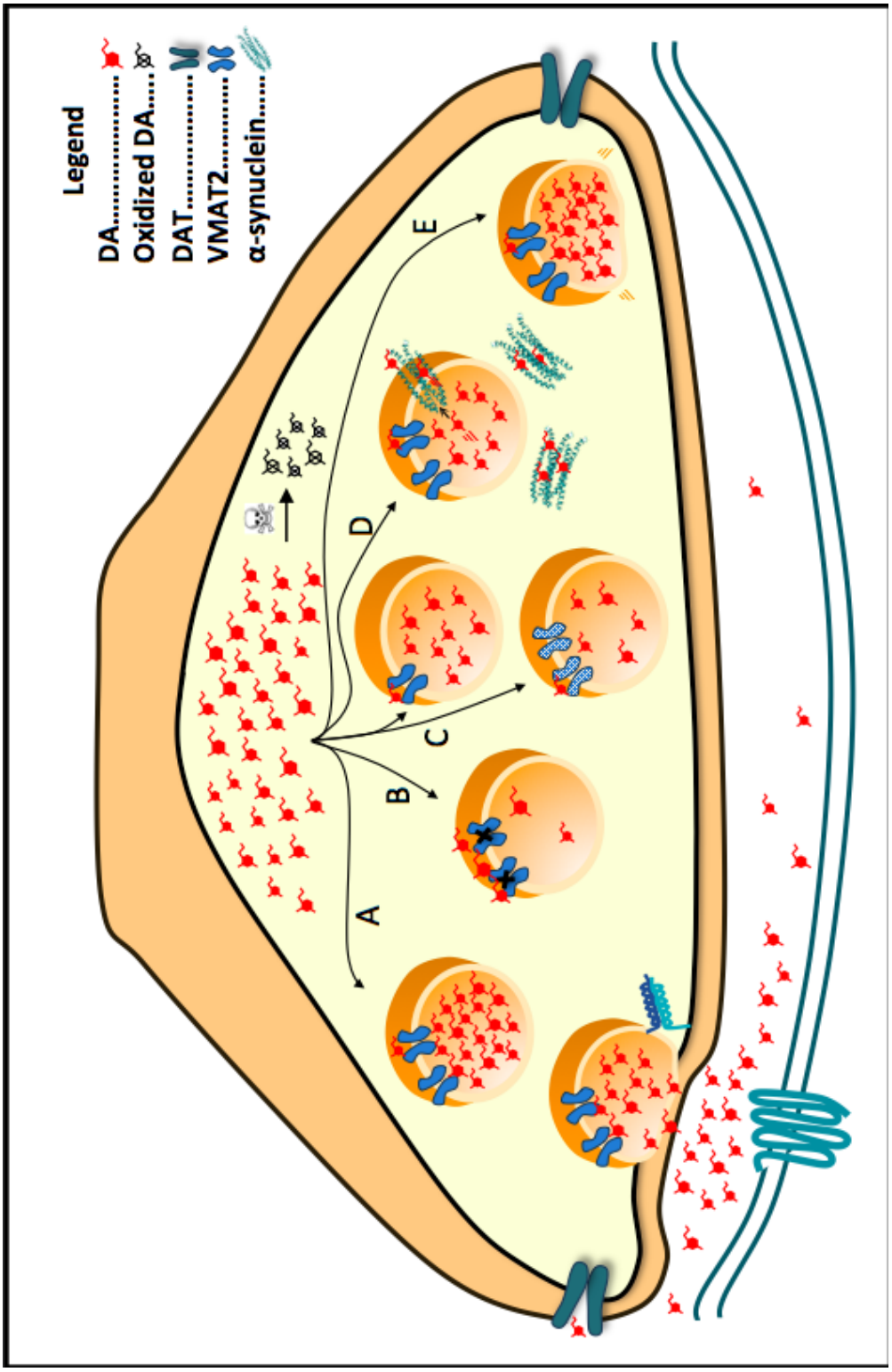
Legend
DA.....
Oxidized DA.....
DAT.....
VMAT2.....
α-synuclein.....
A
B
C
D
E

**Figure 1-3. Mechanisms of vesicular disruption in Parkinson's disease.**

After synthesis, dopamine is transported into vesicles. Cytoplasmic dopamine can be oxidized; in excess, this can lead to cellular injury. A) Vesicles in the readily releasable pool dock at the presynaptic membrane. In response to an action potential and calcium influx, vesicle membranes fuse to the plasma membrane and release their contents into the synaptic space. Dopamine is then reclaimed by the dopamine transporter (DAT) and then subsequently repackaged into the vesicle. B) Pharmacological inhibition of VMAT2 prevents uptake of dopamine leading to a depleted vesicle and reduced release. C) Genetic reduction of VMAT2 expression via promoter polymorphisms in humans or genetic manipulation in mice (upper vesicle) or VMAT2 function (lower vesicle) causes a reduction in vesicular filling and subsequent release. D) α-synuclein can form pores in the vesicle and cause depletion of dopamine from the vesicle or interact with cytoplasmic dopamine to form toxic species. E) Altered trafficking of the vesicle to the presynaptic membrane has been proposed to occur in the presence of overabundant α-synuclein or mutated LRRK2.

**References**


Aarsland D, Pahlhagen S, Ballard CG, Ehrt U, and Svenningsson P (2012) Depression in Parkinson disease--epidemiology, mechanisms and management. *Nat Rev Neurol* **8**:35–47.

Albin RL, Nichols TE, and Frey KA (2002) Brain imaging to assess the effects of dopamine agonists on progression of Parkinson disease. *JAMA* **288**:311–313.

Asanuma M, Miyazaki I, and Ogawa N (2003) Dopamine- or L-DOPA-induced neurotoxicity: The role of dopamine quinone formation and tyrosinase in a model of Parkinson's disease. *Neurotox Res* **5**:165–176.

Barker LA, Dowdall MJ, and Whittaker VP (1972) Choline metabolism in the cerebral cortex of guinea pigs. Stable-bound acetylcholine. *Biochem J* **130**:1063–1075.

Baumgarten HG, and Lachenmayer L (2004) Serotonin neurotoxins--past and present. *Neurotox Res* **6**:589–614.

Bédard C, Wallman M-J, Pourcher E, Gould P V, Parent A, and Parent M (2011) Serotonin and dopamine striatal innervation in Parkinson's disease and Huntington's chorea. *Park Relat Disord* **17**:593–598.

Belluzzi E, Greggio E, and Piccoli G (2012) Presynaptic dysfunction in Parkinson's disease: a focus on LRRK2. *Biochem Soc Trans* **40**:1111–1116.

Bemis JC, and Seegal RF (2004) PCB-induced inhibition of the vesicular monoamine transporter predicts reductions in synaptosomal dopamine content. *Toxicol Sci* **80**:288–295.

Benshachar D, Zuk R, and Glinka Y (1995) Dopamine Neurotoxicity - Inhibition of Mitochondrial Respiration. *J Neurochem* **64**:718–723.

Bernheimer H, Birkmayer W, and Hornykiewicz O (1961) [Distribution of 5-hydroxytryptamine (serotonin) in the human brain and its behavior in patients with Parkinson's syndrome]. *Klin Wochenschr* **39**:1056–1059.

Bertler A, Carlsson A, Nilsson J, and Rosengren E (1957) Effect of reserpine on the metabolism of catechol amines. *Acta Physiol Scand* **42**:22–23.

Birkmayer W, and Hornykiewicz O (1961) [The L-3,4-dioxyphenylalanine (DOPA)-effect in Parkinson-akinesia]. *Wien Klin Wochenschr* **73**:787–788.

Blondeau F, Ritter B, Allaire PD, Wasiak S, Girard M, Hussain NK, Angers A, Legendre-Guillemin V, Roy L, Boismenu D, Kearney RE, Bell AW, Bergeron JJ, and McPherson PS (2004) Tandem MS analysis of brain clathrin-coated vesicles reveals their critical involvement in synaptic vesicle recycling. *Proc Natl Acad Sci U S A* **101**:3833–3838.

Bohnen NI, Albin RL, Koeppe RA, Wernette KA, Kilbourn MR, Minoshima S, and Frey KA (2006) Positron emission tomography of monoaminergic vesicular binding in aging and Parkinson disease. *J Cereb Blood Flow Metab* **26**:1198–1212.

Braak H, Del Tredici K, Rub U, de Vos RA, Jansen Steur EN, and Braak E (2003) Staging of brain pathology related to sporadic Parkinson's disease. *Neurobiol Aging* **24**:197–211.

Brighina L, Riva C, Bertola F, Saracchi E, Fermi S, Goldwurm S and Ferrarese C (2013) Analysis of vesicular monoamine transporter 2 polymorphisms in Parkinson's disease. *Neurobiology of aging* **34**(6): 1712 e1719-1713.

Brodie BB, Shore PA, and Silver SL (1955) Potentiating action of chlorpromazine and reserpine. *Nature* **175**:1133–1134.

Burke WJ, Li SW, Chung HD, Ruggiero DA, Kristal BS, Johnson EM, Lampe P, Kumar VB, Franko M, Williams EA, and Zahm DS (2004) Neurotoxicity of MAO Metabolites of Catecholamine Neurotransmitters: Role in Neurodegenerative Diseases. *Neurotoxicology* **25**:101–115.

Burman J, Tran CH, Glatt C, Freimer NB, and Edwards RH (2004) The effect of rare human sequence variants on the function of vesicular monoamine transporter 2. *Pharmacogenetics* **14**:587–594.

Burn JH, and Rand MJ (1958) The action of sympathomimetic amines in animals treated with reserpine. *J Physiol* **144**:314–336.

Burre J, Beckhaus T, Schagger H, Corvey C, Hofmann S, Karas M, Zimmermann H, and Volknandt W (2006) Analysis of the synaptic vesicle proteome using three gel-based protein separation techniques. *Proteomics* **6**:6250–6262.

Callaghan RC, Cunningham JK, Sykes J, and Kish SJ (2012) Increased risk of Parkinson's disease in individuals hospitalized with conditions related to the use of methamphetamine or other amphetamine-type drugs. *Drug Alcohol Depend* **120**:35–40.

Carlsson A, Lindqvist M, and Magnusson T (1957) 3,4-Dihydroxyphenylalanine and 5-hydroxytryptophan as reserpine antagonists. *Nature* **180**:1200.

Caudle WM, Guillot TS, Lazo CR, and Miller GW (2012) Industrial toxicants and Parkinson's disease. *Neurotoxicology* **33**:178–188.

Caudle WM, Richardson JR, Wang MZ, Taylor TN, Guillot TS, McCormack AL, Colebrooke RE, Di Monte DA, Emson PC, and Miller GW (2007) Reduced

vesicular storage of dopamine causes progressive nigrostriatal neurodegeneration. *J Neurosci* **27**:8138–8148.

Caughey B, and Lansbury PT (2003) Protofibrils, pores, fibrils, and neurodegeneration: separating the responsible protein aggregates from the innocent bystanders. *Annu Rev Neurosci* **26**:267–298.

Ceccarelli B, and Hurlbut WP (1980) Vesicle hypothesis of the release of quanta of acetylcholine. *Physiol Rev* **60**:396–441.

Chao KT, Tsao HH, Weng YH, Hsiao IT, Hsieh CJ, Wey SP, Yen TC, Kung MP, and Lin KJ (2012) Quantitative analysis of binding sites for 9-fluoropropyl-(+)-dihydrotetrabenazine ( 18F AV-133) in a MPTP-lesioned PD mouse model. *Synapse* **66**:823–831.

Chaudhry FA, Boulland JL, Jenstad M, Bredahl MK, and Edwards RH (2008) Pharmacology of neurotransmitter transport into secretory vesicles. *Handb Exp Pharmacol* 77–106.

Chaudhry FA, Edwards RH, and Fonnum F (2008) Vesicular neurotransmitter transporters as targets for endogenous and exogenous toxic substances. *Annu Rev Pharmacol Toxicol* **48**:277–301.

Chen L, Ding Y, Cagniard B, Van Laar AD, Mortimer A, Chi W, Hastings TG, Kang UJ, and Zhuang X (2008) Unregulated cytosolic dopamine causes neurodegeneration associated with oxidative stress in mice. *J Neurosci* **28**:425–433.

Cheshire P, Ayton S, Bertram KL, Ling H, Li A, McLean C, Halliday GM, O'Sullivan SS, Revesz T, Finkelstein DI, Storey E, and Williams DR (2015) Serotonergic

markers in Parkinson's disease and levodopa-induced dyskinesias. *Mov Disord*, doi: 10.1002/mds.26144.

Choi BK, Choi MG, Kim JY, Yang Y, Lai Y, Kweon DH, Lee NK, and Shin YK (2013) Large alpha-synuclein oligomers inhibit neuronal SNARE-mediated vesicle docking. *Proc Natl Acad Sci U S A*, doi: 10.1073/pnas.1218424110.

Conway KA, Rochet J-C, Bieganski RM, and Lansbury Jr PT (2001) Kinetic Stabilization of the Alpha-Synuclein Protofibril by a Dopamine-Alpha-Synuclein Adduct. *Science (80- )* **294**:1346.

Corrigan FM, Murray L, Wyatt CL, and Shore RF (1998) Diorthosubstituted polychlorinated biphenyls in caudate nucleus in Parkinson's disease. *Exp Neurol* **150**:339–342.

Corrigan FM, Wienburg CL, Daniel SE, and Mann D (2000) Organochlorine insecticides in substantia nigra in Parkinson ' s disease. *J Toxicol Environ Heal Part A* **59**:229–234.

Coughenour HD, Spaulding RS, and Thompson CM (2004) The synaptic vesicle proteome: a comparative study in membrane protein identification. *Proteomics* **4**:3141–3155.

Crino PB, Vogt BA, Chen JC, and Volicer L (1989) Neurotoxic effects of partially oxidized serotonin: tryptamine-4,5-dione. *Brain Res* **504**:247–257.

Damier P, Hirsch EC, Agid Y, and Graybiel AM (1999) The substantia nigra of the human brain: II. Patterns of loss of dopamine-containing neurons in Parkinson's disease. *Brain* **122**:1437–1448.

Davidson WS, Jonas A, Clayton DF, and George JM (1998) Stabilization of alpha-synuclein secondary structure upon binding to synthetic membranes. J Biol Chem 273:9443–9449.

Del Tredici K and Braak H (2013) Dysfunction of the locus coeruleus-norepinephrine system and related circuitry in Parkinson's disease-related dementia. J Neurol Neurosurg Psychiatry 84(7): 774-783.

Edwards RH (2007) The neurotransmitter cycle and quantal size. Neuron 55:835–858.

Ehringer H, and Hornykiewicz O (1960) [Distribution of noradrenaline and dopamine (3-hydroxytyramine) in the human brain and their behavior in diseases of the extrapyramidal system]. *Klin Wochenschr* **38**:1236–1239.

Eiden LE, and Weihe E (2011) VMAT2: a dynamic regulator of brain monoaminergic neuronal function interacting with drugs of abuse. *Ann N Y Acad Sci* **1216**:86–98.

Eisenhofer G, Hovevey-Sion D, Kopin IJ, Miletich R, Kirk KL, Finn R, and Goldstein DS (1989) Neuronal uptake and metabolism of 2- and 6-fluorodopamine: false neurotransmitters for positron emission tomographic imaging of sympathetically innervated tissues. *J Pharmacol Exp Ther* **248**:419–427.

Eisenhofer G, Kopin IJ, and Goldstein DS (2004a) Catecholamine Metabolism: A Contemporary View with Implications for Physiology and Medicine. *Pharmacol Rev* **56**:331–349.

Eisenhofer G, Kopin IJ, and Goldstein DS (2004b) Leaky Catecholamine Stores: Undue Waste or a Stress Response Coping Mechanism? *Ann N Y Acad Sci* **1018**:224–230,

Elbaz A, Clavel J, Rathouz PJ, Moisan F, Galanaud J-P, Delemotte B, Alpérovitch A, and Tzourio C (2009) Professional exposure to pesticides and Parkinson disease. *Ann Neurol* **66**:494–504.

Fahn S (2003) Description of Parkinson's Disease as a Clinical Syndrome. *Ann N Y Acad Sci* **991**:1–14.

Fleming L, Mann JB, Bean J, Briggle T, and Sanchez-Ramos JR (1994) Parkinson's disease and brain levels of organochlorine pesticides. *Ann Neurol* **36**:100–103.

Foley JM, and Baxter D (1958) On the nature of pigment granules in the cells of the locus coeruleus and substantia nigra. *J Neuropathol Exp Neurol* **17**:586–598,

Fonnum F, Mariussen E, and Reistad T (2006) Molecular mechanisms involved in the toxic effects of polychlorinated biphenyls (PCBs) and brominated flame retardants (BFRs). *J Toxicol Env Heal A* **69**:21–35.

Forno LS, Langston JW, DeLanney LE, Irwin I, and Ricaurte GA (1986) Locus ceruleus lesions and eosinophilic inclusions in MPTP-treated monkeys. *Ann Neurol* **20**:449–455.

Frey KA, Koeppe RA, Kilbourn MR, VanderBorght TM, Albin RL, Gilman S, and Kuhl DE (1996) Presynaptic monoaminergic vesicles in Parkinson's disease and normal aging. *Ann Neurol* **40**:873–884.

Fumagalli F, Gainetdinov RR, Wang Y-M, Valenzano KJ, Miller GW, and Caron MG (1999) Increased Methamphetamine Neurotoxicity in Heterozygous Vesicular Monoamine Transporter 2 Knock-Out Mice. *J Neurosci* **19**:2424–2431.

Gaugler MN, Genc O, Bobela W, Mohanna S, Ardah MT, El-Agnaf OM, Cantoni M, Bensadoun JC, Schneggenburger R, Knott GW, Aebischer P, and Schneider BL

(2012) Nigrostriatal overabundance of alpha-synuclein leads to decreased vesicle density and deficits in dopamine release that correlate with reduced motor activity. *Acta Neuropathol* **123**:653–669.

Glatt CE, DeYoung JA, Delgado S, Service SK, Giacomini KM, Edwards RH, Risch N, and Freimer NB (2001) Screening a large reference sample to identify very low frequency sequence variants: comparisons between two genes. *Nat Genet* **27**:435–438.

Glatt CE, Wahner AD, White DJ, Ruiz-Linares A, and Ritz B (2006) Gain-of-function haplotypes in the vesicular monoamine transporter promoter are protective for Parkinson disease in women. *Hum Mol Genet* **15**:299–305.

Goldstein DS, Holmes C, Kopin IJ, and Sharabi Y (2011) Intra-neuronal vesicular uptake of catecholamines is decreased in patients with Lewy body diseases. *J Clin Invest* **121**:3320–3330.

Goldstein DS, Holmes C, Sewell L, Park MY, and Sharabi Y (2012) Sympathetic noradrenergic before striatal dopaminergic denervation: relevance to Braak staging of synucleinopathy. *Clin Aut Res* **22**:57–61.

Goldstein DS, Sullivan P, Holmes C, Kopin IJ, Basile MJ, and Mash DC (2011) Catechols in post-mortem brain of patients with Parkinson disease. *Eur J Neurol* **18**:703–710.

Graham DG, Tiffany SM, Bell Jr. WR, and Gutknecht WF (1978) Autoxidation versus covalent binding of quinones as the mechanism of toxicity of dopamine, 6-hydroxydopamine, and related compounds toward C1300 neuroblastoma cells in vitro. *Mol Pharmacol* **14**:644–653.

Greenfield JG, and Bosanquet FD (1953) The brain-stem lesions in Parkinsonism. *J Neurol Neurosurg Psychiatry* **16**:213–226.

Guillot T, and Miller G (2009) Protective Actions of the Vesicular Monoamine Transporter 2 (VMAT2) in Monoaminergic Neurons. *Mol Neurobiol* **39**:149–170.

Guillot TS, Richardson JR, Wang MZ, Li YJ, Taylor TN, Ciliax BJ, Zachrisson O, Mercer A, and Miller GW (2008) PACAP38 increases vesicular monoamine transporter 2 (VMAT2) expression and attenuates methamphetamine toxicity. *Neuropeptides* **42**:423–434.

Guillot TS, Shepherd KR, Richardson JR, Wang MZ, Li YJ, Emson PC, and Miller GW (2008) Reduced vesicular storage of dopamine exacerbates methamphetamine-induced neurodegeneration and astrogliosis. *J Neurochem* **106**:2205–2217.

Halliday GM, Blumbergs PC, Cotton RG, Blessing WW, and Geffen LB (1990) Loss of brainstem serotonin- and substance P-containing neurons in Parkinson's disease. *Brain Res* **510**:104–107.

Halliday GM, Li YW, Blumbergs PC, Joh TH, Cotton RG, Howe PR, Blessing WW, and Geffen LB (1990) Neuropathology of immunohistochemically identified brainstem neurons in Parkinson's disease. *Ann Neurol* **27**:373–385.

Hallman H, Lange J, Olson L, Stromberg I, and Jonsson G (1985) Neurochemical and histochemical characterization of neurotoxic effects of 1-methyl-4-phenyl-1,2,3,6-tetrahydropyridine on brain catecholamine neurones in the mouse. *J Neurochem* **44**:117–127.

Hannah MJ, Schmidt AA, and Huttner WB (1999) Synaptic vesicle biogenesis. *Annu Rev Cell Dev Biol* **15**:733–798.

Hastings TG, Lewis DA, and Zigmond MJ (1996) Role of oxidation in the neurotoxic effects of intrastriatal dopamine injections. *Proc Natl Acad Sci U S A* **93**:1956–1961.

Hatcher JM, Miller GW, and Pennell KD (2008) Parkinson's disease and pesticides: a toxicological perspective. *Trends Pharmacol Sci* **29**:322–329.

Hatcher-Martin JM, Gearing M, Steenland K, Levey AI, Miller GW, and Pennell KD (2012) Association between polychlorinated biphenyls and Parkinson's disease neuropathology. *Neurotoxicology* **33**:1298–1304.

Hauser RA, Koller WC, Hubble JP, Malapira T, Busenbark K, and Olanow CW (2000) Time course of loss of clinical benefit following withdrawal of levodopa/carbidopa and bromocriptine in early Parkinson' s disease. *Mov Disord* **15**:485–489.

Jain S, and Goldstein DS (2012) Cardiovascular dysautonomia in Parkinson disease: From pathophysiology to pathogenesis. *Neurobiol Dis* **46**:572–580.

Jinsmaa Y, Cooney A, Sullivan P, Sharabi Y, and Goldstein DS (2015) The serotonin aldehyde, 5-HIAL, oligomerizes alpha-synuclein. *Neurosci Lett* **590**:134–137.

Kanaan NM, Kordower JH, and Collier TJ (2008) Age-related changes in dopamine transporters and accumulation of 3-nitrotyrosine in rhesus monkey midbrain dopamine neurons: relevance in selective neuronal vulnerability to degeneration. *Eur J Neurosci* **27**:3205–3215.

Kilbourn MR, Frey KA, Vander Borght T, and Sherman PS (1996) Effects of dopaminergic drug treatments on in vivo radioligand binding to brain vesicular monoamine transporters. *Nucl Med Biol* **23**:467–471.

Kish SJ, Zhong XH, Hornykiewicz O, and Haycock JW (1995) Striatal 3,4-dihydroxyphenylalanine decarboxylase in aging: disparity between postmortem and positron emission tomography studies? *Ann Neurol* **38**:260–264.

Kostic VS, Djuricic BM, Covickovic-Sternic N, Bumbasirevic L, Nikolic M, and Mrsulja BB (1987) Depression and Parkinson's disease: possible role of serotonergic mechanisms. *J Neurol* **234**:94–96.

Kruger R, Kuhn W, Muller T, Woitalla D, Graeber M, Kosel S, Przuntek H, Epplen JT, Schols L, and Riess O (1998) Ala30Pro mutation in the gene encoding alpha-synuclein in Parkinson's disease. *Nat Genet* **18**:106–108.

Langston JW, Ballard P, Tetrud JW, and Irwin I (1983) Chronic Parkinsonism in humans due to a product of meperidine-analog synthesis. *Science (80- )* **219**:979–980.

Larsen KE, Fon EA, Hastings TG, Edwards RH, and Sulzer D (2002) Methamphetamine-induced degeneration of dopaminergic neurons involves autophagy and upregulation of dopamine synthesis. *J Neurosci* **22**:8951–8960.

LaVoie MJ, and Hastings TG (1999) Dopamine quinone formation and protein modification associated with the striatal neurotoxicity of methamphetamine: evidence against a role for extracellular dopamine. *J Neurosci* **19**:1484–1491.

Li S-T, Dendi R, Holmes C, and Goldstein DS (2002) Progressive loss of cardiac sympathetic innervation in Parkinson's disease. *Ann Neurol* **52**:220–223.

Lill CM, Roehr JT, McQueen MB, Kavvoura FK, Bagade S, Schjeide BM, Schjeide LM, Meissner E, Zauft U, Allen NC, Liu T, Schilling M, Anderson KJ, Beecham G, Berg D, Biernacka JM, Brice A, DeStefano AL, Do CB, Eriksson N, Factor SA, Farrer MJ, Foroud T, Gasser T, Hamza T, Hardy JA, Heutink P, Hill-Burns EM, Klein C,

Latourelle JC, Maraganore DM, Martin ER, Martinez M, Myers RH, Nalls MA, Pankratz N, Payami H, Satake W, Scott WK, Sharma M, Singleton AB, Stefansson K, Toda T, Tung JY, Vance J, Wood NW, Zabetian CP, Young P, Tanzi RE, Khoury MJ, Zipp F, Lehrach H, Ioannidis JP, and Bertram L (2012) Comprehensive research synopsis and systematic meta-analyses in Parkinson's disease genetics: The PDGene database. *PLoS Genet* **8**:e1002548.

Lin ZC, Zhao Y, Chung CY, Zhou YH, Xiong NA, Glatt CE, and Isacson O (2010) High regulatability favors genetic selection in SLC18A2, a vesicular monoamine transporter essential for life. *Faseb J* **24**:2191–2200.

Liu Y, Peter D, Roghani A, Schuldiner S, Prive GG, Eisenberg D, Brecha N, and Edwards RH (1992) A cDNA that suppresses MPP+ toxicity encodes a vesicular amine transporter. *Cell* **70**:539–551.

Liu YJ, and Edwards RH (1997) The role of vesicular transport proteins in synaptic transmission and neural degeneration. *Annu Rev Neurosci* **20**:125–156.

Lotharius J, and Brundin P (2002) Impaired dopamine storage resulting from alpha-synuclein mutations may contribute to the pathogenesis of Parkinson's disease. *Hum Mol Genet* **11**:2395–2407.

Manning-Bog AB, Caudle WM, Perez XA, Reaney SH, Paletzki R, Isla MZ, Chou VP, McCormack AL, Miller GW, Langston JW, Gerfen CR, and Dimonte DA (2007) Increased vulnerability of nigrostriatal terminals in DJ-1-deficient mice is mediated by the dopamine transporter. *Neurobiol Dis* **27**:141–150.

Masilamoni GJ, Bogenpohl JW, Alagille D, Delevich K, Tamagnan G, Votaw JR, Wichmann T, and Smith Y (2011) Metabotropic glutamate receptor 5 antagonist

protects dopaminergic and noradrenergic neurons from degeneration in MPTP-treated monkeys. *Brain* **134**:2057–2073.

Maximov A, and Sudhof TC (2005) Autonomous function of synaptotagmin 1 in triggering synchronous release independent of asynchronous release. *Neuron* **48**:547–554.

McCann UD, Wong DF, Yokoi F, Villemagne V, Dannals RF, and Ricaurte GA (1998) Reduced striatal dopamine transporter density in abstinent methamphetamine and methcathinone users: Evidence from positron emission tomography studies with C-11 WIN-35,428. *J Neurosci* **18**:8417–8422.

Melega WP, Williams AE, Schmitz DA, DiStefano EW, and Cho AK (1995) Pharmacokinetic and pharmacodynamic analysis of the actions of D-amphetamine and D-methamphetamine on the dopamine terminal. *J Pharmacol Exp Ther* **274**:90–96.

Miller GW, Erickson JD, Perez JT, Penland SN, Mash DC, Rye DB, and Levey AI (1999) Immunochemical Analysis of Vesicular Monoamine Transporter (VMAT2) Protein in Parkinson's Disease. *Exp Neurol* **156**:138–148.

Miller GW, Erickson JD, Perez JT, Penland SN, Mash DC, Rye DB, and Levey AI (1999) Immunochemical analysis of vesicular monoamine transporter (VMAT2) protein in Parkinson's disease. *Exp Neurol* **156**:138–148.

Miller GW, Gainetdinov RR, Levey a I, and Caron MG (1999) Dopamine transporters and neuronal injury. *Trends Pharmacol Sci* **20**:424–9.

Miller GW, Kirby ML, Levey AI, and Bloomquist JR (1999) Heptachlor alters expression and function of dopamine transporters. *Neurotoxicology* **20**:631–637.

Mooslehner KA, Chan PM, Xu W, Liu L, Smadja C, Humby T, Allen ND, Wilkinson LS, and Emson PC (2001) Mice with very low expression of the vesicular monoamine transporter 2 gene survive into adulthood: potential mouse model for parkinsonism. *Mol Cell Biol* **21**:5321–5331.

Morciano M, Burre J, Corvey C, Karas M, Zimmermann H, and Volknandt W (2005) Immunoisolation of two synaptic vesicle pools from synaptosomes: a proteomics analysis. *J Neurochem* **95**:1732–1745.

Murthy VN, and Stevens CF (1999) Reversal of synaptic vesicle docking at central synapses. *Nat Neurosci* **2**:503–507.

Narboux-Neme N, Sagne C, Doly S, Diaz SL, Martin CB, Angenard G, Martres MP, Giros B, Hamon M, Lanfumey L, Gaspar P, and Mongeau R (2011) Severe serotonin depletion after conditional deletion of the vesicular monoamine transporter 2 gene in serotonin neurons: neural and behavioral consequences. *Neuropsychopharmacology* **36**:2538–2550.

Navailles S, Carta M, Guthrie M, and De Deurwaerdere P (2011) L-DOPA and serotonergic neurons: functional implication and therapeutic perspectives in Parkinson's disease. *Cent Nerv Syst Agents Med Chem* **11**:305–320.

Okamura N, Villemagne VL, Drago J, Pejoska S, Dhamija RK, Mulligan RS, Ellis JR, Ackermann U, O'Keefe G, Jones G, Kung HF, Pontecorvo MJ, Skovronsky D, and Rowe CC (2010) In Vivo Measurement of Vesicular Monoamine Transporter Type 2 Density in Parkinson Disease with F-18-AV-133. *J Nucl Med* **51**:223–228.

Orimo S, Ozawa E, Nakade S, Sugimoto T, and Mizusawa H (1999) I-123-metaiodobenzylguanidine myocardial scintigraphy in Parkinson's disease. *J Neurol Neurosurg Psychiatry* **67**:189–194.

Orimo S, Suzuki M, Inaba A, and Mizusawa H (2012) 123I-MIBG myocardial scintigraphy for differentiating Parkinson's disease from other neurodegenerative parkinsonism: A systematic review and meta-analysis. *Park Relat Disord* **18**:494–500.

Orimo S, Takahashi A, Uchihara T, Mori F, Kakita A, Wakabayashi K, and Takahashi H (2007) Degeneration of cardiac sympathetic nerve begins in the early disease process of Parkinson's disease. *Brain Pathol* **17**:24–30.

Paisan-Ruiz C, Nath P, Washecka N, Gibbs JR, and Singleton AB (2008) Comprehensive analysis of LRRK2 in publicly available Parkinson's disease cases and neurologically normal controls. *Hum Mutat* **29**:485–490.

Pang ZP, Sun J, Rizo J, Maximov A, and Sudhof TC (2006) Genetic analysis of synaptotagmin 2 in spontaneous and Ca2+-triggered neurotransmitter release. *EMBO J* **25**:2039–2050.

Paul SM, Rehavi M, Skolnick P, Ballenger JC, and Goodwin FK (1981) Depressed-patients have decreased binding of tritiated imipramine to platelet serotonin transporter. *Arch Gen Psychiatry* **38**:1315–1317.

Paulus W, and Jellinger K (1991) The Neuropathologic Basis of Different Clinical Subgroups of Parkinsons-Disease. *J Neuropathol Exp Neurol* **50**:743–755.

Pifl C, Rajput A, Reither H, Blesa J, Cavada C, Obeso JA, Rajput AH, and Hornykiewicz O (2014) Is Parkinson's Disease a Vesicular Dopamine Storage Disorder? Evidence

from a Study in Isolated Synaptic Vesicles of Human and Nonhuman Primate Striatum. *J Neurosci* **34**:8210–8218.

Pletscher A (1988) Platelets as models: Use and limitations. *Experientia* **44**:152–155.

Pletscher A, Shore PA, and Brodie BB (1955) Serotonin release as a possible mechanism of reserpine action. *Science (80- )* **122**:374–375.

Politis M, Oertel WH, Wu K, Quinn NP, Pogarell O, Brooks DJ, Bjorklund A, Lindvall O, and Piccini P (2011) Graft-induced dyskinesias in Parkinson's disease: High striatal serotonin/dopamine transporter ratio. *Mov Disord* **26**:1997–2003.

Polymeropoulos MH, Lavedan C, Leroy E, Ide SE, Dehejia A, Dutra A, Pike B, Root H, Rubenstein J, Boyer R, Stenroos ES, Chandrasekharappa S, Athanassiadou A, Papapetropoulos T, Johnson WG, Lazzarini AM, Duvoisin RC, Di Iorio G, Golbe LI, and Nussbaum RL (1997) Mutation in the alpha-synuclein gene identified in families with Parkinson's disease. *Science (80- )* **276**:2045–2047.

Priyadarshi A, Khuder SA, Schaub EA, and Priyadarshi SS (2001) Environmental risk factors and Parkinson's disease: a metaanalysis. *Environ Res* **86**:122–127.

Priyadarshi A, Khuder SA, Schaub EA, and Shrivastava S (2000) A meta-analysis of Parkinson's disease and exposure to pesticides. *Neurotoxicology* **21**:435–440.

Pyle JL, Kavalali ET, Piedras-Renteria ES, and Tsien RW (2000) Rapid reuse of readily releasable pool vesicles at hippocampal synapses. *Neuron* **28**:221–231.

Rees JN, Florang VR, Eckert LL, and Doorn JA (2009) Protein Reactivity of 3,4-Dihydroxyphenylacetaldehyde, a Toxic Dopamine Metabolite, Is Dependent on Both the Aldehyde and the Catechol. *Chem Res Toxicol* **22**:1256–1263.

Richman A, and Tyhurst JS (1955) An extrapyramidal syndrome with reserpine. *Can Med Assoc J* **72**:457–458.

Rilstone JJ, Alkhater RA, and Minassian BA (2013) Brain Dopamine-Serotonin Vesicular Transport Disease and Its Treatment. N Engl J Med. 368(6): 543-550.

Ritz B, and Costello S (2006) Geographic model and biomarker-derived measures of pesticide exposure and Parkinson's disease. *Ann N Y Acad Sci* **1076**:378–387.

Rizo J, and Sudhof TC (2012) The membrane fusion enigma: SNAREs, Sec1/Munc18 proteins, and their accomplices--guilty as charged? *Annu Rev Cell Dev Biol* **28**:279–308.

Rochet JC, Outeiro TF, Conway KA, Ding TT, Volles MJ, Lashuel HA, Bieganski RM, Lindquist SL, and Lansbury PT (2004) Interactions among alpha-synuclein, dopamine, and biomembranes - Some clues for understanding neurodegeneration in Parkinson's disease. *J Mol Neurosci* **23**:23–33.

Sala G, Brighina L, Saracchi E, Fermi S, Riva C, Carrozza V, Pirovano M, and Ferrarese C (2010) Vesicular monoamine transporter 2 mRNA levels are reduced in platelets from patients with Parkinson's disease. *J Neural Transm* **117**:1093–1098.

Schikorski T, and Stevens CF (1997) Quantitative Ultrastructural Analysis of Hippocampal Excitatory Synapses. *J Neurosci* **17**:5858–5867.

Scott D, and Roy S (2012) alpha-Synuclein inhibits intersynaptic vesicle mobility and maintains recycling-pool homeostasis. *J Neurosci* **32**:10129–10135.

Segovia M, Ales E, Montes MA, Bonifas I, Jemal I, Lindau M, Maximov A, Sudhof TC, and Alvarez de Toledo G (2010) Push-and-pull regulation of the fusion pore by synaptotagmin-7. *Proc Natl Acad Sci U S A* **107**:19032–19037.

Semchuk KM, Love EJ, and Lee RG (1992) Parkinson's disease and exposure to agricultural work and pesticide chemicals. *Neurology* **42**:1328–1335.

Semchuk KM, Love EJ, and Lee RG (1991) Parkinson's disease and exposure to rural environmental factors: a population based case-control study. *Can J Neurol Sci* **18**:279–286.

Shore PA, Pletscher A, Tomich EG, Carlsson A, Kuntzman R, and Brodie BB (1957) Role of brain serotonin in reserpine action. *Ann N Y Acad Sci* **66**:609–15; discussion, 615–7.

Singleton AB, Farrer M, Johnson J, Singleton A, Hague S, Kachergus J, Hulihan M, Peuralinna T, Dutra A, Nussbaum R, Lincoln S, Crawley A, Hanson M, Maraganore D, Adler C, Cookson MR, Muenter M, Baptista M, Miller D, Blancato J, Hardy J, and Gwinn-Hardy K (2003) alpha-Synuclein locus triplication causes Parkinson's disease. *Science (80- )* **302**:841.

Smith Y, Wichmann T, Factor SA, and DeLong MR (2012) Parkinson's disease therapeutics: new developments and challenges since the introduction of levodopa. *Neuropsychopharmacology* **37**:213–246.

Speciale SG, Liang CL, Sonsalla PK, Edwards RH, and German DC (1998) The neurotoxin 1-methyl-4-phenylpyridinium is sequestered within neurons that contain the vesicular monoamine transporter. *Neuroscience* **84**:1177–1185.

Steenland K, Hein MJ, Cassinelli RT, Prince MM, Nilsen NB, Whelan E a., Waters M a., Ruder AM, and Schnorr TM (2006) Polychlorinated Biphenyls and Neurodegenerative Disease Mortality in an Occupational Cohort. *Epidemiology* **17**:8–13.

Sudhof TC (2004) The synaptic vesicle cycle. *Annu Rev Neurosci* **27**:509–547.

Südhof TC (2000) The Synaptic VesicleCycle Revisited. *Neuron* **28**:317–320.

Sulzer D (2011a) How Addictive Drugs Disrupt Presynaptic Dopamine Neurotransmission. *Neuron* **69**:628–649.

Sulzer D (2011b) How Addictive Drugs Disrupt Presynaptic Dopamine Neurotransmission. *Neuron* **69**:628–649.

Sulzer D, and Surmeier DJ (2012) Neuronal vulnerability, pathogenesis, and Parkinson's disease. *Mov Disord* n/a–n/a, Wiley Subscription Services, Inc., A Wiley Company.

Sulzer D, and Zecca L (1999) Intraneuronal dopamine-quinone synthesis: A review. *Neurotox Res* **1**:181–195.

Takahashi N, Miner LL, Sora I, Ujike H, Revay RS, Kostic V, Jackson-Lewis V, Przedborski S, and Uhl GR (1997) VMAT2 knockout mice: Heterozygotes display reduced amphetamine-conditioned reward, enhanced amphetamine locomotion, and enhanced MPTP toxicity. *Proc Natl Acad Sci* **94**:9938–9943.

Takamori S, Holt M, Stenius K, Lemke EA, Gronborg M, Riedel D, Urlaub H, Schenck S, Brugger B, Ringler P, Muller SA, Rammner B, Grater F, Hub JS, De Groot BL, Mieskes G, Moriyama Y, Klingauf J, Grubmuller H, Heuser J, Wieland F, and Jahn R (2006) Molecular anatomy of a trafficking organelle. *Cell* **127**:831–846.

Tanner CM (1990) Parkinson's disease: environmental etiologic factors. *Curr Opin Neurol* **3**.

Taylor TN, Alter SP, Wang M, Goldstein DS, and Miller GW (2014) Reduced vesicular storage of catecholamines causes progressive degeneration in the locus ceruleus. *Neuropharmacology* **76 Pt A**:97–105.

Taylor TN, Caudle WM, Shepherd KR, Noorian A, Jackson CR, Iuvone PM, Weinshenker D, Greene JG, and Miller GW (2009) Nonmotor symptoms of Parkinson's disease revealed in an animal model with reduced monoamine storage capacity. *J Neurosci* **29**:8103–8113.

Tedroff J, Ekesbo A, Rydin E, Langstrom B, and Hagberg G (1999) Regulation of dopaminergic activity in early Parkinson's disease. *Ann Neurol* **46**:359–365.

Tijero B, Gomez-Esteban JC, Llorens V, Lezcano E, Gonzalez-Fernandez MC, de Pancorbo MM, Ruiz-Martinez J, Cembellin JC, and Zarranz JJ (2010) Cardiac sympathetic denervation precedes nigrostriatal loss in the E46K mutation of the alpha-synuclein gene (SNCA). *Clin Aut Res* **20**:267–269.

Toren P, Rehavi M, Luski A, Roz N, Laor N, Lask M, and Weizman A (2005) Decreased platelet vesicular monoamine transporter density in children and adolescents with attention deficit/hyperactivity disorder. *Eur Neuropsychopharmacol* **15**:159–162, Netherlands.

Ulusoy A, Björklund T, Buck K, and Kirik D (2012) Dysregulated dopamine storage increases the vulnerability to α-synuclein in nigral neurons. *Neurobiol Dis* **47**:367–377.

Velseboer DC, de Haan RJ, Wieling W, Goldstein DS, and de Bie RM (2011) Prevalence of orthostatic hypotension in Parkinson's disease: a systematic review and meta-analysis. *Park Relat Disord* **17**:724–729.

Villemagne V, Yuan J, Wong DF, Dannals RF, Hatzidimitriou G, Mathews WB, Ravert HT, Musachio J, McCann UD, and Ricaurte GA (1998) Brain dopamine neurotoxicity in baboons treated with doses of methamphetamine comparable to

those recreationally abused by humans: Evidence from C-11 WIN-35,428 positron emission tomography studies and direct in vitro determinations. *J Neurosci* **18**:419–427.

Volles MJ, and Lansbury PT (2002) Vesicle permeabilization by protofibrillar alpha-synuclein is sensitive to Parkinson's disease-linked mutations and occurs by a pore-like mechanism. *Biochemistry* **41**:4595–4602.

Wagner GC, Ricaurte GA, Seiden LS, Schuster CR, Miller RJ, and Westley J (1980) Long-lasting depletions of striatal dopamine and loss of dopamine uptake sites following repeated administration of methamphetamine. *Brain Res* **181**:151–160.

Wang YM, Gainetdinov RR, Fumagalli F, Xu F, Jones SR, Bock CB, Miller GW, Wightman RM, and Caron MG (1997) Knockout of the vesicular monoamine transporter 2 gene results in neonatal death and supersensitivity to cocaine and amphetamine. *Neuron* **19**:1285–1296.

Weisskopf MG, Knekt P, O'Reilly EJ, Lyytinen J, Reunanen a, Laden F, Altshul L, and Ascherio a (2010) Persistent organochlorine pesticides in serum and risk of Parkinson disease. *Neurology* **74**:1055–1061.

Wey MC, Fernandez E, Martinez PA, Sullivan P, Goldstein DS, and Strong R (2012) Neurodegeneration and motor dysfunction in mice lacking cytosolic and mitochondrial aldehyde dehydrogenases: implications for Parkinson's disease. *PLoS One* **7**:e31522.

Wichmann T, and DeLong MR (1996) Functional and pathophysiological models of the basal ganglia. *Curr Opin Neurobiol* **6**:751–758.

Yamamoto BK, Moszczynska A, and Gudelsky GA (2010) Amphetamine toxicities. Ann N Y Acad Sci 1187:101–121.

Yubero-Lahoz S, Robledo P, Farre M and de laTorre R (2013) Platelet SERT as a peripheral biomarker of serotonergic neurotransmission in the central nervous system. Current medicinal chemistry 20(11): 1382-1396.

Zahid M, Saeed M, Yang L, Beseler C, Rogan E, and Cavalieri EL (2011) Formation of dopamine quinone-DNA adducts and their potential role in the etiology of Parkinson's disease. IUBMB Life 63:1087–1093.

Zalsman G, Rehavi M, Roz N, Laor N, Weizman A, and Toren P (2011) Altered affinity of the platelet vesicular monoamine transporter 2 to dihydrotetrabenazine in children with major depression. *J Neural Transm* **118**:1383–1387..

Zarow C, Lyness SA, Mortimer JA, and Chui HC (2003) Neuronal loss is greater in the locus coeruleus than nucleus basalis and substantia nigra in Alzheimer and Parkinson diseases. *Arch Neurol* **60**:337–341.

Zucker M, Weizman A, and Rehavi M (2001) Characterization of high-affinity [3H]TBZOH binding to the human platelet vesicular monoamine transporter. *Life Sci* **69**:2311–2317.

# CHAPTER 2

## Reduced vesicular storage of catecholamines causes progressive degeneration in the locus ceruleus

This work has been published:
*Taylor TN, *Alter SP, Wang M, Goldstein DS and Miller GW (2014) Reduced vesicular storage of catecholamines causes progressive degeneration in the locus ceruleus. *Neuropharmacology* **76 Pt A**: 97-105.
*denotes equal contribution.

**Abstract**

Parkinson's disease (PD) is the most common neurodegenerative motor disease. Pathologically, PD is characterized by Lewy body deposition and subsequent death of dopamine neurons in the substantia nigra pars compacta. PD also consistently features degeneration of the locus ceruleus, the main source of norepinephrine in the central nervous system. We have previously reported a mouse model of dopaminergic neurodegeneration based on reduced expression of the vesicular monoamine transporter (VMAT2 LO). To determine if reduced vesicular storage can also cause noradrenergic degeneration, we examined indices of damage to the catecholaminergic systems in brain and cardiac tissue of VMAT2 LO mice. At two months of age, neurochemical analyses revealed substantial reductions in striatal dopamine (94%), cortical dopamine (57%) and norepinephrine (54%), as well as cardiac norepinephrine (97%). These losses were accompanied by increased conversion of dopamine and norepinephrine to their deaminated metabolites. VMAT2 LO mice exhibited loss of noradrenergic innervation in the cortex, as determined by norepinephrine transporter immunoreactivity and [$^3$H]-nisoxetine binding. Using unbiased stereological techniques, we observed progressive degeneration in the locus ceruleus that preceded degeneration of the substantia nigra pars compacta. In contrast, the ventral tegmental area, which is spared in human PD, remained unaffected. The coordinate loss of dopamine and norepinephrine neurons in VMAT2-LO mice parallels the pattern of neurodegeneration that occurs in human PD, and demonstrates that insufficient catecholamine storage can cause spontaneous degeneration in susceptible neurons, underscoring cytosolic catecholamine catabolism as a determinant of neuronal susceptibility in PD.

## Introduction

Parkinson's disease (PD) is primarily characterized by motor deficits due to the loss of dopamine (DA) producing cells of the substantia nigra pars compacta (SNpc). However, PD is not restricted to the SNpc, as there is significant neurodegeneration in the locus ceruleus (LC), which is the primary source of brain norepinephrine (NE). The degree and rate of LC loss have been reported to be similar to, if not greater than, that of the SNpc (Braak et al., 2003; Zarow et al., 2003). Noradrenergic degeneration in PD has been implicated in parkinsonian motor deficits, neuropsychiatric symptoms (including depression, dementia, and psychosis), and sleep disturbances (Del Tredici and Braak, 2012; Gesi et al., 2000; Paulus and Jellinger, 1991). Noradrenergic deficits in PD also extend into the periphery; cardiac sympathetic denervation occurs in most PD cases, and can manifest in the pre-motor phases of the disease (Goldstein et al., 2007). Loss of sympathetic noradrenergic nerves in the myocardium may be as profound as the loss of dopaminergic terminals in the striatum (Amino et al., 2005).

Each of these affected neuronal populations is of the catecholaminergic phenotype. The shared vulnerability of catecholamine neurons in PD can be ascribed in part to ongoing cytoplasmic neurotransmitter breakdown. Due to ongoing synthesis, plasmalemmal uptake, and vesicular leak, catecholamines are continuously present in the cytosol. The vesicular monoamine transporter 2 (Slc18a2; VMAT2) transports catecholamines from the cytosol into acidic synaptic vesicles, where they are stored for exocytic release. In noradrenergic neurons, NE is synthesized from DA via dopamine-β-hydroxylase inside the vesicle. Products of cytoplasmic catecholamine breakdown by autoxidation and enzymatic deamination are toxic (Burke et al., 2004; Caudle et al., 2007; Cubells et al.,

1994). This burden is characteristic of catecholamine neurons and may be a critical determinant of their susceptibility to neurotoxicity in PD (Caudle et al., 2008; Sulzer and Surmeier, 2012).

Because VMAT2 is essential for vesicular catecholamine storage, its dysregulation can be deleterious to neuronal health. In mice, genetic ablation of VMAT2 is fatal, and while heterozygote knockout animals develop normally, they are more susceptible than wild-type mice to MPTP- and amphetamine- induced neurotoxicity (Guillot et al., 2008; Takahashi et al., 1997; Wang et al., 1997). We previously reported that VMAT2 LO mice, which have a 95% reduction in VMAT2 expression, exhibit progressive nigrostriatal degeneration, highly dysregulated DA homeostasis, α-synuclein accumulation, L-DOPA-responsive motor deficits, and nonmotor features of PD, including depressive and anxiety-like behaviors (Caudle et al., 2007; Taylor et al., 2009).

In this study, we tested whether VMAT2 LO mice exhibit noradrenergic degeneration. We assayed concentrations of DA, NE, and their metabolites in the cortex, striatum, and heart. Changes in noradrenergic innervation were assessed by immunochemistry for the norepinephrine transporter (NET) and by [$^3$H]-nisoxetine binding. To quantify the extent of neuronal loss, we performed stereological analyses of catecholaminergic cell bodies in the LC and SNpc as well as in the ventral tegmental area (VTA), a dopaminergic nucleus less affected in PD.

## Materials and Methods

**Animals.** Male and female VMAT2 LO mice were generated as previously described (Caudle et al., 2007; Taylor et al., 2009). Briefly, the laboratory of Piers Emson (Mooslehner et al., 2001) generated a VMAT2 hypomorphic mouse on a C57BL/6 background. It was later revealed that the C57BL/6 subpopulation from which these mice were derived contained a spontaneous deletion spanning the α-synuclein gene locus (Specht and Schoepfer, 2001). Through outbreeding to mice of the 129 strain, we reintroduced the deleted locus while maintaining the hypomorphic VMAT2 allele. These mice (VMAT2 LO) have been maintained on a C57/BL6 and 129 mixed background. The genotypes of all mice were confirmed by PCR of genomic DNA extracted from tail snips. This report represents the fourth set of data on VMAT2 LO mice with a normal α-synuclein background (Caudle et al., 2007; Guillot et al., 2008; Taylor et al., 2009). All procedures were conducted in accordance with the National Institutes of Health Guide for Care and Use of Laboratory Animals and approved by the Institutional Animal Care and Use Committee at Emory University.

**HPLC determination of catecholamines and metabolites.** Mice were decapitated and their brains immediately dissected. From the brain, we collected the isocortex and ventral and dorsal striata between Bregma coordinates 2.0 mm and -1.9 mm. Tissues were frozen in liquid nitrogen, and catechol levels were measured by liquid chromatography with electrochemical detection after batch alumina extraction at the Clinical Neurochemistry Laboratory of the Clinical Neurocardiology Section in intramural NINDS (Goldstein et al., 2011; Holmes et al., 1994). Catechols of interest included the catecholamines, the catecholamine precursor L-DOPA, dihydroxyphenylacetic acid

(DOPAC, the main neuronal metabolite of DA), and dihydroxyphenylglycol (DHPG, the main neuronal metabolite of NE). Mice of two months of age were used to determine catechol levels prior to the onset of neurodegeneration.

**[$^3$H]-Nisoxetine binding to quantify norepinephrine transporter expression.** [$^3$H]-Nisoxetine binding in brain homogenates was performed as previously described (Tejani-Butt, 1992), with minor modifications. Briefly, mice were decapitated and their brains rapidly removed and dissected (described above). Cortical tissue was homogenized in 0.32 M sucrose, 10 mM HEPES at 1000 RPM with a Teflon homogenizer and Wheaton glass tube and centrifuged at 48,000xg. The resulting pellet was resuspended, homogenized, and centrifuged again. The final pellet was resuspended in 500 µl assay buffer (50 mM Tris, 300mM NaCl, 5mM KCl, pH 6.8). 200-400 µg (post-hoc determination) of sample was incubated in a 400 µL reaction mixture of 5 nM [$^3$H]-nisoxetine (American Radiolabeled Chemicals, St. Louis, MO) for total binding, and with 10 µM desipramine (Sigma-Aldrich, St. Louis, MO) to determine nonspecific binding. Mice of 12 months of age were used to examine NET expression at the start of LC degeneration.

**Immunohistochemical analysis of tyrosine hydroxylase and norepinephrine transporter.** Tissue staining was completed as previously described (Caudle et al., 2006; Miller et al., 1999; Miller et al., 1997). Briefly, we transcardially perfused phosphate buffered saline and 4% paraformaldehyde into mice. Tissue was removed and fixed in 4% paraformaldehyde for 24 h, followed by cryoprotectection in 30% sucrose for 48 h. The brains were sliced to a thickness of 40 µm on a freezing microtome (Microm, Kalamazoo, MI). For fluorescent immunohistochemistry, sections were incubated with

mouse monoclonal anti-TH (1:1,000; Millipore) and rabbit polyclonal anti-VMAT2 (1:15,000, custom-made). Rabbit antisera was raised against the C-terminal VMAT2 peptide sequence CTQNNVQPYPVGDDEESESD (immunizations and sera collection performed by Covance, Princeton, NJ). Sections were then incubated with fluorophore-linked secondary antibodies against rabbit and mouse IgG, raised in goats (1:800, Life Technologies, Grand Island, NY). For DAB-peroxidase staining, free-floating sections were incubated with either rabbit polyclonal anti-tyrosine hydroxylase (TH) (1:2000; Millipore), or mouse monoclonal anti-NET (1:1,000, MAb Technologies, Stone Mountain, GA) overnight, followed by incubation in a biotinylated goat anti-rabbit secondary antibody (TH) or biotinylated goat anti-mouse (1:200; Jackson Immunoresearch) for 1 h at room temperature. NET detection was optimized with Citra citrate antigen retrieval kit (Biogenex, Fremont, CA). Visualization was performed using 3, 3′-diaminobenzidine (DAB, St. Louis, MO) for 2 min at room temperature. After DAB, all sections were counterstained in hematoxylin, mounted on slides, dehydrated, and coverslipped using Permount (Fisher Scientific, Waltham, MA) with sections viewed using a light microscope (Olympus, San Jose, CA).

**Stereological analysis of cell bodies.** Stereological sampling (West et al., 1991) was performed using the Stereo Investigator software (MicroBrightField, Colchester, VT). Tissue staining was performed as described previously (McCormack et al., 2002; Reveron et al., 2002). Whole brains were removed and processed for frozen sections as described above, and serially sectioned at 50 μm (final mounted thickness of 26 μm) for systematic analysis of randomly placed counting frames (size, 50 × 50 μm) on a counting grid (size of 120 × 160 μm) and sampled using an 22 μm optical dissector with 2 μm

upper and lower guard zones. The boundaries of SNpc, LC, and VTA were outlined under magnification of the 4X objective as per the atlas of Paxinos and Franklin (2001). Cells were counted with a 40X objective (1.3 numerical aperture) using an Eclipse e800 microscope (Nikon, Melville, NY). Guard zones of 2 μm ensured the exclusion of lost profiles on the top and bottom of the section sampled. A dopaminergic or noradrenergic neuron was defined as an in-focus TH-immunoreactive (TH-IR) cell body with a TH-negative nucleus within the counting frame. For the SNpc and VTA, every other section was processed for TH-IR, resulting in 20-25 sections sampled per mouse. For the LC, every section was stained for TH-IR and counterstained with hematoxylin, resulting in 15 sections sampled per mouse. The number of neurons in the SNpc, VTA, and LC was estimated using the optical fractionator method, which is unaffected by changes in the volume of reference of the structure sampled. Between 100 and 250 objects were counted to generate the stereological estimates. Gundersen (m=1) coefficients of error were less than 0.1.

**Statistics.** Statistical analyses were performed using GraphPad Prism 5.0 (La Jolla, CA) Experiments with two factors (HPLC analysis of genotype and brain region, stereological analyses between genotypes) were analyzed by two-way ANOVA, followed by Bonferroni post-hoc tests for pairwise comparisons. One-factor experiments (HPLC of cardiac tissue, radioligand binding) were analyzed with t-tests for independent means. Results were reported as mean ± SEM, and statistical significance set at $\alpha=0.05$. In figures, *$p<0.05$, **$p<0.01$, ***$p<0.001$.

## Results

### Immunohistochemical assessment of VMAT2 loss in SNpc and LC neurons.

In this study, we sought to compare the effects of very low VMAT2 expression on the dopaminergic and noradrenergic systems. We thus evaluated VMAT2 expression in the SNpc and LC of VMAT2 LO mice using immunohistochemistry to confirm comparable reductions of the protein (Figure 2-1). Wildtype animals exhibited a cytosolic distribution of VMAT2 immunoreactivity in TH+ neurons of the SNpc and LC. Consistent with an earlier report (Mooslehner et al., 2001), VMAT2 immunoreactivity in the SNpc of VMAT2 LO brains was essentially absent, save for trace somatic staining. In the LC, TH+ neurons were also nearly devoid of VMAT2 immunoreactivity, indicating very low Slc18a2 gene product in both regions.

### VMAT2 LO mice have markedly reduced tissue catecholamine contents and increased relative deamination of catecholamines.

Cortical and striatal tissues of 2-month old VMAT2 LO animals had reduced levels of both NE and DA (Figure 2-2A, B). ANOVA revealed an effect of genotype on NE ($F(1,18)=110.3$, $p<0.0001$) and DA ($F(1,18)=171.8$, $p<0.0001$). In the cerebral cortex, we observed a 54% decrease in NE (wild-type: 268.8 ± 22.9 pg/mg, VMAT2 LO: 124.8 ± 11.81 pg/mg, $p<0.001$) and a tendency toward decrease in DA (wild-type: 557.5 ± 243.3 pg/mg, VMAT2 LO: 50.0 ± 9.9 pg/mg, $p>0.05$). In the striatum, we observed a 67% decrease in NE (wild-type: 284.2 ± 16.7 pg/mg, VMAT2 LO: 92.6 ± 6.9 pg/mg, $p<0.001$) and 94% reduction in DA (wild-type: 6125.8 ± 349.2 pg/mg, VMAT2 LO: 379.2 ± 70.7 pg/mg, $p<0.001$).

In both the cortex and striatum of 2-month old VMAT2 LO mice, we observed a genotype-dependent increase in tissue DHPG:NE ratios (Figure 2-2C) ($F(2,18)=23.73$, $p<0.0001$). There were significant increases in both tissues (cortex: $p<0.05$, striatum: $p<0.05$). These mice also had genotype-dependent increase in DOPAC:DA (Figure 2-2D) ($F(2,18)=47.4$, $p<0.0001$) in the cortex ($p<0.001$) and striatum ($p<0.01$). L-DOPA levels were unchanged between genotypes ($F(1,18)=0.02$, $p=0.9$; striatum, wild-type: 20.3 ± 10.8, VMAT2 LO: 19.4 ± 4.4; cortex, wild-type: 12.8 ± 0.9, VMAT2 LO: 12.1 ± 1.9).

**VMAT2 LO mice have decreased cortical expression of NET**

We examined NET expression using immunohistochemistry in the somatomotor cortex of 12-month old wild-type and VMAT2 LO mice (Figure 2-3A, B) and observed a reduction in NET immunoreactivity. We quantified the reduction of NET expression in the cortex with [$^3$H]-nisoxetine binding (Figure 2-3C), VMAT2 LO animals had a 20% reduction in [$^3$H]-nisoxetine binding, compared to wild type (40.8 ± 2.2 vs. 49.5 ± 3.2 fmol/mg, $p<0.05$).

**VMAT2 LO mice have age-related catecholaminergic degeneration in the LC and SNpc, but not in the VTA.**

At 12 months of age, VMAT2 LO mice did not differ from age-matched controls in TH expression or evidence of neurodegeneration, as measured by silver deposition, in the SNpc or LC (data not shown). At 18 months of age, the VMAT2 LO group had mildly reduced TH staining in the SNpc. The extent of abnormality progressed with age

(Figure 2-4). Larger reductions in TH staining were observed in the LC than the SNpc at 18, 24, and 30 months of age.

To quantify the extent of neuronal loss in the SNpc and LC in the VMAT2 LO mice, unbiased stereological cell counts were performed on TH- and hematoxylin-stained cells. In the SNpc, two-way ANOVA revealed an effect of genotype ($F(1,35)=44.14$, $p<0.001$) and age ($F(4,35)=120.6$, $p<0.0001$) on the number of TH+ neurons (Figure 2-5A), although there was no interaction ($F(4,35)=4.219$, $p=0.6$). Hematoxylin+ cells followed the same pattern. At all ages, VMAT2 LO brains had fewer TH+ SNpc neurons than did wild-type littermates, though Bonferroni post-hoc tests did not reveal significance between genotypes at any single time point. Within genotypes, wild-type and VMAT2 LO mice underwent significant SNpc degeneration at 24 months of age, with respect to counts at 6 months (wild-type, 6 months: 5999 ± 176, wild-type, 24 months: 4039 ± 252, $p<0.001$; VMAT2 LO, 6 months: 5691 ± 286, 24 months: 3347 ± 331, $p<0.001$). At 30 months, wild-type mice (30 months: 3943 ± 159) had lost 34% of TH+ SNpc neurons, while VMAT2 LO mice (2614 ± 344) lost 54% of TH+ neurons with respect to the corresponding 6 month value for each groups.

Within the LC, neuronal survival was an effect of age ($F(4,37)=44.14$, $p<0.0001$) and genotype ($F(1,37)=120.6$, $p<0.0001$). There was an interaction between these factors ($F(4,37)=4.219$, $p<0.01$). Hematoxylin+ cell loss followed the same pattern as TH+ neuron loss. Bonferroni post-hoc tests revealed that degeneration of TH+ LC neurons was significantly greater in VMAT2 LO mice than in wild-type littermates beginning at 12 months (wild-type: 2695 ± 255, VMAT2 LO: 2001 ± 104, $p<0.05$) proceeding through 30 months (wild-type: 1969 ± 155, VMAT2 LO: 744 ± 76, $p<0.001$). Within genotype,

LC degeneration was first significant in wild-type mice at 18 months of age (wild-type, 6 months: 3079 ± 137, wild-type, 18 months: 2274 ± 107, $p<0.05$) and first significant in VMAT2 LO mice at 12 months of age (VMAT2 LO, 6 months: 2683 ± 182, VMAT2 LO, 12 months: 2001 ± 104). At 30 months, wild-type mice lost 36% ($p<0.001$) of TH+ LC neurons, while VMAT2 LO mice lost 72% ($p<0.001$) of TH+ LC neurons with respect to the corresponding 6 month value for each group.

When the VTA was examined for evidence of neuronal loss, no change was seen in wild-type or VMAT2 LO animals at 6 or 30 months of age (Figure 2-6). At 6 months of age, wild-type and VMAT2 LO animals displayed similar numbers of TH-positive (wild-type: 4684 ± 544, VMAT2 LO: 4590 ± 159; $p>0.05$) and hematoxylin-positive neurons (wild-type: 6594 ± 694, VMAT LO: 6413 ± 236; $p>0.05$). Moreover, at 30 months of age, we observed no difference in the quantity of TH+ neurons in the VTA between wild-type and VMAT2 LO animals (wild-type: 4784 ± 429, VMAT2 LO: 4948 ± 349, $p>0.05$; hematoxylin-positive: wild-type: 7470 ± 813, VMAT2 LO: 7461 ± 567, $p>0.05$).

**Discussion**

Our findings demonstrate that dramatically reduced VMAT2 expression augments the age-related loss of noradrenergic neurons in the locus ceruleus. We observed that genetic VMAT2 deficiency in vivo drives catecholamine depletion in the central nervous system and increases relative cytosolic catecholamine catabolism by MAO. These findings in transgenic mice bear particular relevance to the pathology of PD where vesicular function may be compromised as a consequence of exogenous insult (Corrigan et al., 1998; Hatcher-Martin et al., 2012), genetic polymorphism (Brighina et al., 2013; Glatt et al., 2006; Uhl et al., 2000), or a cytosolic milieu that favors an oxidative state, especially with mitochondrial dysfunction (Schapira, 2011) and aging (Cruz-Muros et al., 2008). Indeed, post-mortem analysis of putamen tissue has revealed that PD patients exhibit neurochemical indices of reduced vesicular uptake of DA and buildup of DOPAL, a toxic MAO metabolite of DA (Goldstein et al., 2013).

In young (2 months) VMAT2 LO mice, we observed baseline deficits in striatal and cortical NE and DA, a direct result of insufficient vesicular catecholamine storage (Figure 2-2). Cytosolic catecholamines are subject to enzymatic deamination and autoxidation. Cytosolic autoxidation of catecholamines and their metabolites generates reactive quinone species and other oxidative metabolites (Sulzer and Zecca, 1999). We previously reported that the striata of VMAT2 LO mice showed elevated indices of cytosolic DA oxidation, in the form of cysteinyl-catechol adducts, as well as relatively increased generation of DOPAC (Caudle et al., 2007). Here, we have additionally reported that the cortices and striata of VMAT2 LO mice have increased conversion of NE to DHPG. These neurochemical aberrations are life-long in VMAT2 LO mice, and

set the stage for the eventual age-related neuronal loss we observed in the LC and SNpc (Figure 2-5).

We observed that the LC of VMAT2 LO mice degenerated earlier (12 months) and to a greater extent than did the SNpc (24 months) (Figure 2-5). Clinically, the LC consistently degenerates in PD patients (Chan-Palay and Asan, 1989; Del Tredici and Braak, 2012; Forno, 1996) with severe decreases (as great as 78%) in neuronal number, possibly contributing to the neuropsychiatric symptoms of PD (Mann, 1983; Zarow et al., 2003). It has been theorized that the trophic signaling from the LC compensates for the debilitating effects of progressive nigrostriatal death and delays the onset of clinical signs until greater DA depletion has occurred (Antelman and Caggiula, 1977). Moreover, it has been demonstrated that noradrenergic neurons of the LC are responsible for dopaminergic signaling within the mouse hippocampus (Smith and Greene, 2012); this may occur elsewhere, especially in a setting of dopaminergic degeneration. The relationship between noradrenergic and dopaminergic degeneration established in this study suggests that NE loss could play a significant role in parkinsonian manifestations ranging from olfactory disturbances observed at 4 months of age in VMAT2 LO mice to depressive-like behaviors seen at 12-15 months (Taylor et al., 2009). Degeneration of the noradrenergic LC and other non-dopaminergic centers have been inferred in post-mortem PD brains. These monoaminergic centers are not directly related to the motor phenotype, yet contribute significantly to disease progression (Braak et al., 2003; Del Tredici and Braak, 2012; Gesi et al., 2000; Halliday et al., 1990; Murai et al., 2001; Rommelfanger and Weinshenker, 2007). Braak and colleagues propose that PD begins in the dorsal motor and olfactory nuclei of the brainstem and progresses topographically through

susceptible regions (Braak et al., 2002; Braak et al., 2003). Motor disturbances do not present clinically until approximately 70-80% of striatal dopaminergic terminals have been lost; however, other non-motor symptoms are evident before the onset of motor disturbances. In the VMAT2 LO mice, it has been observed that the major motor deficits (e.g. shortened stride length) do not appear until 28 months of age, coinciding with the most severe SNpc cell loss (Figure 2-5A) (Taylor et al., 2011). The preceding phenotypes seen in the VMAT2 LO mice may be attributed to extra-dopaminergic changes (Taylor et al., 2009).

An intriguing finding in this study is that while the LC and SNpc of VMAT2 LO mice degenerated, the dopaminergic VTA remained unaffected (Figure 2-6). The VTA is less affected or spared in human PD and is resistant to degeneration in toxicant models (Dauer and Przedborski, 2003; German et al., 1992). Physiological differences between the VTA and SNpc may explain their disparate susceptibilities to neurotoxicity. The VTA is phenotypically distinct from the neighboring SNpc in its expression of calbindin, a calcium buffering protein, and unlike the SNpc it is not reliant on calcium influx for autonomous pacemaking (Surmeier et al., 2005). It has been demonstrated that cytosolic calcium increases conversion of L-DOPA to DA by amino acid decarboxylase, which occurs to a greater extent in SNpc neurons than in the VTA; this mechanism was shown to be responsible for the selective susceptibility of the SNpc over the VTA to L-DOPA-induced neurotoxicity in mice (Mosharov et al., 2009; Surmeier, 2009).

While the focus of this work examined the neurotoxic effects of cytoplasmic catecholamines, we should not overlook the role of α-synuclein in this pathology. VMAT2 LO mice do not undergo spontaneous neurodegeneration in the absence of

endogenous α-synuclein (Colebrooke et al., 2006). Similarly, VMAT2 deficiency potentiates the toxic effects of lentiviral α-synuclein overexpression in mice (Ulusoy et al., 2012). Lastly, knockout of α–synuclein dramatically abrogates the effects of L-DOPA- and calcium-induced neurotoxicity in midbrain DA neurons (Mosharov et al., 2009). This interplay is supported by in vitro experiments which have demonstrated that products of cytoplasmic dopamine breakdown oligomerize α-synuclein (Burke et al., 2008) and stabilize subsequent protofibril formation (Conway et al., 2001); it is hypothesized that this mechanism could drive Lewy body pathology in vivo (Sulzer, 2001). Collectively, these findings indicate that cytoplasmic catecholamine catabolism and α-synuclein may synergistically participate in PD pathogenesis.

Our findings in VMAT2 LO mice demonstrate that insufficient catecholamine storage is capable of driving noradrenergic neurodegeneration in an in vivo setting. Despite the deleterious effects of reduced VMAT2 expression on the SNpc and LC, the VTA remained unaffected, likely due to physiological differences that make this region resilient in animal models and human PD. The combination of LC and SNpc degeneration and the absence of VTA degeneration is strikingly consistent with human PD and underscores the importance of proper catecholamine sequestration to neuronal health. VMAT2 activity, with its role in catecholamine homeostasis, may be a critical determinant in noradrenergic and dopaminergic susceptibility to neurotoxicity.

Acknowledgements: This work was supported by funding from F31 ES017247 (Taylor), T32 ES012870, T32 GM008602 (Alter), and P01 ES01673 (Miller). The authors are grateful for the technical assistance provided by Patricia Sullivan in acquisition of HPLC data. We would like to thank Dr. Alison Bernstein for generating and characterizing the VMAT2 antibody.

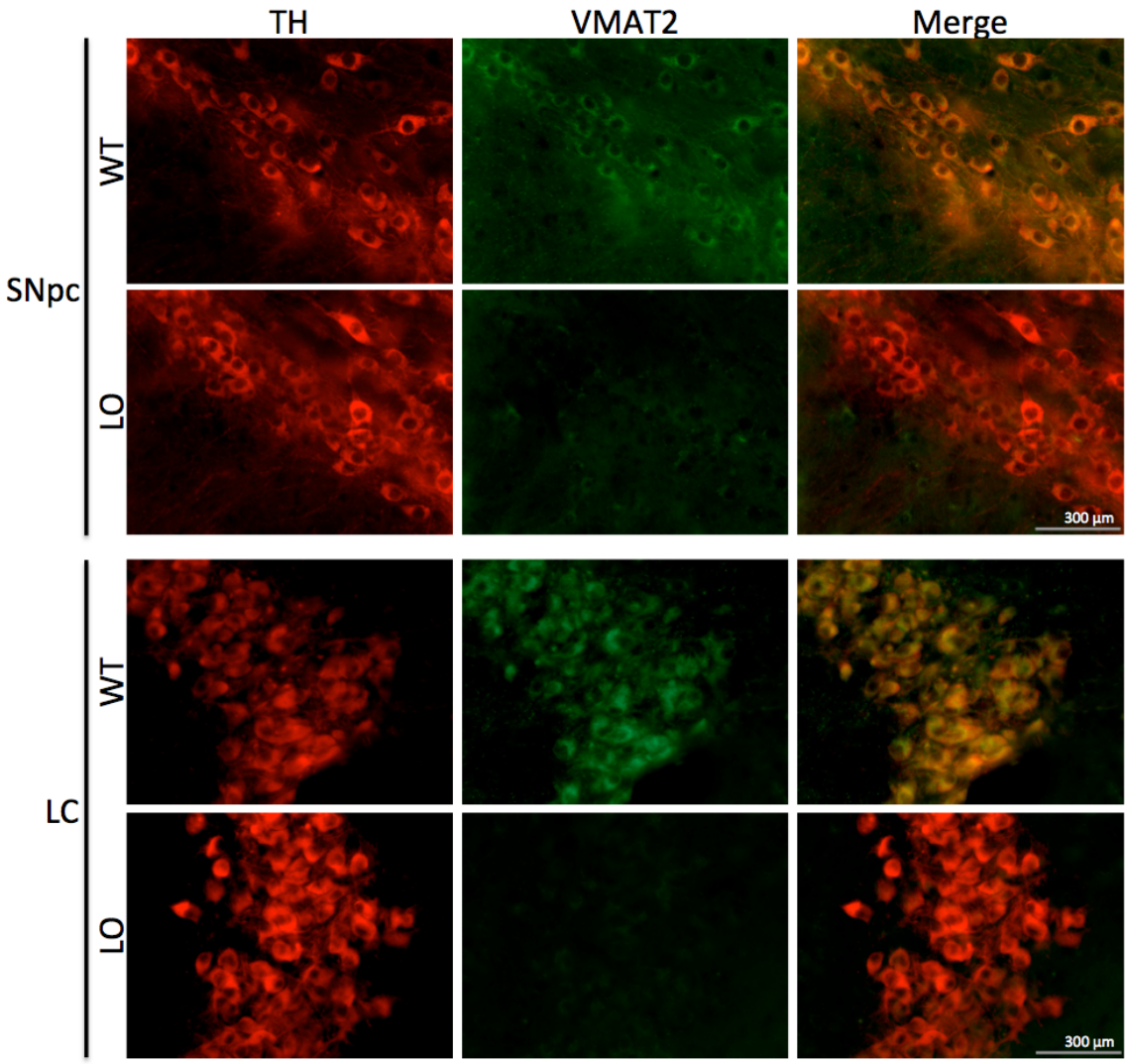
TH
VMAT2
Merge
SNpc
WT
LO
300 µm
LC
WT
LO
300 µm

**Figure 2-1. Immunohistochemical analysis of VMAT2 expression in the substantia nigra and locus ceruleus.**

Widefield immunofluorescent images of TH and VMAT2 expression in the SNpc and LC. Top panels, WT mice exhibited normal TH (red) and VMAT2 (green) immunoreactivity in the SNpc, while VMAT2 LO mice had normal TH immunoreactivity, but trace somatic VMAT2 immunoreactivity. Lower panels, WT mice had marked TH and VMAT2 immunoreactivity in the LC, while VMAT2 LO mice exhibited normal TH immunoreactivity and trace VMAT2 immunoreactivity, as in the SNpc. Scale bars represent 300 μm.

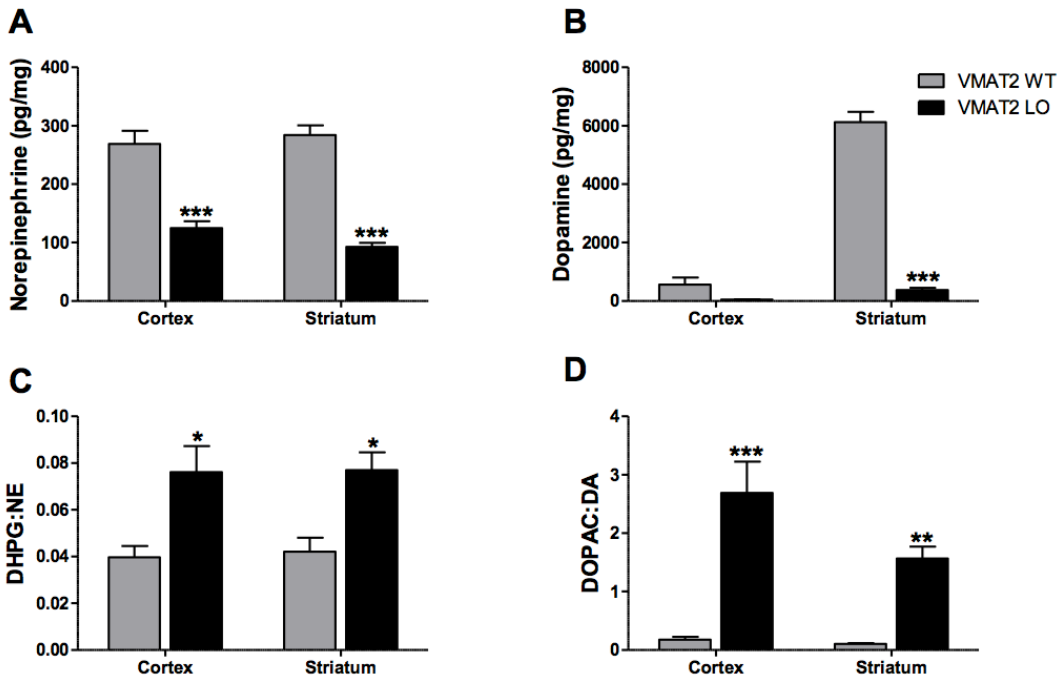
A
Norepinephrine (pg/mg)
400
300
200
100
0
***
***
Cortex
Striatum
B
Dopamine (pg/mg)
8000
6000
4000
2000
0
***
VMAT2 WT
VMAT2 LO
Cortex
Striatum
C
DHPG:NE
0.10
0.08
0.06
0.04
0.02
0.00
*
*
Cortex
Striatum
D
DOPAC:DA
4
3
2
1
0
***
**
Cortex
Striatum

**Figure 2-2. VMAT2 LO mice have reduced brain catecholamines and increased catecholamine turnover at 2 months of age.**

A and B: NE and DA content varied with respect to genotype (n=4). A, Brain NE was reduced in the cortex and striatum of VMAT2 LO mice. B, DA was reduced in the striatum of VMAT2 LO animals; DA content in the cortex trended toward reduction. C and D: In all brain regions surveyed, VMAT2 LO mice exhibited increased relative conversion of NE (C) and DA (D) to their metabolites DHPG and DOPAC, respectively. Results represent the mean ± SEM for 4 animals per genotype at each age. *$p<0.05$, **$p<0.01$, ***$p<0.001$.

A
B
C
$^3$H- nisoxetine bound
(fmol / mg tissue)
60
50
40
30
20
10
0
*
VMAT2 WT
VMAT2 LO

**Figure 2-3. VMAT2 LO mice have reduced expression of the norepinephrine transporter.**

A and B: Immunohistochemical labeling in the somatomotor cortex. At 12 months of age, VMAT2 LO mice showed a reduction in NET immunoreactivity throughout the cortex, compared to wild-type (representative images of somatomotor area shown at 20x magnification). C: [$^3$H]-nisoxetine-binding was performed to quantify changes in NET abundance. There was a reduction (20%) in nisoxetine binding sites in 12-month VMAT2 LO cortices (n=6). Results represent the mean ± SEM for 6 animals per genotype at each age. *$p<0.05$.

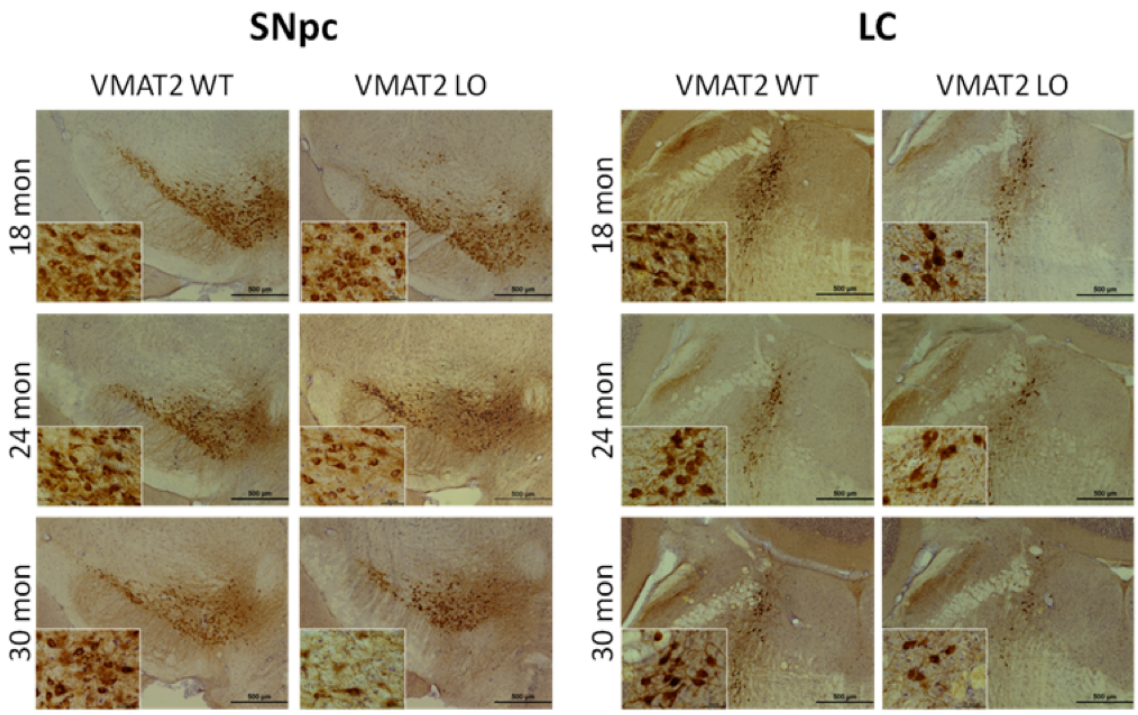
SNpc
LC
VMAT2 WT
VMAT2 LO
VMAT2 WT
VMAT2 LO
18 mon
24 mon
30 mon
18 mon
24 mon
30 mon

**Figure 2-4. VMAT2 LO animals undergo progressive catecholaminergic cell loss.**

Immunohistochemical analysis of tyrosine hydroxylase in locus ceruleus of aged VMAT2 LO mice. TH immunoreactivity was substantially reduced in VMAT2 LO mice at 18, 24, and 30 months of age, preceding loss observed in the substantia nigra. Analysis was performed on 5 animals per genotype at each age. Representative sections are shown. Scale bars, 500 μm.

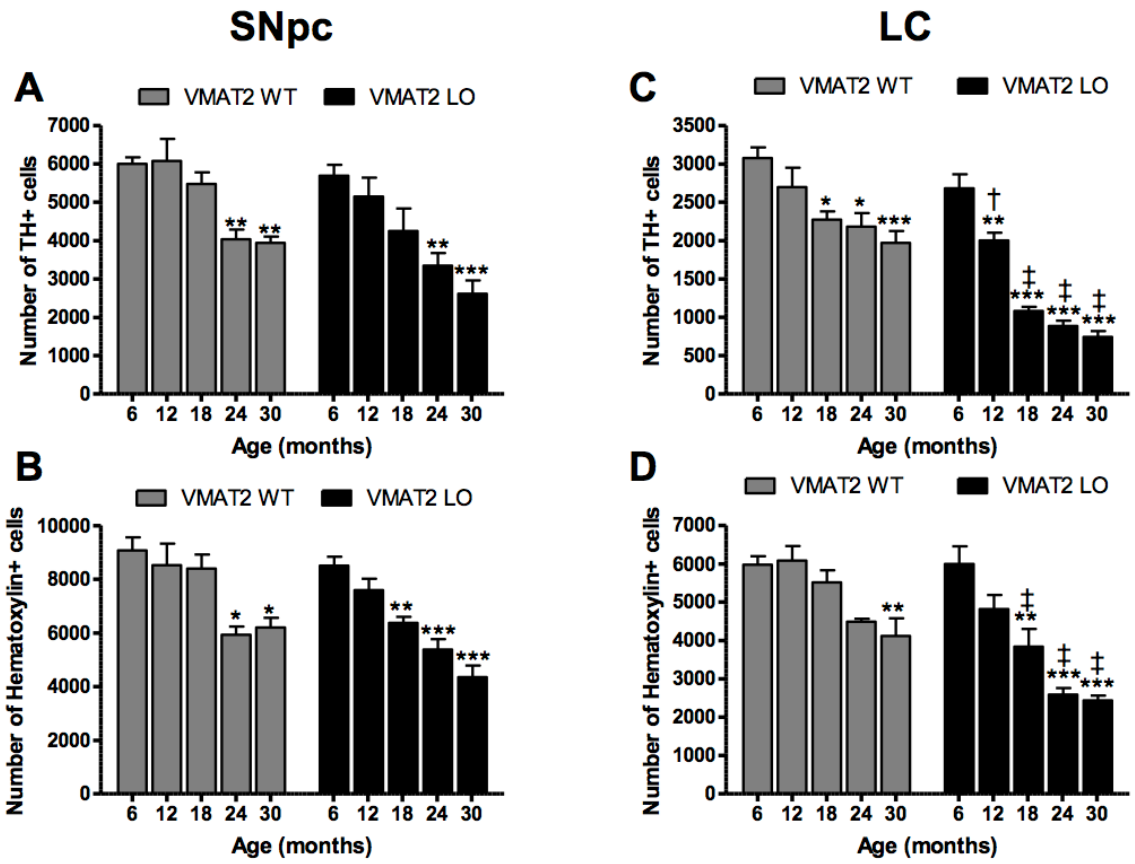
SNpc
LC
A
B
C
D
VMAT2 WT
VMAT2 LO
Number of TH+ cells
Number of Hematoxylin+ cells
Age (months)
6 12 18 24 30 6 12 18 24 30

**Figure 2-5. Quantitative analysis of catecholaminergic cell loss reveals degeneration of LC precedes that of SNpc.** TH and hematoxylin cell counts in the SNpc and LC of 6, 12 18, 24, and 30 month wild-type and VMAT2 LO mice. A: Significant reductions in TH cell counts in the SNpc were observed beginning at 24 months in wild-type and VMAT2 LO mice, with VMAT2 LO mice having fewer TH cells overall. B: Furthermore, a similar age-dependent reduction in hematoxylin cells in the SNpc was seen in wild-type and VMAT2 LO mice. C: Wildtype and VMAT2 LO mice underwent progressive loss of TH cells in the LC, with VMAT2 LO mice having accelerated loss compared to wild-type, beginning at 12 months of age. D: A significant reduction was also seen in hematoxylin cells in the LC at 18, 24, and 30 months of age in VMAT2 LO mice compared to wild-type in the LC. Results represent the mean ±SEM for 5 animals per genotype at each age. *$p<0.05$, ** $p<0.01$; ***$p<0.001$ (with respect to 6 month mice within genotype) †$<0.05$, ‡$<0.001$ (between genotypes).

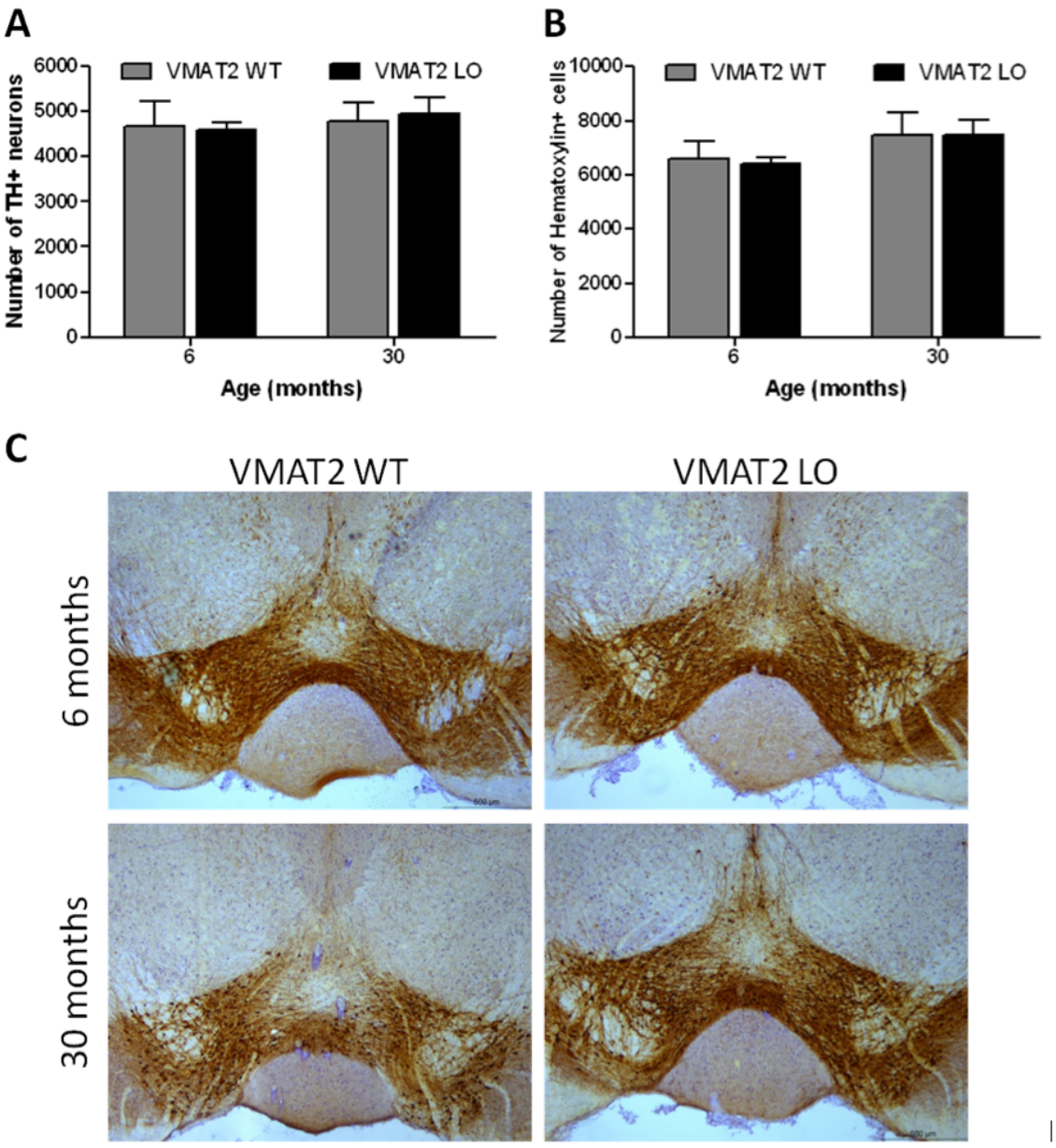
A
Number of TH+ neurons
6000
5000
4000
3000
2000
1000
0
VMAT2 WT
VMAT2 LO
6
30
Age (months)
B
Number of Hematoxylin+ cells
10000
8000
6000
4000
2000
0
VMAT2 WT
VMAT2 LO
6
30
Age (months)
C
VMAT2 WT
VMAT2 LO
6 months
30 months

**Figure 2-6. VMAT2 LO mice do not display neuronal loss in the VTA.** TH and hematoxylin cell counts in the VTA of 6 and 30 month wild-type and VMAT2 LO animals. A: No differences in TH-positive neurons were seen in 6 or 30 month VMAT2 LO mice when compared with age-matched WT controls ($p>0.05$). B: Similarly, no changes were seen in the number of hematoxylin stained cells in the VTA at either age. Results represent the mean ± SEM for 5 animals per genotype at each age. C: Immunohistochemical analysis of tyrosine hydroxylase in the VTA demonstrates that TH immunoreactivity is not significantly changed in VMAT2 WT or LO animals from 6 to 30 months of age. Representative sections are shown. Scale bars, 500 μm.

## References


Amino T, Orimo S, Itoh Y, Takahashi A, Uchihara T and Mizusawa H (2005) Profound cardiac sympathetic denervation occurs in Parkinson disease. *Brain pathology (Zurich, Switzerland)* **15**(1): 29-34.

Antelman SM and Caggiula AR (1977) Norepinephrine-dopamine interactions and behavior. *Science* **195**(4279): 646-653.

Braak H, Del Tredici K, Bratzke H, Hamm-Clement J, Sandmann-Keil D and Rub U (2002) Staging of the intracerebral inclusion body pathology associated with idiopathic Parkinson's disease (preclinical and clinical stages). *Journal of neurology* **249 Suppl 3**: III/1-5.

Braak H, Del Tredici K, Rub U, de Vos RA, Jansen Steur EN and Braak E (2003) Staging of brain pathology related to sporadic Parkinson's disease. *Neurobiology of aging* **24**(2): 197-211.

Brighina L, Riva C, Bertola F, Saracchi E, Fermi S, Goldwurm S and Ferrarese C (2013) Analysis of vesicular monoamine transporter 2 polymorphisms in Parkinson's disease. *Neurobiology of aging* **34**(6): 1712 e1719-1713.

Burke WJ, Kumar VB, Pandey N, Panneton WM, Gan Q, Franko MW, O'Dell M, Li SW, Pan Y, Chung HD and Galvin JE (2008) Aggregation of alpha-synuclein by DOPAL, the monoamine oxidase metabolite of dopamine. *Acta Neuropathologica* **115**(2): 193-203.

Burke WJ, Li SW, Chung HD, Ruggiero DA, Kristal BS, Johnson EM, Lampe P, Kumar VB, Franko M, Williams EA and Zahm DS (2004) Neurotoxicity of MAO

Metabolites of Catecholamine Neurotransmitters: Role in Neurodegenerative Diseases. *NeuroToxicology* **25**(1-2): 101-115.

Caudle WM, Colebrooke RE, Emson PC and Miller GW (2008) Altered vesicular dopamine storage in Parkinson's disease: a premature demise. *Trends in Neurosciences* **31**(6): 303-308.

Caudle WM, Richardson JR, Delea KC, Guillot TS, Wang M, Pennell KD and Miller GW (2006) Polychlorinated biphenyl-induced reduction of dopamine transporter expression as a precursor to Parkinson's disease-associated dopamine toxicity. *Toxicol Sci* **92**(2): 490-499.

Caudle WM, Richardson JR, Wang MZ, Taylor TN, Guillot TS, McCormack AL, Colebrooke RE, Di Monte DA, Emson PC and Miller GW (2007) Reduced vesicular storage of dopamine causes progressive nigrostriatal neurodegeneration. *J Neurosci* **27**(30): 8138-8148.

Chan-Palay V and Asan E (1989) Quantitation of catecholamine neurons in the locus coeruleus in human brains of normal young and older adults and in depression. *J Comp Neurol* **287**(3): 357-372.

Colebrooke RE, Humby T, Lynch PJ, McGowan DP, Xia J and Emson PC (2006) Age-related decline in striatal dopamine content and motor performance occurs in the absence of nigral cell loss in a genetic mouse model of Parkinson's disease. *The European Journal of Neuroscience* **24**(9): 2622-2630.

Conway KA, Rochet J-C, Bieganski RM and Lansbury Jr PT (2001) Kinetic Stabilization of the Alpha-Synuclein Protofibril by a Dopamine-Alpha-Synuclein Adduct. *Science* **294**(5545): 1346.

Corrigan FM, Murray L, Wyatt CL and Shore RF (1998) Diorthosubstituted polychlorinated biphenyls in caudate nucleus in Parkinson's disease. *Experimental neurology* **150**(2): 339-342.

Cruz-Muros I, Afonso-Oramas D, Abreu P, Rodríguez M, González MC and González-Hernández T (2008) Deglycosylation and subcellular redistribution of VMAT2 in the mesostriatal system during normal aging. *Neurobiology of Aging* **29**(11): 1702-1711.

Cubells J, Rayport S, Rajendran G and Sulzer D (1994) Methamphetamine neurotoxicity involves vacuolation of endocytic organelles and dopamine-dependent intracellular oxidative stress. *The Journal of Neuroscience* **14**(4): 2260-2271.

Dauer W and Przedborski S (2003) Parkinson's disease: mechanisms and models. *Neuron* **39**(6): 889-909.

Del Tredici K and Braak H (2012) Dysfunction of the locus coeruleus–norepinephrine system and related circuitry in Parkinson's disease-related dementia. *Journal of Neurology, Neurosurgery & Psychiatry*.

Forno LS (1996) Neuropathology of Parkinson's disease. *J Neuropathol Exp Neurol* **55**(3): 259-272.

German DC, Manaye KF, Sonsalla PK and Brooks BA (1992) Midbrain Dopaminergic Cell Loss in Parkinson's Disease and MPTP-Induced Parkinsonism: Sparing of Calbindin-D25k—Containing Cells. *Annals of the New York Academy of Sciences* **648**(1): 42-62.

Gesi M, Soldani P, Giorgi FS, Santinami A, Bonaccorsi I and Fornai F (2000) The role of the locus coeruleus in the development of Parkinson's disease. *Neuroscience and Biobehavioral Reviews* **24**(6): 655-668.

Glatt CE, Wahner AD, White DJ, Ruiz-Linares A and Ritz B (2006) Gain-of-function haplotypes in the vesicular monoamine transporter promoter are protective for Parkinson disease in women. *Human Molecular Genetics* **15**(2): 299-305.

Goldstein DS, Sharabi Y, Karp BI, Bentho O, Saleem A, Pacak K and Eisenhofer G (2007) Cardiac sympathetic denervation preceding motor signs in Parkinson disease. *Clinical Autonomic Research : official journal of the Clinical Autonomic Research Society* **17**(2): 118-121.

Goldstein DS, Sullivan P, Holmes C, Kopin IJ, Basile MJ and Mash DC (2011) Catechols in post-mortem brain of patients with Parkinson disease. *European Journal of Neurology* **18**(5): 703-710.

Goldstein DS, Sullivan P, Holmes C, Miller GW, Alter S, Strong R, Mash DC, Kopin IJ and Sharabi Y (2013) Determinants of Buildup of the Toxic Dopamine Metabolite DOPAL in Parkinson Disease. *J Neurochem*.

Guillot TS, Shepherd KR, Richardson JR, Wang MZ, Li Y, Emson PC and Miller GW (2008) Reduced vesicular storage of dopamine exacerbates methamphetamine-induced neurodegeneration and astrogliosis. *Journal of Neurochemistry* **106**(5): 2205-2217.

Halliday GM, Blumbergs PC, Cotton RG, Blessing WW and Geffen LB (1990) Loss of brainstem serotonin- and substance P-containing neurons in Parkinson's disease. *Brain Res* **510**(1): 104-107.

Hatcher-Martin JM, Gearing M, Steenland K, Levey AI, Miller GW and Pennell KD (2012) Association between polychlorinated biphenyls and Parkinson's disease neuropathology. *NeuroToxicology* **33**(5): 1298-1304.

Holmes C, Eisenhofer G and Goldstein DS (1994) Improved assay for plasma dihydroxyphenylacetic acid and other catechols using high-performance liquid chromatography with electrochemical detection. *Journal of Chromatography B: Biomedical Sciences and Applications* **653**(2): 131-138.

Mann DM (1983) The locus coeruleus and its possible role in ageing and degenerative disease of the human central nervous system. *Mech Ageing Dev* **23**(1): 73-94.

Miller GW, Erickson JD, Perez JT, Penland SN, Mash DC, Rye DB and Levey AI (1999) Immunochemical analysis of vesicular monoamine transporter (VMAT2) protein in Parkinson's disease. *Experimental Neurology* **156**(1): 138-148.

Miller GW, Staley JK, Heilman CJ, Perez JT, Mash DC, Rye DB and Levey AI (1997) Immunochemical analysis of dopamine transporter protein in Parkinson's disease. *Annals of Neurology* **41**(4): 530-539.

Mooslehner KA, Chan PM, Xu W, Liu L, Smadja C, Humby T, Allen ND, Wilkinson LS and Emson PC (2001) Mice with Very Low Expression of the Vesicular Monoamine Transporter 2 Gene Survive into Adulthood: Potential Mouse Model for Parkinsonism. *Molecular and Cellular Biology* **21**(16): 5321-5331.

Mosharov EV, Larsen KE, Kanter E, Phillips KA, Wilson K, Schmitz Y, Krantz DE, Kobayashi K, Edwards RH and Sulzer D (2009) Interplay between Cytosolic Dopamine, Calcium, and α-Synuclein Causes Selective Death of Substantia Nigra Neurons. *Neuron* **62**(2): 218-229.

Murai T, Muller U, Werheid K, Sorger D, Reuter M, Becker T, von Cramon DY and Barthel H (2001) In vivo evidence for differential association of striatal dopamine and midbrain serotonin systems with neuropsychiatric symptoms in Parkinson's disease. *The Journal of Neuropsychiatry and Clinical Neurosciences* **13**(2): 222-228.

Paulus W and Jellinger K (1991) The Neuropathologic Basis of Different Clinical Subgroups of Parkinsons-Disease. *J Neuropathol Exp Neurol* **50**(6): 743-755.

Rommelfanger KS and Weinshenker D (2007) Norepinephrine: The redheaded stepchild of Parkinson's disease. *Biochem Pharmacol* **74**(2): 177-190.

Schapira AH (2011) Mitochondrial pathology in Parkinson's disease. *The Mount Sinai Journal of Medicine, New York* **78**(6): 872-881.

Smith CC and Greene RW (2012) CNS Dopamine Transmission Mediated by Noradrenergic Innervation. *The Journal of Neuroscience* **32**(18): 6072-6080.

Specht CG and Schoepfer R (2001) Deletion of the alpha-synuclein locus in a subpopulation of C57BL/6J inbred mice. *BMC Neurosci* **2**: 11.

Sulzer D (2001) [alpha]-synuclein and cytosolic dopamine: Stabilizing a bad situation. *Nat Med* **7**(12): 1280-1282.

Sulzer D and Surmeier DJ (2013) Neuronal vulnerability, pathogenesis, and Parkinson's disease. Mov Disord 28(1): 41-50.

Sulzer D and Zecca L (1999) Intraneuronal dopamine-quinone synthesis: A review. *Neurotoxicity Research* **1**(3): 181-195.

Surmeier DJ (2009) A Lethal Convergence of Dopamine and Calcium. *Neuron* **62**(2): 163-164.

Surmeier DJ, Mercer JN and Chan CS (2005) Autonomous pacemakers in the basal ganglia: who needs excitatory synapses anyway? *Current Opinion in Neurobiology* **15**(3): 312-318.

Takahashi N, Miner LL, Sora I, Ujike H, Revay RS, Kostic V, Jackson-Lewis V, Przedborski S and Uhl GR (1997) VMAT2 knockout mice: Heterozygotes display reduced amphetamine-conditioned reward, enhanced amphetamine locomotion, and enhanced MPTP toxicity. *Proceedings of the National Academy of Sciences* **94**(18): 9938-9943.

Taylor TN, Caudle WM and Miller GW (2011) VMAT2-Deficient Mice Display Nigral and Extranigral Pathology and Motor and Nonmotor Symptoms of Parkinson's Disease. *Parkinson's disease* **2011**: 124165.

Taylor TN, Caudle WM, Shepherd KR, Noorian A, Jackson CR, Iuvone PM, Weinshenker D, Greene JG and Miller GW (2009) Nonmotor Symptoms of Parkinson's Disease Revealed in an Animal Model with Reduced Monoamine Storage Capacity. *The Journal of Neuroscience* **29**(25): 8103-8113.

Tejani-Butt SM (1992) [3H]nisoxetine: a radioligand for quantitation of norepinephrine uptake sites by autoradiography or by homogenate binding. *Journal of Pharmacology and Experimental Therapeutics* **260**(1): 427-436.

Uhl GR, Li S, Takahashi N, Itokawa K, Lin Z, Hazama M and Sora I (2000) The VMAT2 gene in mice and humans: amphetamine responses, locomotion, cardiac arrhythmias, aging, and vulnerability to dopaminergic toxins. *FASEB journal : official publication of the Federation of American Societies for Experimental Biology* **14**(15): 2459-2465.

Ulusoy A, Björklund T, Buck K and Kirik D (2012) Dysregulated dopamine storage increases the vulnerability to α-synuclein in nigral neurons. *Neurobiology of Disease* **47**(3): 367-377.

Wang YM, Gainetdinov RR, Fumagalli F, Xu F, Jones SR, Bock CB, Miller GW, Wightman RM and Caron MG (1997) Knockout of the vesicular monoamine transporter 2 gene results in neonatal death and supersensitivity to cocaine and amphetamine. *Neuron* **19**(6): 1285-1296.

West MJ, Slomianka L and Gundersen HJ (1991) Unbiased stereological estimation of the total number of neurons in thesubdivisions of the rat hippocampus using the optical fractionator. *The Anatomical record* **231**(4): 482-497.

Zarow C, Lyness SA, Mortimer JA and Chui HC (2003) Neuronal loss is greater in the locus coeruleus than nucleus basalis and substantia nigra in Alzheimer and Parkinson diseases. *Arch Neurol* **60**(3): 337-341.

# CHAPTER 3

## Reduced vesicular monoamine function drives noradrenergic depletion in the hearts of mice and men

## Introduction

Not only is VMAT2 essential for the neuronal function and viability of monoaminergic neurons within the brain, but it is critical to the function of the peripheral nervous system as well. VMAT2 stores norepinephrine in postganglionic neurons of the sympathetic nervous system and thus, VMAT2 plays a critical role in mediating the homeostatic and "fight-or-flight", feeding, and mating functions of the autonomic nervous system. The noradrenergic sympathetic nervous system mediates numerous autonomic functions throughout the body, including increasing the strength and rate of cardiac contraction, vasodilation of blood vessels in skeletal muscles and skin, pupillary dilation, and increasing adrenal medullary output; at the same time, noradrenergic signaling achieves inhibition of activity of tissues associated with the "rest-and-digest" functions of the parasympathetic nervous system.

Increasing cardiac output to the brain is important not only in responding to "fight-or-flight" stimuli, but also in mediating the pressor effects of the baroreceptor reflex when a patient moves from sitting or lying to standing. Insufficient orthostatic response to this change is described as orthostatic hypotension, and is clinically diagnosable if a person's systolic blood pressure falls in pressure least 10 mmHg when changing orientation from supine to standing. A salient effect of this reduction in blood pressure is that patients experience lightheadedness when standing from a prone or seated position, and may become dizzy, lose consciousness, and fall.

The myriad nonmotor symptoms experienced by patients of Parkinson's disease include irregularities of the autonomic nervous system (dysautonomias), the most prevalent of which is orthostatic hypotension (Jankovic, 2008; Langston, 2006). The

prevalence of orthostatic hypotension in Parkinson's disease is estimated to be 30% (Fereshtehnejad and Lökk, 2014). The high incidence of orthostatic hypotension in Parkinson's disease was once ascribed to a hypotensive side effect of levodopa therapy (Dhasmana and Spilker, 1973), while a distinct pathology remained obscure. Following the advent of imaging techniques to assess the presence and integrity sympathetic terminals of the peripheral nervous system in humans (Dae, 1994), researchers achieved the means by which to investigate the presence, integrity, and function of noradrenergic innervation in the hearts of patients with PD and orthostatic hypotension. Using radionuclide ligands and substrates for the norepinephrine transporter and VMAT, clinical researchers observed pathology suggesting sympathetic denervation of cardiac tissue in patients with PD and orthostatic hypotension (PD+OH) (Goldstein et al., 1997; Orimo et al.).

In 1997, Goldstein and colleagues presented the first evidence of sympathetic denervation in patients with PD+OH, by administering the catecholamine analog [$^{18}$F]-6-dopamine, and observing reduced uptake in the myocardial walls of the heart. This finding would be confirmed by others, including Orimo and colleagues, who used [$^{123}$I]-MIBG, another radionuclide catecholamine analog (Orimo et al., 1999). Virtually all PD patients who exhibit orthostatic hypotension show evidence of sympathetic denervation of the heart (Jain and Goldstein, 2012), and this mechanism is now acknowledged to be the primary cause of comorbid OH in PD. Moreover, noradrenergic denervation of the hearts of PD+OH patients parallels and can even precede dopaminergic degeneration of brain's nigrostriatal tract (Goldstein et al., 2012; Wong et al., 2012).

The pathogenesis of cardiac sympathetic denervation in Parkinson's disease is no more well understood than the cause of catecholaminergic degeneration within the brain. Growing evidence supports a role for reduced vesicular function causing catecholaminergic toxicity in both systems. By coupling neuroimaging with neurochemical metabolic analysis, Goldstein and colleagues recently observed that the sympathetic nerves in patients with PD+OH have reduced capacity to uptake the analog 6-fluorodopamine (6-FDA), and exhibit relatively increased neuronal conversion to 6-fluoroDOPAC. Together, these data indicate that the sympathetic cardiac nerves of PD+OH patients have reduced vesicular storage capability (Goldstein et al., 2011a).

Because reduced vesicular function appears to correlate with cardiac sympathetic denervation and parallels Parkinsonian pathology observed in patients, the VMAT2 LO mouse model of Parkinson's disease presents an excellent platform by which to test the hypothesis that reduced catecholamine storage can cause catecholaminergic dysfunction in the heart, as it does in the brain (Taylor et al., 2014). Moreover, by virtue of their genetic phenotype, VMAT2 LO mice can provide a neurochemical index by which to judge the vesicular function in clinical samples, as we have previously demonstrated from the striatal tissue of VMAT2 LO mice and post mortem PD cases (Goldstein et al., 2013). In the current work, I present data from the myocardial tissue of VMAT2 LO mice that was used in our group's independent comparison to samples from post mortem PD cases (Goldstein et al., 2014). To these ends, we assessed evidence of noradrenergic depletion in VMAT2 LO mice by assessing the abundance of norepinephrine transporter expression in cardiac tissue, observed changes to cardiac norepinephrine content and

metabolism, and assessed the ability of cardiac tissue to uptake and metabolize the catecholamine analog, 6-FDA.

## Materials and Methods

**HPLC determination of cardiac catecholamines.** HPLC determination of catecholamines and metabolites was performed as previously described (Taylor, 2014).. Mice were decapitated and their brains and hearts immediately dissected. From the brain, we collected the isocortex and ventral and dorsal striata between Bregma coordinates 2.0 mm and -1.9 mm. Tissues were frozen in liquid nitrogen, and catechol levels were measured by liquid chromatography with electrochemical detection after batch alumina extraction at the Clinical Neurochemistry Laboratory of the Clinical Neurocardiology Section in intramural NINDS (Goldstein et al., 2011b; Holmes et al., 1994). Catechols of interest included DA, NE, the catecholamine precursor L-DOPA, dihydroxyphenylacetic acid (DOPAC, the main neuronal metabolite of DA), and dihydroxyphenylglycol (DHPG, the main neuronal metabolite of NE). Mice of two months of age were used to determine catechol levels prior to the onset of neurodegeneration.

**[$^3$H]-Nisoxetine binding to quantify norepinephrine transporter expression.** [$^3$H]-Nisoxetine binding was performed as previously described (Tejani-Butt, 1992), with minor modifications. Briefly, mice were decapitated and their hearts rapidly removed and dissected (described above). Cardiac tissue was minced with a steel razor blade and homogenized in 0.32 M sucrose, 10 mM HEPES at 1000 RPM with a Teflon homogenizer and Wheaton glass tube and centrifuged at 48,000xg. The resulting pellet was resuspended, homogenized, and centrifuged again. The final pellet was resuspended in 500 µl assay buffer (50 mM Tris, 300mM NaCl, 5mM KCl, pH 6.8). 200-400 µg (post-hoc determination) of sample was incubated in a 400 µL reaction mixture of 5 nM [$^3$H]-nisoxetine (American Radiolabeled Chemicals, St. Louis, MO) for total binding, and

with 10 μM desipramine (Sigma-Aldrich, St. Louis, MO) to determine nonspecific binding. Hearts were processed similarly, with the addition of first homogenizing cardiac tissue in ice cold 0.1M phosphate-buffered with a Tissue-Tearor tissue homogenizer (Bio Spec Products, Bartlesville, OK). Mice of 12 months of age were used to examine NET expression at the start of LC degeneration.

**Measurement of 6-fluorinated cardiac dopamine uptake.** Mice were placed under isoflurane anesthesia (5% for induction, 3% for maintenance), and intravenously administered 100 ng of 6-fluorodomine (1 μg/ml in NaCl; stock produced in the Clinical Neurochemistry Laboratory of NINDS, NIH, Bethesda, MD). Mice were placed under a heat lamp to achieve vasodilation. Following a time course of 5 min, mice were euthanized by pentobarbital and sympathetically innervated tissues were rapidly dissected. The heart, striata, and liver and from each animal were rapidly dissected, frozen on dry ice, and shipped to the Clinical Neurocardiology Lab as described above.

Statistical analyses. Two-tailed t-tests were used to compare results between genotypes; analyses were performed on GraphPad Prism 5.0.

## Results

### Reduced VMAT2 expression disrupts norepinephrine synthesis and storage.

We assayed cardiac tissue for neurochemical aberrations in 2-month VMAT2 LO hearts (Figure 3-1). At this time point, we observed a 97% reduction in cardiac NE (Figure 3-1A, wild-type: 469.1 ± 24.5 pg/mg, VMAT2 LO: 13.73 ± 13.6 pg/mg, $p<0.0001$). VMAT2 LO mice also showed reductions in cardiac DA (wild-type: 11.15 ± 1.1, VMAT2 LO: 4.03 ± 1.1, $p<0.01$), though to a lesser extent (64%; Figure 3-1B). As conversion of DA to NE requires the intra-vesicular protein dopamine-β-hydroxylase VMAT2 LO mice accordingly had a 14-fold higher DA:NE ratio than wild-type mice, indicating reduced conversion of DA to NE, a process which is dependent on vesicular transport (WT: 0.024 ± 0.003 pg/mg; LO: 0.338 ± 0.042 pg/mg; $p=0.0003$). VMAT2 LO mice had an 11-fold increase in DHPG:NE, indicative of increased intraneuronal catabolism of NE (WT: 0.01306 ± 0.0005 pg/mg; LO: 0.1386 ± 0.0263 ; $p= 0.003$).

### VMAT2 LO mice have drastically impaired 6-fluorodopamine sequestration in sympathetic terminals of cardiac tissue.

In a parallel approach to assay functional catecholaminergic innervation in the heart, we measured the uptake and metabolism of intravenously administered 6-fluorodopamine in the sympathetic terminals of cardiac tissue. Five minutes after intravenous administration of 6-FDA (100 ng, via tail vein), we assessed levels of 6-FDA, 6-FNE, and 6-FDOPAC with HPLC (Figure 3-2). Wildtype hearts all contained 6F-catechols (12 of 12 mice), whereas only 50% VMAT2 LO hearts contained detectable levels of 6-F-catechols (4 of 8). Total 6-F-catechol levels (the molar sum of 6-FDA, 6-FNE, and 6-FDOPAC) were

reduced in VMAT2 LO hearts by 73% (WT: 26.9±4.1 fmol/mg; LO: 7.2±3.8 fmol/mg; p=0.005).

The presence of 6-FDA and 6-FNE are indicative of sympathetic 6-FDA sequestration (Chang et al., 1990). Compared to wild-type littermates, VMAT2 LO hearts had 92% less 6-FDA (WT: 2.77±0.43 pg/mg, LO: 0.18±0.14pg/mg; p=0.0002) and 77% less 6-FNE (WT: 1.80±0.27 pg/mg; LO: 0.36±0.16 pg/mg p=0.0007). Despite low 6-F catechol uptake, VMAT2 LO mice had a trend toward increased total 6-FDOPAC in cardiac tissue (WT:0.14±0.14 pg/mg; LO: 1.00±0.55 pg/mg; p=0.15), indicating rapid cytosolic deamination of 6FDA after uptake.

**Reductions in cardiac NET expression do not account for VMAT2 NE depletion**

To assess noradrenergic innervation in the heart, we quantified norepinephrine transporter abundance in cardiac homogenates of VMAT2 LO mice (Figure 3-3). VMAT2 LO animals had 38% less nisoxetine binding in contrast to their wild-type littermates (wild-type: 16.00 ± 1.64 fmol bound/mg tissue, VMAT2 LO: 10.09 ± 0.73, $p<0.05$).

**Discussion**

Just as there is strong support for reduced vesicular function contributing to nigrostriatal degeneration in PD (Goldstein et al., 2013; Miller et al., 1997; Pifl et al., 2014), there is mounting evidence that reduced vesicular function also contributes to cardiologic abnormalities in PD as well. Loss of sympathetic tone in cardiac tissue is indeed a pervasive pathological feature of PD, with 30% of patients meeting the diagnostic criteria for orthostatic hypotension (Velseboer et al., 2011). In this work, we present data from VMAT2 LO mice that parallel the neurochemical pathology in the hearts of PD patients (Goldstein et al., 2014)(Figures 3-1 and 3-4).

The first indication that vesicular catecholamine storage is impaired in the hearts of PD patients came from a study by Goldstein and colleagues that combined scintigraphic imaging of cardiac $^{18}$F-DA uptake and neurochemical assessment of its metabolic fate in serum (Goldstein et al., 2011a). In the present work, we demonstrate that VMAT2 LO mice have impaired also have 6-FDA uptake, as reflected in the HPLC results of cardiac tissue following intravenous administration of 6-FDA. In contrast to scintigraphy in humans, this approach in mice allows us to measure not only sympathetic uptake of 6-FDA, but its catabolism to 6-FDOPAC and conversion to 6-FNE, as well. Based off of total 6-F catechol levels in cardiac tissue, we can infer that sympathetic uptake of 6-FDA in VMAT2 LO mice was approximately 30% of WT. Stable storage of 6-FDA in VMAT2 LO hearts was more severely impaired (7% of WT) as was total vesicular synthesis of 6-FNE (23% of WT). Of VMAT2 LO mice that exhibited sympathetic uptake of 6-FDA, there was a 10-fold increase in its cytosolic conversion to 6-FDOPAC

However, neither of these approaches shows the effect of reduced vesicular transport on endogenous cardiac norepinephrine, which led our groups (Miller and Goldstein) to perform parallel studies in the cardiac tissue of VMAT2 LO mice and post mortem PD cases. In VMAT2 LO mice, we observed a drastic, 97% reduction in cardiac NE, coupled with an 11-fold increase in relative cytosolic NE turnover (DHPG:NE; Figure 3-1). The magnitude of cardiac NE depletion is in contrast to the more modest reductions in the striatal and cortical norepinephrine of VMAT2 LO mice (Chapter 2; Taylor, 2014) and may reflect variability between neuron types with respect to synthesis and release patterns, extraneuronal milieu, and expression of catecholamine metabolizing enzymes.

These results draw a striking parallel to the catechol levels in cardiac tissue from post mortem PD cases, analyzed in parallel by Goldstein and colleagues (Figure 3-4, as published in Goldstein, 2014). From a study of 23 postmortem cases, 16 of 23 (70%) were "NE-depleted" compared to case controls, having a 98% mean reduction of cardiac norepinephrine. The NE-depleted PD cases had an 11-fold increase in cardiac DHPG:NE, indicating that vesicular sequestration in sympathetic terminals was impaired to the same extent as in VMAT2 LO mice. Of the non-depleted PD cases, DHPG:NE was still significantly elevated, further supporting a shift from vesicular storage to cytosolic metabolism as a consistent molecular event in PD pathogenesis.

As demonstrated by our neurochemical data, VMAT2 underexpression and PD contribute to nearly identical cardiac NE depletion. It is worth noting that disrupted vesicular function is one of two main determinants of cardiac NE. PD patients exhibit up to an 85% reduction in sympathetic innervation (Goldstein et al., 2000), which partially

accounts for the stark NE depletion. Similarly, we observed that the hearts of VMAT2 LO mice have substantial preservation of noradrenergic cardiac innervation, as demonstrated by nisoxetine-binding in cardiac homogenates (60% of WT) (Figure 3-3), though their reduced 6-FDA uptake (30% of WT, Figure 3-2) suggests a reduction in functional integrity.

**Conclusion**

Disrupted vesicular storage of catecholamines in mice drives a neurochemical cardiac pathology that is nearly identical in magnitude to that of human PD. While indirect measures of vesicular function in PD patients and post mortem cases have demonstrated that sympathetic vesicular impairment occurs in PD, the present work in VMAT2 LO mice demonstrates that this disruption drives this pathology.

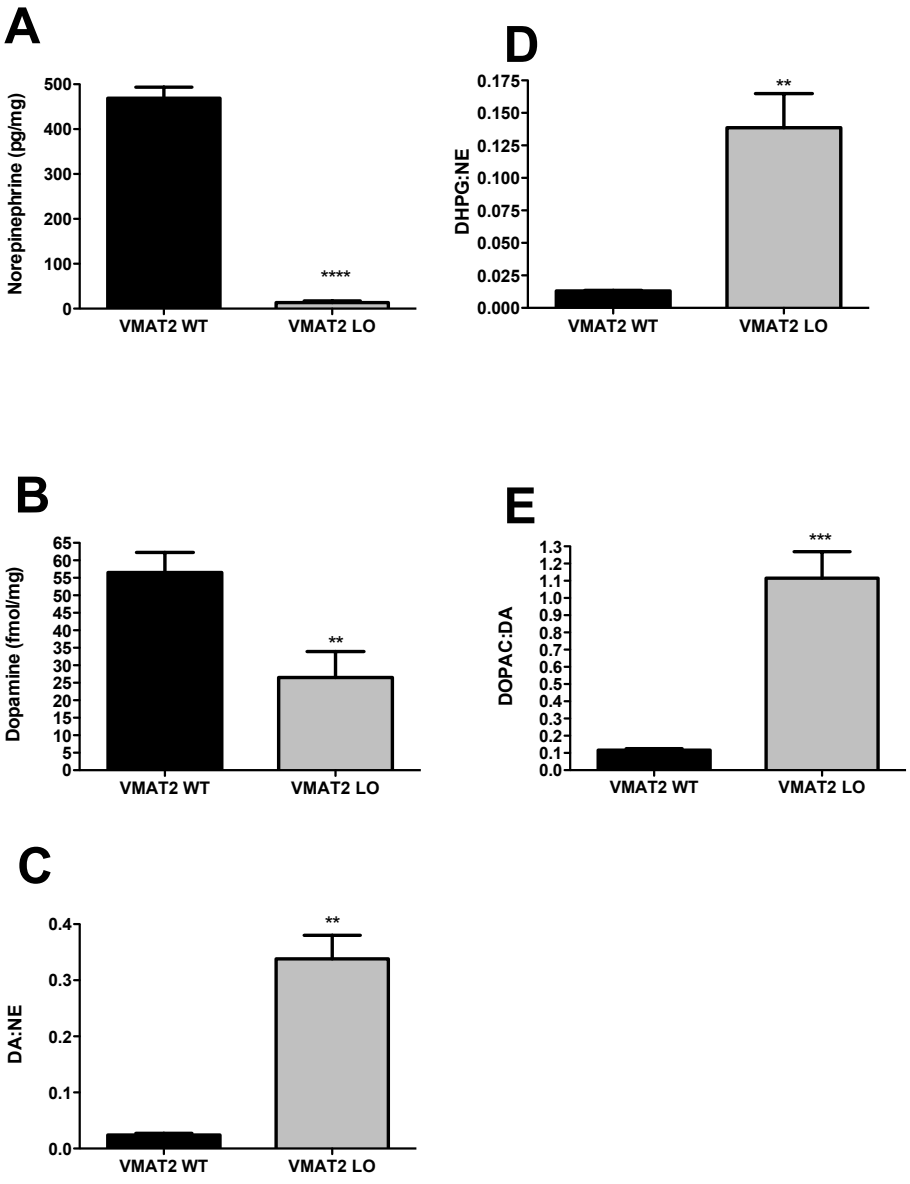
A
Norepinephrine (pg/mg)
500
400
300
200
100
0
****
VMAT2 WT
VMAT2 LO
D
DHPG:NE
0.175
0.150
0.125
0.100
0.075
0.050
0.025
0.000
**
VMAT2 WT
VMAT2 LO
B
Dopamine (fmol/mg)
65
60
55
50
45
40
35
30
25
20
15
10
5
0
**
VMAT2 WT
VMAT2 LO
E
DOPAC:DA
1.3
1.2
1.1
1.0
0.9
0.8
0.7
0.6
0.5
0.4
0.3
0.2
0.1
0.0
***
VMAT2 WT
VMAT2 LO
C
DA:NE
0.4
0.3
0.2
0.1
0.0
**
VMAT2 WT
VMAT2 LO

**Figure 3-1. Reduced vesicular function disrupts sympathetic norepinephrine homeostasis.**

HPLC levels of cardiac catecholamines shows a drastic (97%) depletion in cardiac norepinephrine (A), as well as a substantial, but less drastic reduction in its precursor dopamine (B). This is reflected in the increased ratio of DA:NE (C), an index of reduced conversion of DA to NE. D and E. Reduced vesicular function causes a relative increase in intraneuronal MAO-mediated metabolism of NE to DHPG (D) and DA to DOPAC (E). n=4 mice for each analyte **p<0.01, ***p<0.001; ****<0.0001.

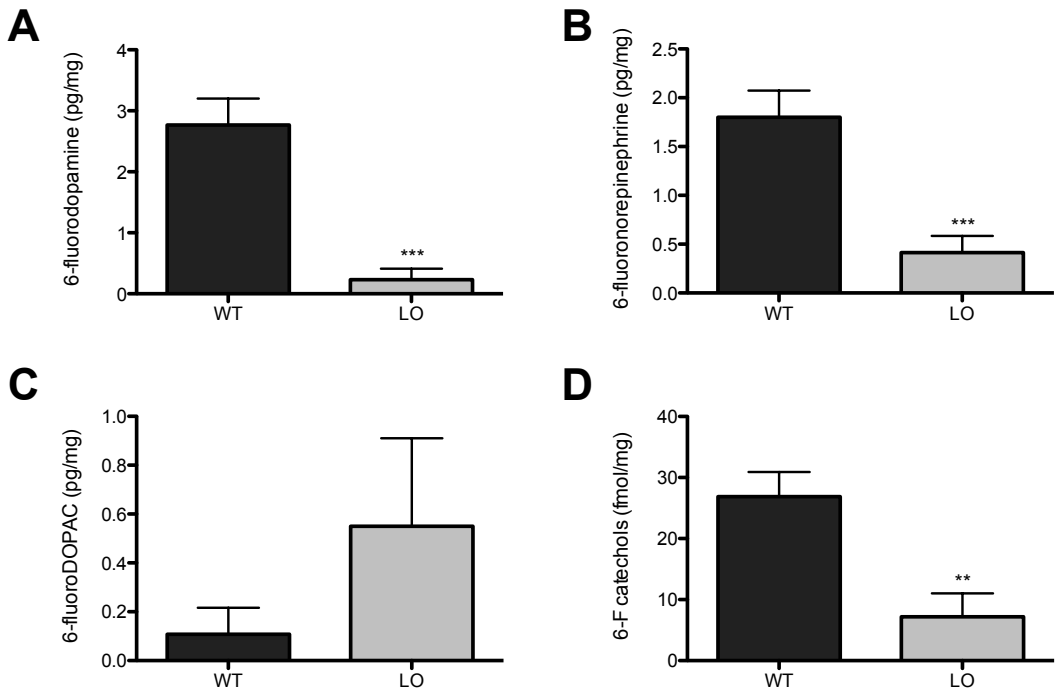
A
6-fluorodopamine (pg/mg)
4
3
2
1
0
***
WT
LO
B
6-fluoronorepinephrine (pg/mg)
2.5
2.0
1.5
1.0
0.5
0.0
***
WT
LO
C
6-fluoroDOPAC (pg/mg)
1.0
0.8
0.6
0.4
0.2
0.0
WT
LO
D
6-F catechols (fmol/mg)
40
30
20
10
0
**
WT
LO

**Figure 3-2. VMAT2 LO mice have impaired uptake and storage of 6-FDA.**

Five minutes after administration of 6-fluorodopamine (100ng, i.v.), wild-type and VMAT2 transgenic mice had markedly reduced sympathetic cardiac storage of the dopamine analog 6-fluorodopamine (A) and reduced sympathetic synthesis of 6-FNE (B). C, VMAT2 LO animals exhibited a trend of increased cytosolic breakdown of 6-FDA. D, Total fluorinated catechol levels in VMAT2 WT and LO hearts. N= 8-11 mice. ***$p<0.001$.

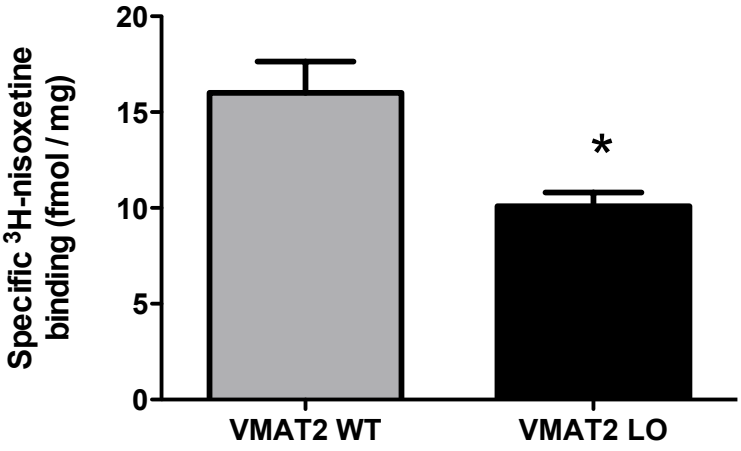
Specific ³H-nisoxetine binding (fmol / mg)
20
15
10
5
0
*
VMAT2 WT
VMAT2 LO

**Figure 3-3. VMAT2 LO mice have reduced abundance of cardiac norepinephrine transporter.**

[$^3$H]-nisoxetine binding in cardiomyocyte homogenates revealed that VMAT2 LO mice had reduced specific [$^3$H]-nisoxetine binding sites at 12 months. N= 4 animals, *$p<0.05$,

HUMANS
CONCENTRATION RATIO
100
10
1
0.1
0.01
<0.0001
<0.0001
0.0004
<0.0001
0.0002
CON
PD NE Depl.
DHPG:NE
DOPAC:DA
DA:NE
DOPAC:NE
DOPAC:DHPG
MICE
1
0.1
0.01
0.001
<0.0001
<0.0001
<0.0001
<0.0001
<0.0001
WT
VMAT2-Lo
DHPG:NE
DOPAC:DA
DA:NE
DOPAC:NE
DOPAC:DHPG

**Figure 3-4. Cardiac neurochemistry in PD patients and VMAT2 LO mice.**

Myocardial mean (±SEM) ratios of 3,4-dihydroxyphenylglycol (DHPG): norepinephrine (NE), 3,4-dihydroxyphenylacetic acid, (DOPAC): dopamine (DA), DA:NE, DOPAC:NE in control subjects. (CON, light colors) and patients with Parkinson's disease (PD, dark colors) and in wildtype (WT) mice (light colors) and mice with very low activity of the type 2 vesicular monoamine transporter (VMAT2 LO,,dark colors). p values are for PD versus CON and WT versus VMAT2 LO groups for each ratio. Reproduced with permission from the authors, (Goldstein et al, 2014).

**References**

Chang PC, Szemeredi K, Grossman E, Kopin IJ and Goldstein DS (1990) Fate of tritiated 6-fluorodopamine in rats: a false neurotransmitter for positron emission tomographic imaging of sympathetic innervation and function. *The Journal of Pharmacology and Experimental Therapeutics* **255**(2): 809-817.

Dae M (1994) Imaging of myocardial sympathetic innervation with metaiodobenzylguanidine. *Journal of Nuclear Cardiology* **1**(0): S23-S30.

Dhasmana KM and Spilker BA (1973) On the mechanism of L-DOPA-induced postural hypotension in the cat. *British Journal of Pharmacology* **47**(3): 437-451.

Fereshtehnejad S-M and Lökk J (2014) Orthostatic Hypotension in Patients with Parkinson's Disease and Atypical Parkinsonism. *Parkinson's disease* **2014**: 475854.

Goldstein DS, Holmes C, Kopin IJ and Sharabi Y (2011a) Intra-neuronal vesicular uptake of catecholamines is decreased in patients with Lewy body diseases. *J Clin Invest* **121**(8): 3320-3330.

Goldstein DS, Holmes C, Li ST, Bruce S, Metman LV and Cannon RO, 3rd (2000) Cardiac sympathetic denervation in Parkinson disease. *Ann Intern Med* **133**(5): 338-347.

Goldstein DS, Holmes C, Sewell L, Park MY and Sharabi Y (2012) Sympathetic noradrenergic before striatal dopaminergic denervation: relevance to Braak staging of synucleinopathy. *Clinical autonomic research : official journal of the Clinical Autonomic Research Society* **22**(1): 57-61.

Goldstein DS, Holmes C, Stuhlmuller JE, Lenders JW and Kopin IJ (1997) 6-[18F]fluorodopamine positron emission tomographic scanning in the assessment of cardiac sympathoneural function--studies in normal humans. *Clinical Autonomic Research : Official Journal of the Clinical Autonomic Research Society* **7**(1): 17-29.

Goldstein DS, Sullivan P, Holmes C, Kopin IJ, Basile MJ and Mash DC (2011b) Catechols in post-mortem brain of patients with Parkinson disease. *European Journal of Neurology* **18**(5): 703-710.

Goldstein DS, Sullivan P, Holmes C, Miller GW, Alter S, Strong R, Mash DC, Kopin IJ and Sharabi Y (2013) Determinants of buildup of the toxic dopamine metabolite DOPAL in Parkinson's disease. *Journal of Neurochemistry.* **126**(5): 591-603.

Goldstein DS, Sullivan P, Holmes C, Miller GW, Sharabi Y and Kopin IJ (2014) A vesicular sequestration to oxidative deamination shift in myocardial sympathetic nerves in Parkinson's disease. *Journal of Neurochemistry* **131**(2): 219-228.

Holmes C, Eisenhofer G and Goldstein DS (1994) Improved assay for plasma dihydroxyphenylacetic acid and other catechols using high-performance liquid chromatography with electrochemical detection. *Journal of Chromatography B: Biomedical Sciences and Applications* **653**(2): 131-138.

Jain S and Goldstein DS (2012) Cardiovascular dysautonomia in Parkinson disease: From pathophysiology to pathogenesis. *Neurobiology of Disease* **46**(3): 572-580.

Jankovic J (2008) Parkinson's disease: clinical features and diagnosis. *J Neurol Neurosurg Psychiatry* **79**(4): 368-376.

Langston JW (2006) The Parkinson's complex: parkinsonism is just the tip of the iceberg. *Annals of Neurology* **59**(4): 591-596.

Miller GW, Staley JK, Heilman CJ, Perez JT, Mash DC, Rye DB and Levey AI (1997) Immunochemical analysis of dopamine transporter protein in Parkinson's disease. *Annals of Neurology* **41**(4): 530-539.

Orimo S, Ozawa E, Nakade S, Sugimoto T and Mizusawa H (1999) I-123-metaiodobenzylguanidine myocardial scintigraphy in Parkinson's disease. *J Neurol Neurosurg Psychiatry* **67**(2): 189-194.

Pifl C, Rajput A, Reither H, Blesa J, Cavada C, Obeso JA, Rajput AH and Hornykiewicz O (2014) Is Parkinson's Disease a Vesicular Dopamine Storage Disorder? Evidence from a Study in Isolated Synaptic Vesicles of Human and Nonhuman Primate Striatum. *The Journal of Neuroscience* **34**(24): 8210-8218.

Taylor TN, Alter SP, Wang M, Goldstein DS and Miller GW (2014) Reduced vesicular storage of catecholamines causes progressive degeneration in the locus ceruleus. *Neuropharmacology* **76 Pt A**: 97-105.

Tejani-Butt SM (1992) [3H]nisoxetine: a radioligand for quantitation of norepinephrine uptake sites by autoradiography or by homogenate binding. *Journal of Pharmacology and Experimental Therapeutics* **260**(1): 427-436.

Velseboer DC, de Haan RJ, Wieling W, Goldstein DS and de Bie RM (2011) Prevalence of orthostatic hypotension in Parkinson's disease: a systematic review and meta-analysis. *Parkinsonism & Related Disorders* **17**(10): 724-729.

Wong KK, Raffel DM, Koeppe RA, Frey KA, Bohnen NI and Gilman S (2012) Pattern of Cardiac Sympathetic Denervation in Idiopathic Parkinson Disease Studied with 11C Hydroxyephedrine PET. *Radiology*. **265**(1): 240-247.

# CHAPTER 4

## Reduced vesicular storage disrupts signaling but does not cause degeneration of serotonin neurons

**Abstract**

Parkinson's disease (PD) features disruptions of the dopaminergic, noradrenergic, and serotonergic neurotransmitter systems. Presynaptic storage of monoamines by the vesicular monoamine transporter (VMAT) 2 is impaired in PD pathologenesis. We previously demonstrated that mice with reduced expression of the vesicular monoamine transporter 2 (VMAT2 LO) undergo age-related degeneration of the catecholamine-producing neurons of the substantia nigra pars compacta and locus ceruleus and exhibit motor and nonmotor symptoms of PD. In this work, we investigated the effect of reduced vesicular transport on the viability and function of serotonin neurons in these mice. In contrast to the degenerated catecholaminergic nuclei, aged VMAT2 LO mice do not exhibit a change in the number of serotonergic (TPH2+) neurons within the dorsal raphe compared to wild-type mice, as measured by unbiased stereology. We also observed sparing of serotonergic terminals throughout the forebrain by SERT immunoreactivity and evaluated [$^3$H]-paroxetine binding in striatal homogenates. While reduced VMAT2 expression did not result in loss of serotonergic markers throughout the brain, serotonin storage, release, and signaling were significantly affected.

VMAT2 LO mice displayed reduced serotonin storage and release capacity, as measured by HPLC and fast scan cyclic voltammetry. In *in vivo* tests of serotonin receptor responsivity, we observed changes to serotonin-mediated signaling correlates of depression. VMAT2 LO mice exhibited abolished 5HT1A autoreceptor sensitivity as determined by 8-OH-DPAT induction of hypothermia. When challenged with the 5HT2 agonist, 2,5-dimethoxy-4-iodamphetamine, VMAT2 LO mice exhibited a 50% increase in head twitch response. Collectively, these data indicate that (unlike catecholamine

neurons) reduced vesicular storage does not induce serotonergic autotoxicity, but can sufficiently disrupt signaling to cause a depressive phenotype.

## Introduction

Parkinson's disease consistently features disruption and preferential degeneration of monoaminergic neurotransmitter systems, resulting in the destruction of the nigrostriatal dopamine system and the noradrenergic locus ceruleus (Braak et al., 2003). The serotonergic raphe nuclei also degenerate in PD, though this pathology is more variable (Bernheimer et al.; D'Amato et al.; Halliday et al., 1990; Paulus and Jellinger). In contrast to striatal dopamine system, serotonergic pathology is less consistent, with serotonergic innervation of forebrain structures often being preserved through later stages of PD (Bédard et al.; Politis et al., 2010). Despite this resilience, reduced levels of serotonin (Kish et al., 2008; Ohara and Kondo, 1998) disruptions in serotonergic signaling likely underlie the high incidence of comorbid depression and other psychiatric symptoms in PD (Fahn, 2003), and may underlie the pathophysiology of L-DOPA induced dyskinesia (Navailles et al., 2011).

The basis for the shared vulnerability of monoaminergic neurons in Parkinson's disease may lie in their common molecular processes, which include the synthesis, storage, and metabolism of reactive neurotransmitters, all of which are influenced by the vesicular monoamine transporter (VMAT) 2. Following synthesis or plasmalemmal uptake of monoamines, VMAT2 sequesters these transmitters from the cytosol into acidic synaptic vesicles for stable storage and exocytic release. Clinical and epidemiological research has revealed that reduced function of VMAT2 likely contributes to PD pathology (as reviewed in Alter, 2013). Epidemiological studies have shown that *Slc18a2* promoter haplotypes that confer increased expression or function of VMAT2 are protective against Parkinson's disease (Brighina et al.; Glatt et al., 2006), while reduced *Slc18a2* mRNA

expression has been detected in the platelets of PD patients (Sala et al., 2010). From immunohistochemical analyses of postmortem brain tissue, we know that there is substantially less VMAT2 in caudate and putamen of PD cases than would be expected from degenerative loss (Miller et al., 1997). This was recently confirmed to have a functional effect, when Pifl and colleagues demonstrated that vesicular transport of dopamine via VMAT2 is reduced in synaptic vesicles isolated from the striata of Parkinson's disease patients in comparison to control cases (Pifl et al., 2014).

While there is strong support for the role of reduced vesicular function in dopaminergic degeneration in PD, there has been less direct investigation into the relationship between vesicular function and the vulnerability of noradrenergic and serotonergic neurons in PD. However, these neurotransmitters are subject to similar cytosolic degradation pathways, which lead us to hypothesize that reduced vesicular function contributes to their dysfunction and degeneration as well. In settings of reduced vesicular function, monoamines accumulate in the alkaline conditions of the cytosol, where they are subject to breakdown by spontaneous and enzymatic oxidative processes. In the cytosolic milieu, monoamines autoxidize to form reactive semiquinone (in the case of DA and NE) or dione (5-HT) intermediates and yield reactive oxygen species (Graham et al., 1978; Jiang et al., 1999); alternatively, DA, NE, and 5-HT are metabolized by monoamine oxidase to form reactive aldehyde intermediates—DOPAL, DOPEGAL, and 5-HIAL, respectively—prior to their enzymatic conversion to the benign neuronal metabolites DOPAC, DHPG, and 5-HIAA (Eisenhofer et al., 2004). Excessive cytosolic breakdown of DA, NE, and 5-HT by either fate (enzymatic deamniation or autoxidation) has been

demonstrated to be neurotoxic (Caudle et al.; Crino et al., 1989; Hastings et al.; Mosharov et al.; Taylor et al., 2014; Ulusoy et al., 2012).

We have previously demonstrated that mice with drastically reduced (~95%) expression of VMAT2 (VMAT2 LO) undergo accelerated age-related degeneration of the SNpc and LC, and display motor and nonmotor symptoms of PD (Caudle et al., 2007; Taylor et al., 2014; Taylor et al., 2009), while mice that overexpress VMAT2 exhibit enhanced dopamine release and are protected against MPTP-induced nigral degeneration (Lohr et al., 2014). Given the ability of reduced vesicular function to drive age-related catecholaminergic neurodegeneration, we investigated if VMAT2 deficiency can also drive degeneration of serotonergic neurons in the aging VMAT2 LO mouse model of Parkinson's disease.

## Materials and Methods

### Chemicals and reagents.

8-OH-DPAT was purchased from Abcam (#ab1210507, Cambridge, MA), DOI was purchased from (#D153, St. Louis, MO), [$^3$H]-Paroxetine was purchased from American Radiolabeled Chemical Inc. (#Art1777, St. Louis, MO),

**Mice.** Male and female VMAT2 LO mice were generated as previously described (Caudle et al., 2007). Briefly, the laboratory of Piers Emson (Mooslehner et al., 2001) generated a VMAT2 hypomorphic mouse on a C57BL/6 background. It was later revealed that the C57BL/6 subpopulation from which these mice were derived contained a spontaneous deletion spanning the α-synucleicn gene locus (SpecHT and Schoepfer, 2001). Through outbreeding to mice of the 129 strain, we reintroduced the deleted locus while maintaining the hypomorphic VMAT2 allele. These mice (VMAT2 LO) have been maintained on a C57/BL6 and 129 mixed background. The genotypes of all mice were confirmed by PCR of genomic DNA extracted from tail snips. This report represents the fifth set of data on VMAT2 LO mice with a normal α-synuclein background (Caudle et al., 2007; Guillot et al., 2008; Taylor et al., 2009; Taylor et al., 2014). All procedures were conducted in accordance with the National Institutes of Health Guide for Care and Use of Laboratory Animals and approved by the Institutional Animal Care and Use Committee at Emory University.

### HPLC determination of monoamines and metabolites

HPLC was performed as previously described (Richardson and Miller, 2004; Caudle et al., 2006, 2007). Briefly, dissected right striata, cortex, and hippocampus were sonicated

in 0.1 M perchloric acid containing 347 μM sodium bisulfate and 134 μM EDTA. Homogenates were centrifuged at 10,000 μg for 10 min at 4°C; the supernatant was removed and filtered through a 0.22 μm filter by centrifugation at 5000xg for 3 min. The supernatants were then analyzed for levels of DA, DOPAC, homovanillic acid, NE, 5-HT, and 5-HIAA. Levels were measured using HPLC with an eight-channel coulometric electrode array (ESA Coularray; ESA Laboratories). Quantification was made by reference to calibration curves made with individual standards.

**Immunohistochemistry**

Mice were transcardially perfused with phosphate-buffered saline and 4% paraformaldehyde. Their brains were then removed and stored in 4% paraformaldehyde for 24 hours, and cryopreserved in 30% sucrose for 48 hours. Brains were then sliced on a freezing microtome at 40 μm and collected into cryopreservative. Immunohistochemistry was performed as previously described (Caudle et al., 2007; Taylor et al., 2014). Briefly, sections were washed in phosphate buffered saline, incubated in 3% hydrogen peroxide to quench peroxidase activity, incubated in Citra (Biogenex, HK087-5K) antigen retrieval buffer for 10 minutes, and blocked in PBS with 10% normal goat serum and 0.1% Triton-X 100. Sections were incubated with a polyclonal rabbit antibody against TPH2 (1,5:000; Novus NB100-74555) overnigHT at 4° or SERT for 48 hours at room temperature (1:10,000; Immunostar 24330). Secondary incubations were performed with biotinylated polyclonal goat anti-rabbit antibody (Jackson 111-065-003, Hudson, WI).

**Stereology of the dorsal raphe nucleus**

Following immunohistochemistry against TPH2, tissue slices were mounted on microscope slides and counterstained with cresyl violet (Taylor, 2014). Stereological sampling (West et al., 1991) was performed using Stereo Investigator software (MicroBrigHTField, Colchester, VT). Dorsal raphe contours (comprising the dorsal, ventral, and interfascicular regions of the nucleus) were outlined as defined by the atlas of Paxinos and Franklin (2001), using a 4x objective. Final tissue thickness was 24 μm; guard zones of 2 μm were used to exclude lost profiles on the top and bottom of tissue sections. Cells were counted with a 40x objective (1.3x numerical aperture), using a counting frame of 50 x 50 μm, and sampling grid of 80 x 100 μm, at an evaluation interval of three sections (yielding 6-7 sections per animal). A serotonergic neuron was defined as an in-focus TPH2-immunoreactive cell body with a TPH2-negative nucleus. Nissl+ cells were defined as having a cresyl-violet positive nucleus or TPH2+ cell body. The Gunderssen (m=1) coefficient of error was less than 0.1 for each animal.

**Fast scan cyclic voltammetry in substantia nigra pars reticulata**

Fast scan cyclic voltammetry was performed as previously described (Lohr, 2014), with modification to measure serotonin release in the SNr. Mice were decaptitated and their brains quickly transferred ice cold oxygenated (95% $O_2$/5%$CO_2$) artificial cerebrospinal fluid (aCSF). Brains were mounted in aCSF onto the stage of a vibratome (Leica VT100S) and sliced at 300 μm. Midbrain slices were collected and maintained in oxygenated aCSF at room temperature. After 30 minutes, slices were placed in a slice perfusion chamber. Stimulating and carbon-fiber recording electrodes were placed in the

lateral region of the substantia nigra pars reticulata, as defined by Paxinos. A four-recording survey of three different sites within the SNr was taken for each animal with a 5-min rest interval between each stimulation (600 μA). Neurochemical identity of serotonin was confirmed with a serotonin-specific waveform and by observing increased signal in the presence of 10 μM fluoxetine.

Carbon-fiber microelectrodes were calibrated with serotonin standards using a flow-cell injection system. Kinetic constants were extracted using nonlinear regression analysis of release and uptake of serotonin. Application of waveform, stimulus, and current monitoring was controlled by TarHeel CV [University of North Carolina (UNC)] using a custom potentiostat (UEI, UNC Electronics Shop). The waveform for serotonin detection consisted of a −0.2 V holding potential versus an Ag/AgCl (In Vivo Metric) reference electrode. The applied voltage ramp ranged from−0.2V to 1.0V and back to -0.2V, with a phase shift of 13.7%, applied at a rate of 1000 V/s at 10 Hz.

**[$^3$H]-Paroxetine binding to quantify SERT expression**

Mice were decapitated and bilateral striata were dissected and collected into 5 ml assay buffer (50 mM Tris, 120 mM Nacl, 5 mM KCl, pH=7.4), and homogenized with a Teflon homogenizer at 1000 RPM. The homogenate was transferred to a centrifuge with 5 ml assay buffer and centrifuged at 48000 RCF. The resulting pellet was homogenized and centrifuged as before; the resultant pellet was resuspended in ~30 volumes of assay buffer. 100-200 ug of protein were transferred to borosilicate glass test tubes on ice in the presence of 2 nM [$^3$H]-paroxetine. Nonspecific binding was determined in the presence of 10 μM fluoxetine.

**DOI-induced Head Twitch Response.**

Methods were modeled after (Canal and Morgan, 2012). Mice were injected with saline or 2,5-dimethoxy-4-iodoamphetamine (DOI; 1 mg/kg, i.p.), and placed in a clean cage for video-recorded observation. 12 days later, a crossover study was performed. Behavior was recorded from 10 to 20 min post injection. The number of head twitches over a 10 minute interval was counted by a blinded observer. Head twitches were defined as rapid rotational head movements as described by (Canal and Morgan, 2012; Corne et al., 1963).

**8-OH-DPAT-induced hypothermia.**

The 8-OH-DPAT-induced hypothermia assay was performed as described by (Martin et al., 1992). Briefly, mice were injected with saline or 8-OH-DPAT (0.5 mg/kg; s.c.). Core body temperatures were measured with a rectal thermometer and recorded at baseline ($t_0$) and 20 ($t_{20}$) minutes following injection, and the differences between $t_0$ and $t_{20}$ were calculated.

## Results

### Reduced vesicular function does not cause significant age-related neurodegeneration of the dorsal raphe nucleus

As VMAT2 deficiency drives age-related neurodegeneration of the SNpc and LC (Caudle et al., 2007; Taylor et al., 2009), we examined the effects of this genetic disruption on the integrity of the dorsal raphe nucleus. Using immunohistochemistry against tryptophan hydroxylase 2, we observed no apparent changes to the serotonergic cytoarchitechture of the dorsal raphe (Figure 4-1). We counted serotonergic (TPH2+) neurons within the nucleus using unbiased stereology. At 24 months (the age at which LC and SNpc degeneration were severe), we observed no significant change in the serotonergic neuronal population in the dorsal raphe nucleus between genotypes (WT: 3027±210 TPH2+ neurons; LO: 2646 ± 253 neurons; p=0.73*),* and no difference between the number of Nissl+ neurons in the DRN (p=0.84).

### Preservation of serotonin transporter expression

While the quantity of serotonergic cell bodies in the DRN of VMAT2 LO mice was unaffected, we next sought to investigate if serotonergic innervation of rostral brain regions would be affected. Using immunohistochemistry against SERT, we evaluated serotonergic innervation of the SNr, cortex, and striatum (Figure 4-2). In each region surveyed, we observed no overt changes to serotonergic morphology or expression. We quantified striatal SERT expression in striatal homogenates by [$^3$H]-paroxetine binding (Figure 4-2D), and observed no change in the number of specific paroxetine-binding sites (WT: 426 ± 41 fmol/mg; LO: 420 ± 25 fmol/mg; p=0.9).

**VMAT2 LO mice are deficient in 5-HT content and release.**

To evaluate the extent of neurochemical depletion caused by the VMAT2 hypomorph transgene, we evaluated DA and 5-HT levels in the striata and cortex of VMAT2 transgenic mice at 4-6 months of age (Figure 4-3). VMAT2 LO mice had marked reductions of striatal 5-HT (WT, 30.3 ± 1.0 pmol/mg, LO, 3.2 ± 0.2; $p<0.0001$) and DA: (WT, 144.4 ± 6.7, LO, 10.3 ± 1.8; $p<0.0001$), as well as similarly marked reductions in cortical 5-HT (WT, 21.6 ± 1.8; LO, 2.57 ± 0.65; $p<0.0001$) and DA (WT, 20.0 ± 2.3; LO, 0.8 ± 0.2; $p<0.0001$). In the striatum, we assessed the relative conversion of DA and 5-HT to their respective intraneuronal metabolites, DOPAC and 5-HIAA (Figure 4-1B,C). VMAT2 LO mice exhibited an 11-fold increase in conversion of DA to DOPAC and 9-fold increase of 5-HT to 5-HIAA. These effects were also observed in the cortex. Notably, the extent of neurotransmitter depletion and increased metabolite conversion caused by VMAT2 underexpression were comparable between brain regions.

Using fast scan cyclic voltammetry in brain slices (Figure 4-4), we measured the stimulated synaptic release of 5-HT in the substantia pars reticulata, which is the most densely serotonergically innervated structure in the brain and is the major output nucleus of the basal ganglia. In response to electrical stimulation (600 μA, 20p @ 100Hz) VMAT2 LO mice exhibited a 90% decrease in synaptic 5-HT release compared to wild-type littermates (extracellular 5-HT, wild-type: 1.0 ± 0.3 μM 5-HT; VMAT2 LO: 0.1 ± 0.0 μM 5-HT), barely exceeding the threshold of detection. These signals were proportionately enhanced in the presence of fluoxetine (data not shown). We observed no difference in Tau, a measure of synaptic monoamine clearance.

**Reduced vesicular function disrupts serotonergic signaling**

We examined potential changes to serotonergic signaling *in vivo*. 5-HT1A receptors are expressed on somatodendrites and function as an inhibitory autoreceptor. Physiologically, 5HT1A agonism elicits a hypothermic effect in rodents and humans, though this effect is lost in depressive states (Jacobsen et al., 2012a; Lesch, 1991). We sought to test the effects of VMAT2 deficiency on the thermic response to the 5HT1a autoreceptor agonist, 8-OH-DPAT (Figure 4-5A). VMAT2 WT and LO mice had similar baseline core body temperatures (WT: 37.6 ± 0.2; LO: 37.4 ± 0.2; p=0.37). After administration of 8-OH-DPAT (0.5 mg/kg; IP), wild-type mice exhibited a -4.0 ± 0.4˚ decrease in core body temperature 20 minutes following treatment; this response was attenuated in VMAT2 LO mice, which exhibited a -1.0 ± 0.3˚ decrease in core temperature ($p<0.0001$).

5-HT2 receptors are expressed postsynaptically and mediate excitatory signaling. Behaviorally, selective 5-HT2 agonism causes hallucinations in humans and a headtwitch response in rodents (Canal and Morgan, 2012; Corne et al., 1963). To investigate the effect of reduced VMAT2 expression on the responsiveness of 5-HT2 receptors, we evaluated the DOI-induced headtwitch response in wild-type and VMAT2 LO mice (Figure 4-5B). After administration with DOI (1 mg/kg, IP), wild-type animals elicited 29 ± 3 head twitches over ten minutes of recorded observation. VMAT2 LO mice were more sensitive to DOI, and exhibited a 79% increase in head twitches (52 ± 5 HTRs; WT vs LO, p=0.0009).

## Discussion

Significant attention has been directed at exploring the connection between vesicular function and neuronal vulnerability in Parkinson's disease (Alter et al., 2013; German and Sonsalla, 2003). Reduced vesicular function occurs in the substantia nigra pars compacta of PD patients, and has been demonstrated to drive neurodegeneration in the SNpc and LC of mouse models (Taylor et al., 2014; Ulusoy et al., 2012). In this work, we asked if disrupting the vesicular storage of serotonin could also cause dysfunction and degeneration of serotonergic neurons. Because clinical and animal data have shown that drastically reduced VMAT2 function causes neuropsychiatric disturbances associated with PD (Rilstone et al., 2013; Taylor et al., 2009), we also sought to investigate if reducing vesicular 5-HT storage would lead to changes in serotonergic signaling consistent with a depressive phenotype.

### Reduced expression of VMAT2 does not cause degeneration of the dorsal raphe of VMAT2 deficient mice.

As we previously reported severe, age-related degeneration of the SNpc and LC of VMAT2 LO mice (Caudle et al., 2007; Taylor et al., 2014), we asked if the increase in cytosolic breakdown of 5-HT would also drive neurotoxicity in the dorsal raphe. Others have demonstrated that conditional knockout of VMAT2 or TPH2 in serotonergic neurons does not affect the initial development of the raphe cytoarchitecture (Narboux-Neme et al., 2011). In this work, we demonstrate that aged VMAT2 LO mice (24 months) do not undergo significant change to TPH2+ cell populations within the dorsal raphe by unbiased stereological counting. Qualitatively, we did not observe any overt

changes to the cytoarchitecture of the median raphe. The preservation of the raphe nuclei in aged VMAT2 LO mice suggests that the vesicular storage of 5-HT is less critical to serotonergic neuronal health than catecholamine storage is to the neuronal viability of the LC or SNpc. It is worth noting that the dopaminergic VTA of VMAT2-LO mice does not undergo degeneration either (Taylor et al., 2014); we previously ascribed this result differential regulation of cytosolic calcium and its influence on cytosolic dopamine (Chan et al., 2007; German et al., 1992; Mosharov et al., 2009).

Serotonergic cell bodies are resilient even to 5-HT-selective toxicants (2-NH2-MPTP, 5,7-DHT, MDMA), but are indeed sensitive to terminal damage (Baumgarten and Lachenmayer, 2004; Luellen et al., 2006). We thus explored the possibility that our mice may undergo loss of serotonergic terminals in regions relevant to Parkinson's disease but observed no changes to SERT+ innervation pattern or expression (Figure 4-2). We quantified SERT expression in striatal tissue using [$^3$H]-paroxetine binding but detected no change in expression. This is in stark contrast to what we observed of dopaminergic innervation in the striatum, which featured progressive dopamine transporter loss beginning at 12 months of age, with near-complete terminal loss at 24 months. The preservation of striatal serotonergic innervation is of particular interest in the context of depression and levodopa-induced dyskinesia.

In a strongly supported hypothesis of levodopa-induced dyskinesia, serotonin neurons transport L-DOPA, convert it to DA via AADC, and release it in a dysregulated manner (Politis et al., 2014). Moreover, an increased ratio of SERT to DAT expression in the striatum is predictive of the severity of levodopa-induced dyskinesia following fetal midbrain grafts (Politis et al., 2011). Upon observing the resilience of 5-HT striatal

innervation in VMAT2 LO mice, we performed a study modeled after that performed in Pitx3-deficient mice (Ding et al., 2007), but observed no dyskinetic movement in treated animals; it is reasonable to conclude that the 5-HT neurons of our mice do not have the storage capacity to release sufficient L-dopa-derived DA to express LID.

**Reduced vesicular function diminishes serotonin storage and release capacity**

As a consequence of the genetic suppression of VMAT2, we observed drastic (~90%) reduction in cortical and striatal 5-HT and DA (Figure 4-3), consistent with an earlier report (Taylor et al., 2009). In contrast, mice with reduced serotonin synthesis capability (TPH2 loss-of-function) do not have a significant neurochemical 5-HT deficit, despite compromised serotonin synthesis (Mosienko et al., 2014). The authors found that the neurons of these mice compensate for reduced synthesis by decreasing metabolism of 5-HT to 5-HIAA (Mosienko et al., 2014). However, by compromising vesicular sequestration, we did not see such a compensatory effect in our mice, as 5-HT levels were diminished and conversion to 5-HIAA increased. Together, these data indicate that vesicular function is critical to maintaining normal serotonin levels, and that the depleting effects of its disruption are not readily compensated.

While HPLC results revealed drastic reductions in tissue serotonin content, we wanted to determine to what extent synaptic release of serotonin would be affected. In response to electric stimulation, VMAT2 LO mice exhibited a 90% decrease synaptic serotonin release, indicating no compensatory change in the presynaptic regulation of 5-HT release. This is in contrast to another report of the striatal DA system of VMAT2 LO mice, in which there was a 90% reduction in striatal dopamine, but only a 66% reduction

in synaptic DA release (Mooslehner et al., 2001; Patel et al., 2003). However, these experiments were performed in transgenic VMAT2 mice with different genetic backgrounds.

**Depressive-like thermic and behavioral responses**

There is a high comorbidity of depression in PD affecting 35% of patients (Aarsland et al., 2012), and occurring at a rater greater than in patients of other diseases (Nilsson et al., 2002). Pathologogically, this correlates with reductions in midbrain serotonin and serotonergic neurons (Aarsland et al., 2012). We previously reported that VMAT2 LO mice have a depressive-like phenotype, exhibiting increased immobility in the forced swim and tail suspension tests (Taylor et al., 2009). In this study, we evaluated the sensitivity of the 5-HT1A/2 serotonin receptors in tests that correspond with human biomarkers of depression (Jacobsen et al., 2012b). VMAT2 LO mice had an abolished hypothermic response to the 5HT1A autoreceptor agonist 8-OH-DPAT, which is a selective 5HT1A agonist that suppresses serotonin release from raphe neurons, eliciting a hypothermic response (Martin et al., 1992). While it could be expected that 5HT1A sensitivity would increase in a setting of reduced extracellular serotonin (the inverse has been observed in SERT KO mice (Li et al., 1999)), raphe neurons may adaptively blunt the 5HT1A autoinhibition. Our results are consistent with observations in other hyposerotonergic mouse models (Jacobsen et al., 2012b; Mosienko et al., 2014). This bears translational relevance, as unmedicated depressed patients also exhibit a blunted hypothermic response to 5HT1A agonists (Cowen et al., 1994; Lesch, 1991).

VMAT2 LO mice exhibited a markedly increased head-twitch response to the 5-HT2 agonist DOI. DOI is a substituted amphetamine selective for 5-HT2A/C postsynaptic receptors that elicits hallucinations in humans and head-twitches in rodents (Canal and Morgan, 2012). 5-HT2 receptor expression and function have been shown to increase in experimental models of hyposerotonergia and serotonergic denervation (Jacobsen et al., 2012a), while increased 5-HT2A binding has been observed in depression and suicide (Shelton et al., 2009). Observations of the altered responsiveness of 5-HT1A and 5-HT2A have led to their consideration as biomarkers of chronic hyposerotonergia and depression (Jacobsen et al., 2012b). In VMAT2 LO mice, we have demonstrated that these phenotypes are capitulated by disrupting vesicular storage of serotonin. These findings indicate that reduced vesicular function, which exacerbates or drives Parkinsonian pathology, can also cause depressive features in mice, providing a single molecular mechanism that could plausibly drive the comorbidity of PD and depression. We have further supported this argument by demonstrating that overexpression of VMAT2 protects against MPTP-derived neurotoxicity and confers a resilient, euthymic phenotype in depressive behavior tests (Lohr et al., 2014).

**Conclusions**

Disrupting the storage of 5-HT does not cause degeneration of serotonergic neurons in the dorsal raphe, despite greatly accelerated intraneuronal metabolism of 5-HT. VMAT2 LO mice exhibit reduced synaptic release of 5-HT and altered serotonergic signaling, which drive physiological and behavioral correlates of depression. These data, along with our previous reports, demonstrate that disruption of a single neuronal

function—vesicular transport—can exacerbate or drive the motor and nonmotor symptoms of Parkinson's disease.

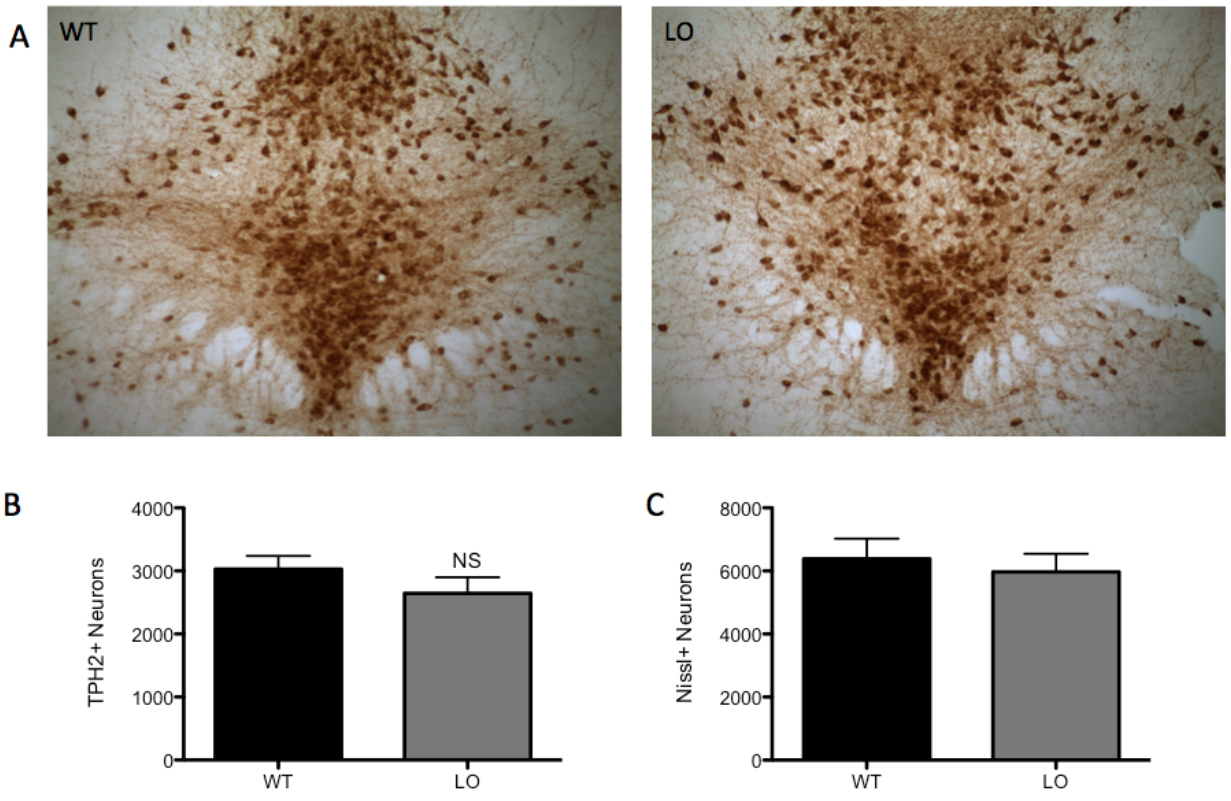
A
WT
LO
B
TPH2+ Neurons
4000
3000
2000
1000
0
NS
WT
LO
C
Nissl+ Neurons
8000
6000
4000
2000
0
WT
LO

**Figure 4-1: Preservation of dorsal raphe in aged VMAT2 LO mice.**

A: Immunohistochemical staining against TPH2 in the dorsal raphe shows normal cytoarchitecture in 24 month old VMAT2 LO mice. B: Unbiased stereological sampling revealed no significant change in the number of TPH2+ neurons between aged WT and VMAT2 LO mice (n=5, p=0.73), while the number of Nissl+ neurons (inclusive of TPH2+ neurons) was also unchanged.

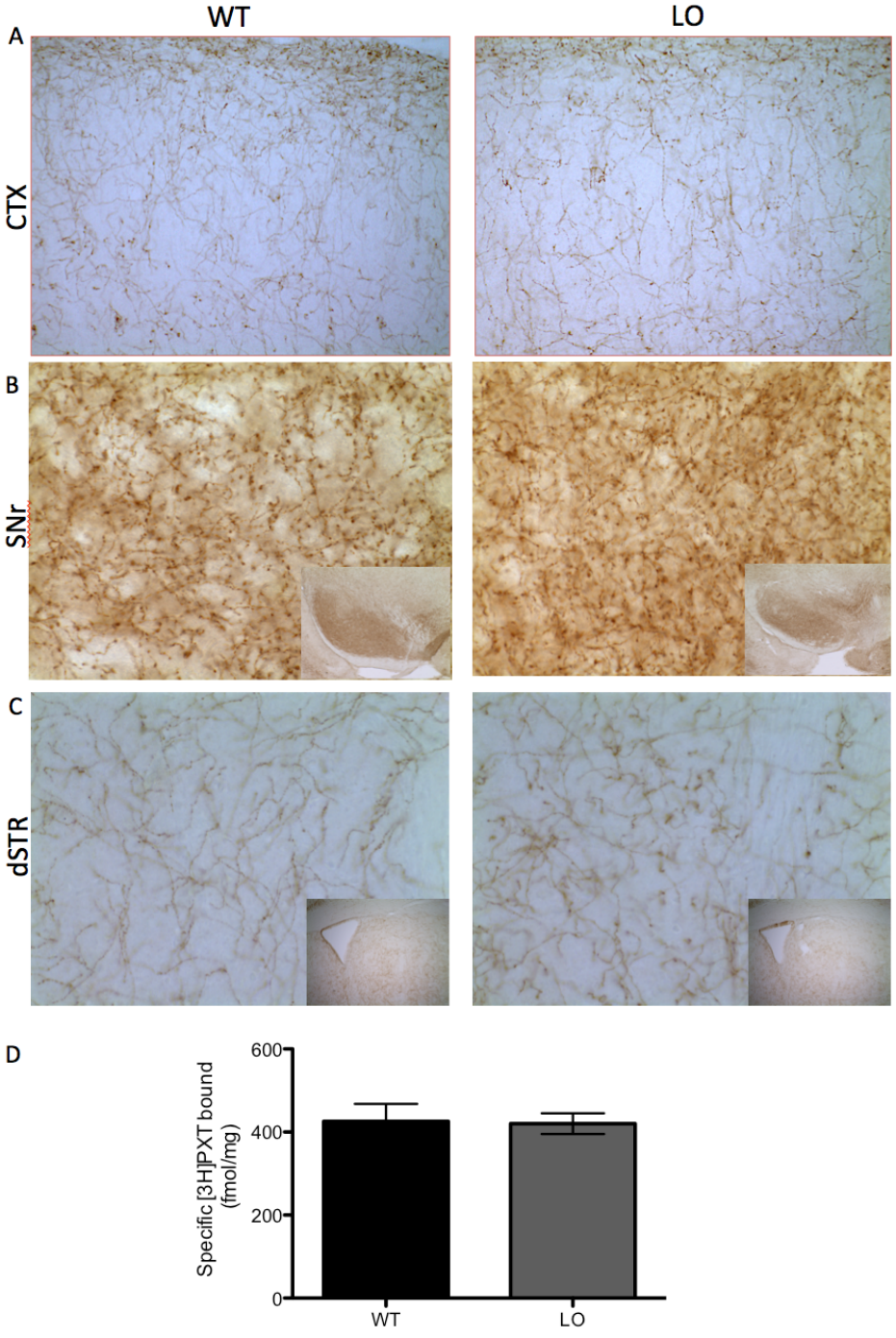
WT
LO
A
CTX
B
SNr
C
dSTR
D
Specific [3H]PXT bound (fmol/mg)
600
400
200
0
WT
LO

**Figure 4-2: Serotonergic Innervation is preserved in VMAT2 LO mice.**

Immunohistochemical staining against SERT reveal no noticeable changes to serotonergic innervation in aged (24 months) wild-type and VMAT2 LO mice, in the motor cortex (A), substantia nigra pars reticulata (B), or dorsal striatum (C). D: There was no change in [$^3$H]-paroxetine binding sites in striatal homogenates between wild-type and VMAT2 LO mice (n=6).

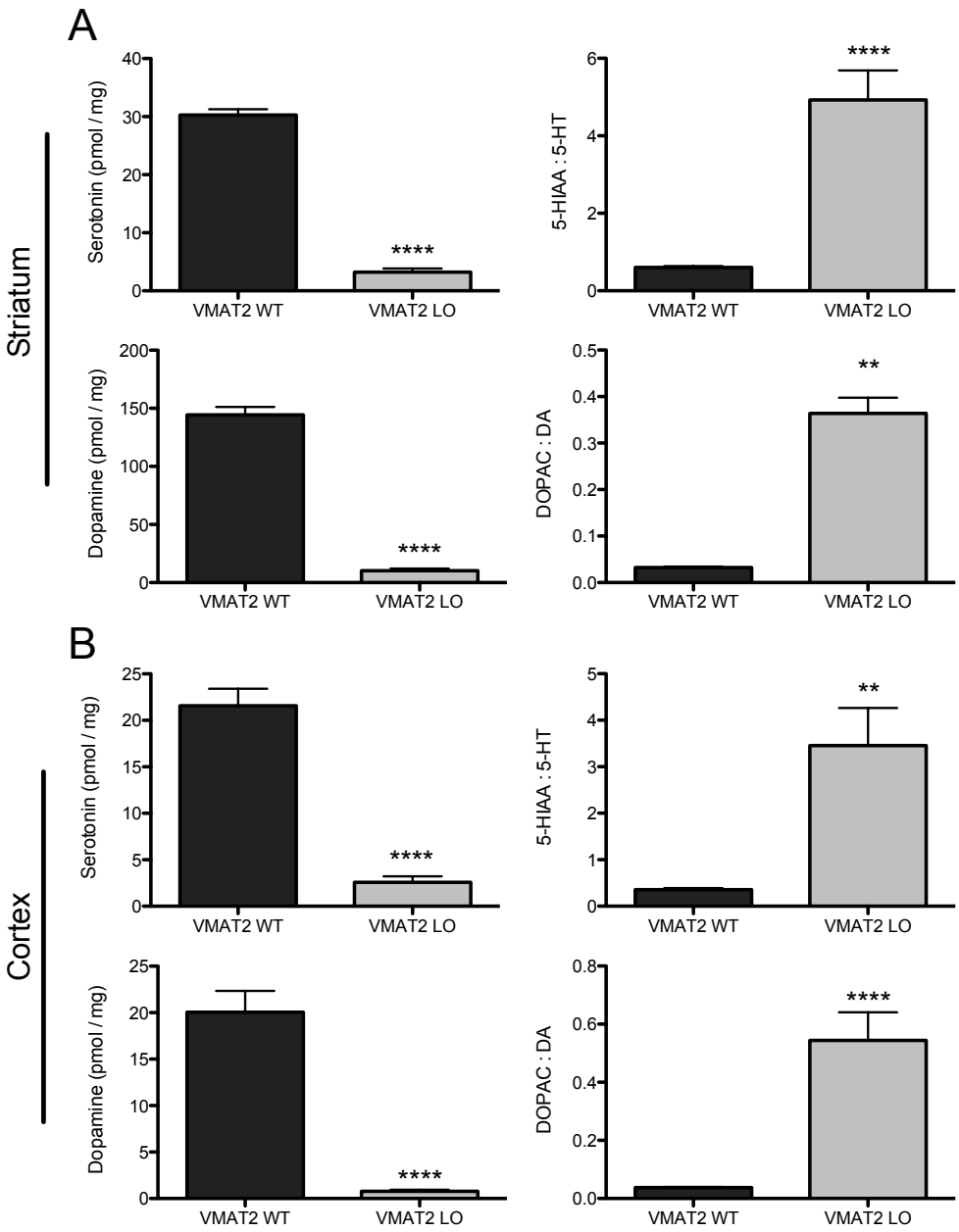
A
Striatum
Serotonin (pmol / mg)
40
30
20
10
0
****
VMAT2 WT
VMAT2 LO
5-HIAA : 5-HT
6
4
2
0
****
VMAT2 WT
VMAT2 LO
Dopamine (pmol / mg)
200
150
100
50
0
****
VMAT2 WT
VMAT2 LO
DOPAC : DA
0.5
0.4
0.3
0.2
0.1
0.0
**
VMAT2 WT
VMAT2 LO
B
Cortex
Serotonin (pmol / mg)
25
20
15
10
5
0
****
VMAT2 WT
VMAT2 LO
5-HIAA : 5-HT
5
4
3
2
1
0
**
VMAT2 WT
VMAT2 LO
Dopamine (pmol / mg)
25
20
15
10
5
0
****
VMAT2 WT
VMAT2 LO
DOPAC : DA
0.8
0.6
0.4
0.2
0.0
****
VMAT2 WT
VMAT2 LO

**Figure 4-3. VMAT2 LO mice have reduced levels and increased catabolism of serotonin and dopamine.**

A: VMAT2 LO mice have reduced levels striatal serotonin and dopamine (left panels), and increased neuronal catabolism to the respective metabolites, 5-HIAA and DOPAC (right panels). B: VMAT2 LO mice had compable reductions in cortical serotonin and dopamine, along with similarly increased catabolism of both monoamines. (**<p<0.1, ****p<0.0001).

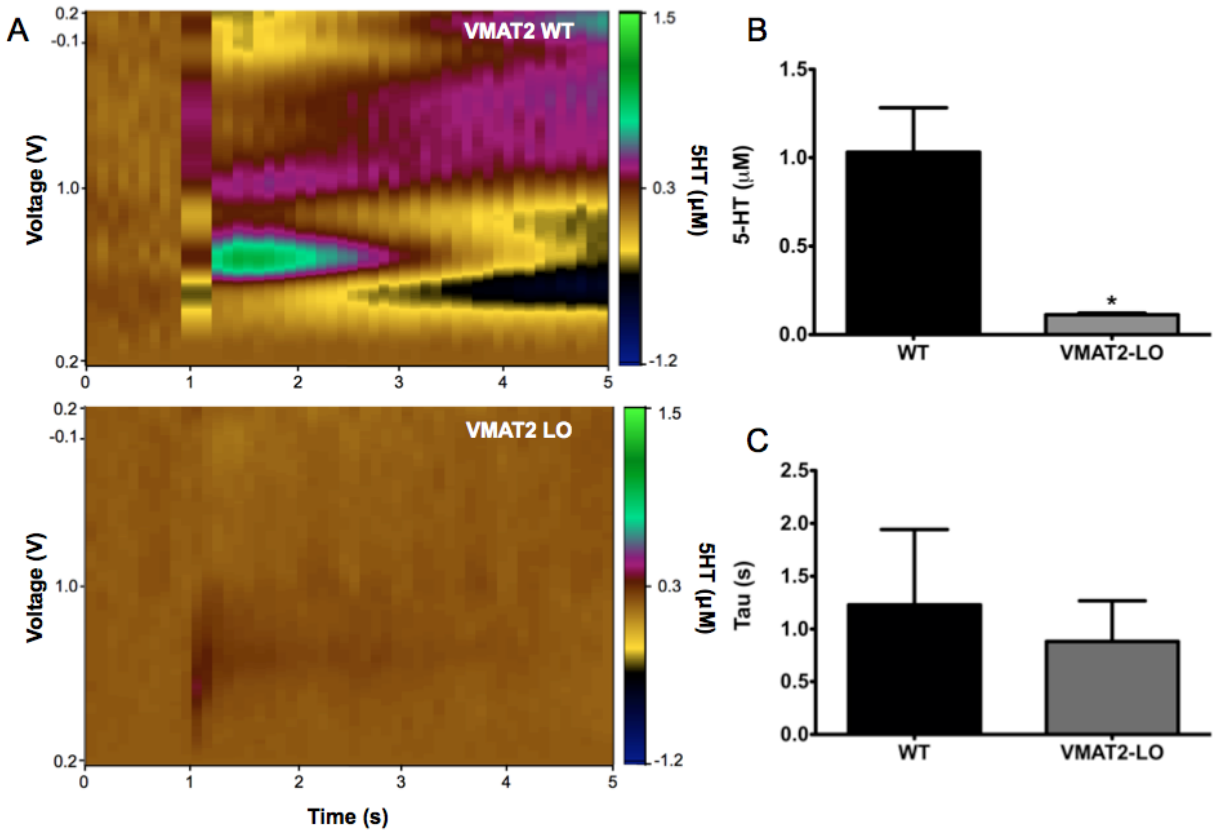
A
VMAT2 WT
VMAT2 LO
Voltage (V)
5HT (μM)
Time (s)
B
5-HT (μM)
WT
VMAT2-LO
*
C
Tau (s)
WT
VMAT2-LO

**Figure 4-4. VMAT2 hypomorphy causes reduced synaptic release of serotonin.**

A: Top colorplot, VMAT2 WT animals exhibited a peak release of 1 μM 5-HT in the substantia nigra pars reticulata in response to electric stimulation. Bottom colorplot, VMAT2 LO mice had drastically reduced signal (~90%), as illustrated in B (*p=0.02; n=3 mice). C: There was no significant change in synaptic clearance rate of 5-HT (Tau).

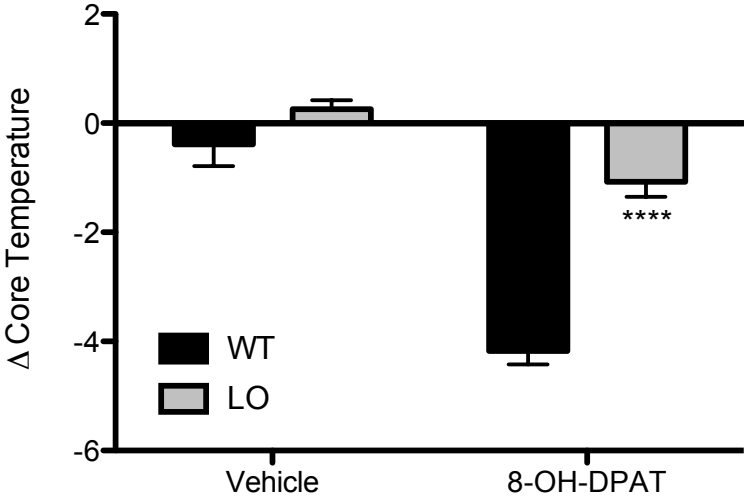
2
0
-2
-4
-6
Δ Core Temperature
WT
LO
****
Vehicle
8-OH-DPAT

**Figure 4-5: VMAT2 LO mice have an ablated hypothermic response to the 5HT1A agonist 8-OH-DPAT.**

Wildtype and VMAT2 LO mice were injected with saline or 8-OHDPAT (0.1 mg/kg; i.p.). Wildtype animals exhibited a -4° change in core body temperature, whereas VMAT2 LO mice had an attenuated response of -1° (n=7-10).

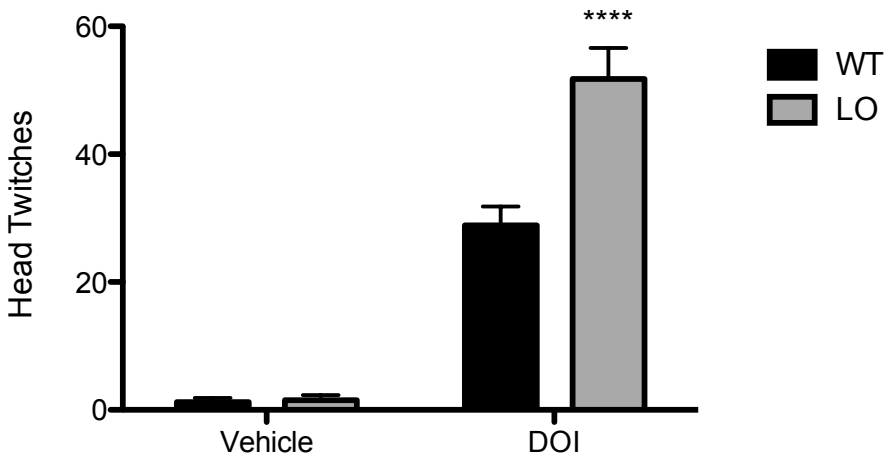
****
60
40
20
0
Head Twitches
Vehicle
DOI
WT
LO

**Figure 4-6. VMAT2 LO mice have increased sensitivity to the 5-HT2 agonist DOI.** When injected with DOI, VMAT2 LO mice exhibited a 79% increase in the number of head twitches over wild-type mice (n=8-9, ****p<0.0001).

**References**

Aarsland, D., Pahlhagen, S., Ballard, C.G., Ehrt, U., Svenningsson, P., 2012. Depression in Parkinson disease--epidemiology, mechanisms and management. Nature reviews. Neurology 8, 35-47.

Alter, S.P., Lenzi, G.M., Bernstein, A.I., Miller, G.W., 2013. Vesicular integrity in Parkinson's disease. Current neurology and neuroscience reports 13, 362.

Baumgarten, H.G., Lachenmayer, L., 2004. Serotonin neurotoxins--past and present. Neurotox Res 6, 589-614.

Bédard, C., Wallman, M.-J., Pourcher, E., Gould, P.V., Parent, A., Parent, M., 2011. Serotonin and dopamine striatal innervation in Parkinson's disease and Huntington's chorea. Parkinsonism & Related disorders 17, 593-598.

Bernheimer, H., Birkmayer, W., Hornykiewicz, O., 1961. [Distribution of 5-hydroxytryptamine (serotonin) in the human brain and its behavior in patients with Parkinson's syndrome]. Klinische Wochenschrift 39, 1056-1059.

Braak, H., Del Tredici, K., Rub, U., de Vos, R.A., Jansen Steur, E.N., Braak, E., 2003. Staging of brain pathology related to sporadic Parkinson's disease. Neurobiology of Aging 24, 197-211.

Brighina, L., Riva, C., Bertola, F., Saracchi, E., Fermi, S., Goldwurm, S., Ferrarese, C., 2013. Analysis of vesicular monoamine transporter 2 polymorphisms in Parkinson's disease. Neurobiology of Aging.

Canal, C.E., Morgan, D., 2012. Head-twitch response in rodents induced by the hallucinogen 2,5-dimethoxy-4-iodoamphetamine: a comprehensive history, a re-

evaluation of mechanisms, and its utility as a model. Drug testing and analysis 4, 556-576.

Caudle, W.M., Richardson, J.R., Wang, M.Z., Taylor, T.N., Guillot, T.S., McCormack, A.L., Colebrooke, R.E., Di Monte, D.A., Emson, P.C., Miller, G.W., 2007. Reduced vesicular storage of dopamine causes progressive nigrostriatal neurodegeneration. J Neurosci 27, 8138-8148.

Chan, C.S., Guzman, J.N., Ilijic, E., Mercer, J.N., Rick, C., Tkatch, T., Meredith, G.E., Surmeier, D.J., 2007. 'Rejuvenation' protects neurons in mouse models of Parkinson's disease. Nature 447, 1081-1086.

Corne, S.J., Pickering, R.W., Warner, B.T., 1963. A method for assessing the effects of drugs on the central actions of 5-hydroxytryptamine. British journal of Pharmacology and Chemotherapy 20, 106-120.

Cowen, P.J., Power, A.C., Ware, C.J., Anderson, I.M., 1994. 5-HT1A receptor sensitivity in major depression. A neuroendocrine study with buspirone. The British Journal of Psychiatry : the Journal of Mental Science 164, 372-379.

Crino, P.B., Vogt, B.A., Chen, J.C., Volicer, L., 1989. Neurotoxic effects of partially oxidized serotonin: tryptamine-4,5-dione. Brain Res 504, 247-257.

D'Amato, R.J., Zweig, R.M., Whitehouse, P.J., Wenk, G.L., Singer, H.S., Mayeux, R., Price, D.L., Snyder, S.H., 1987. Aminergic systems in Alzheimer's disease and Parkinson's disease. Annals of Neurology 22, 229-236.

Ding, Y., Restrepo, J., Won, L., Hwang, D.Y., Kim, K.S., Kang, U.J., 2007. Chronic 3,4-dihydroxyphenylalanine treatment induces dyskinesia in aphakia mice, a novel genetic model of Parkinson's disease. Neurobiol Dis 27, 11-23.

Eisenhofer, G., Kopin, I.J., Goldstein, D.S., 2004. Catecholamine Metabolism: A Contemporary View with Implications for Physiology and Medicine. Pharmacological Reviews 56, 331-349.

Fahn, S., 2003. Description of Parkinson's Disease as a Clinical Syndrome. Annals of the New York Academy of Sciences 991, 1-14.

German, D.C., Manaye, K.F., Sonsalla, P.K., Brooks, B.A., 1992. Midbrain Dopaminergic Cell Loss in Parkinson's Disease and MPTP-Induced Parkinsonism: Sparing of Calbindin-D25k—Containing Cells. Annals of the New York Academy of Sciences 648, 42-62.

German, D.C., Sonsalla, P.K., 2003. A role for the vesicular monoamine transporter (VMAT2) in Parkinson's disease, in: Graybiel, A., Delong, M., Kitai, S. (Eds.), The Basal Ganglia VI. pp. 131-137.

Glatt, C.E., Wahner, A.D., White, D.J., Ruiz-Linares, A., Ritz, B., 2006. Gain-of-function haplotypes in the vesicular monoamine transporter promoter are protective for Parkinson disease in women. Human Molecular Genetics 15, 299-305.

Graham, D.G., Tiffany, S.M., Bell, W.R., Gutknecht, W.F., 1978. Autoxidation Versus Covalent Binding of Quinones as Mechanism of Toxicity of Dopamine, 6-Hydroxydopamine, and Related Compounds toward C1300-Neuroblastoma Cells Invitro. Molecular Pharmacology 14, 644-653.

Halliday, G.M., Blumbergs, P.C., Cotton, R.G., Blessing, W.W., Geffen, L.B., 1990. Loss of brainstem serotonin- and substance P-containing neurons in Parkinson's disease. Brain Res 510, 104-107.

Hastings, T.G., Lewis, D.A., Zigmond, M.J., 1996. Role of oxidation in the neurotoxic effects of intrastriatal dopamine injections. Proc Natl Acad Sci U S A 93, 1956-1961.

Jacobsen, J.P., Medvedev, I.O., Caron, M.G., 2012a. The 5-HT deficiency theory of depression: perspectives from a naturalistic 5-HT deficiency model, the tryptophan hydroxylase 2Arg439His knockin mouse. Philosophical transactions of the Royal Society of London. Series B, Biological sciences 367, 2444-2459.

Jacobsen, J.P.R., Siesser, W.B., Sachs, B.D., Peterson, S., Cools, M.J., Setola, V., Folgering, J.H.A., Flik, G., Caron, M.G., 2012b. Deficient serotonin neurotransmission and depression-like serotonin biomarker alterations in tryptophan hydroxylase 2 (Tph2) loss-of-function mice. Molecular Psychiatry. 17, 694-704.

Jiang, X.R., Wrona, M.Z., Dryhurst, G., 1999. Tryptamine-4,5-dione, a putative endotoxic metabolite of the superoxide-mediated oxidation of serotonin, is a mitochondrial toxin: Possible implications in neurodegenerative brain disorders. Chemical Research in Toxicology 12, 429-436.

Kish, S.J., Tong, J., Hornykiewicz, O., Rajput, A., Chang, L.-J., Guttman, M., Furukawa, Y., 2008. Preferential loss of serotonin markers in caudate versus putamen in Parkinson's disease.

Lesch, K.P., 1991. 5-HT1A receptor responsivity in anxiety disorders and depression. Prog Neuropsychopharmacol Biol Psychiatry 15, 723-733.

Li, Q., Wichems, C., Heils, A., Van De Kar, L.D., Lesch, K.P., Murphy, D.L., 1999. Reduction of 5-hydroxytryptamine (5-HT)(1A)-mediated temperature and

neuroendocrine responses and 5-HT(1A) binding sites in 5-HT transporter knockout mice. The Journal of Pharmacology and Experimental Therapeutics 291, 999-1007.

Lohr, K.M., Bernstein, A.I., Stout, K.A., Dunn, A.R., Lazo, C.R., Alter, S.P., Wang, M., Li, Y., Fan, X., Hess, E.J., Yi, H., Vecchio, L.M., Goldstein, D.S., Guillot, T.S., Salahpour, A., Miller, G.W., 2014. Increased vesicular monoamine transporter enhances dopamine release and opposes Parkinson disease-related neurodegeneration in vivo. Proceedings of the National Academy of Sciences 111, 9977-9982.

Luellen, B.A., Szapacs, M.E., Materese, C.K., Andrews, A.M., 2006. The neurotoxin 2'-NH2-MPTP degenerates serotonin axons and evokes increases in hippocampal BDNF. Neuropharmacology 50, 297-308.

Martin, K.F., Phillips, I., Hearson, M., Prow, M.R., Heal, D.J., 1992. Characterization of 8-OH-DPAT-induced hypothermia in mice as a 5-HT1A autoreceptor response and its evaluation as a model to selectively identify antidepressants. Br J Pharmacol 107, 15-21.

Miller, G.W., Staley, J.K., Heilman, C.J., Perez, J.T., Mash, D.C., Rye, D.B., Levey, A.I., 1997. Immunochemical analysis of dopamine transporter protein in Parkinson's disease. Annals of neurology 41, 530-539.

Mooslehner, K.A., Chan, P.M., Xu, W., Liu, L., Smadja, C., Humby, T., Allen, N.D., Wilkinson, L.S., Emson, P.C., 2001. Mice with Very Low Expression of the Vesicular Monoamine Transporter 2 Gene Survive into Adulthood: Potential Mouse Model for Parkinsonism. Molecular and Cellular Biology 21, 5321-5331.

Mosharov, E.V., Larsen, K.E., Kanter, E., Phillips, K.A., Wilson, K., Schmitz, Y., Krantz, D.E., Kobayashi, K., Edwards, R.H., Sulzer, D., 2009. Interplay between cytosolic dopamine, calcium, and α-synuclein causes selective death of substantia nigra neurons. Neuron 62, 218-229.

Mosienko, V., Matthes, S., Hirth, N., Beis, D., Flinders, M., Bader, M., Hansson, A.C., Alenina, N., 2014. Adaptive changes in serotonin metabolism preserve normal behavior in mice with reduced TPH2 activity. Neuropharmacology 85, 73-80.

Narboux-Neme, N., Sagne, C., Doly, S., Diaz, S.L., Martin, C.B., Angenard, G., Martres, M.P., Giros, B., Hamon, M., Lanfumey, L., Gaspar, P., Mongeau, R., 2011. Severe serotonin depletion after conditional deletion of the vesicular monoamine transporter 2 gene in serotonin neurons: neural and behavioral consequences. Neuropsychopharmacology : official publication of the American College of Neuropsychopharmacology 36, 2538-2550.

Navailles, S., Carta, M., Guthrie, M., De Deurwaerdere, P., 2011. L-DOPA and serotonergic neurons: functional implication and therapeutic perspectives in Parkinson's disease. Central nervous system agents in medicinal chemistry 11, 305-320.

Nilsson, F.M., Kessing, L.V., Sørensen, T.M., Andersen, P.K., Bolwig, T.G., 2002. Major depressive disorder in Parkinson's disease: a register-based study. Acta Psychiatrica Scandinavica 106, 202-211.

Ohara, K., Kondo, N., 1998. Changes of monoamines in post-mortem brains from patients with diffuse Lewy body disease. Prog Neuropsychopharmacol Biol Psychiatry 22, 311-317.

Patel, J., Mooslehner, K.A., Chan, P.M., Emson, P.C., Stamford, J.A., 2003. Presynaptic control of striatal dopamine neurotransmission in adult vesicular monoamine transporter 2 (VMAT2) mutant mice. J Neurochem 85, 898-910.

Paulus, W., Jellinger, K., 1991. The Neuropathologic Basis of Different Clinical Subgroups of Parkinsons-Disease. J. Neuropathol. Exp. Neurol. 50, 743-755.

Pifl, C., Rajput, A., Reither, H., Blesa, J., Cavada, C., Obeso, J.A., Rajput, A.H., Hornykiewicz, O., 2014. Is Parkinson's Disease a Vesicular Dopamine Storage Disorder? Evidence from a Study in Isolated Synaptic Vesicles of Human and Nonhuman Primate Striatum. The Journal of Neuroscience 34, 8210-8218.

Politis, M., Oertel, W.H., Wu, K., Quinn, N.P., Pogarell, O., Brooks, D.J., Bjorklund, A., Lindvall, O., Piccini, P., 2011. Graft-induced dyskinesias in Parkinson's disease: High striatal serotonin/dopamine transporter ratio. Mov Disord 26, 1997-2003.

Politis, M., Wu, K., Loane, C., Brooks, D.J., Kiferle, L., Turkheimer, F.E., Bain, P., Molloy, S., Piccini, P., 2014. Serotonergic mechanisms responsible for levodopa-induced dyskinesias in Parkinson's disease patients. J Clin Invest 124, 1340-1349.

Politis, M., Wu, K., Loane, C., Kiferle, L., Molloy, S., Brooks, D.J., Piccini, P., 2010. Staging of serotonergic dysfunction in Parkinson's Disease: An in vivo 11C-DASB PET study. Neurobiology of Disease 40, 216-221.

Rilstone, J.J., Alkhater, R.A., Minassian, B.A., 2013. Brain dopamine-serotonin vesicular transport disease and its treatment. N Engl J Med. 368(6): 543-550.

Sala, G., Brighina, L., Saracchi, E., Fermi, S., Riva, C., Carrozza, V., Pirovano, M., Ferrarese, C., 2010. Vesicular monoamine transporter 2 mRNA levels are reduced

in platelets from patients with Parkinson's disease. J. Neural Transm. 117, 1093-1098.

Shelton, R.C., Sanders-Bush, E., Manier, D.H., Lewis, D.A., 2009. Elevated 5-HT 2A receptors in postmortem prefrontal cortex in major depression is associated with reduced activity of protein kinase A. Neuroscience 158, 1406-1415.

Taylor, T.N., Alter, S.P., Wang, M., Goldstein, D.S., Miller, G.W., 2014. Reduced vesicular storage of catecholamines causes progressive degeneration in the locus ceruleus. Neuropharmacology 76 Pt A, 97-105.

Taylor, T.N., Caudle, W.M., Shepherd, K.R., Noorian, A., Jackson, C.R., Iuvone, P.M., Weinshenker, D., Greene, J.G., Miller, G.W., 2009. Nonmotor symptoms of Parkinson's disease revealed in an animal model with reduced monoamine storage capacity. J Neurosci 29, 8103-8113.

Ulusoy, A., Björklund, T., Buck, K., Kirik, D., 2012. Dysregulated dopamine storage increases the vulnerability to α-synuclein in nigral neurons. Neurobiology of Disease 47, 367-377.

West, M.J., Slomianka, L., Gundersen, H.J., 1991. Unbiased stereological estimation of the total number of neurons in the subdivisions of the rat hippocampus using the optical fractionator. The Anatomical Record 231, 482-497.

# CHAPTER 5

# Conclusions and Reflections

## Conclusion

At the outset of this dissertation, there was an appreciation for the potential of reduced vesicular function to contribute to degeneration of the SNpc in Parkinson's disease. While noradrenergic and serotonergic pathology have long been recognized in PD, very little attention was directed toward understanding the connection between vesicular function and the pathophysiology of the other nuclei affected in PD. Thus, the goal of this dissertation was to investigate the effect of reduced vesicular function on the noradrenergic and serotonergic systems in the VMAT2 LO mouse model of PD.

During the course of my dissertation, several key clinical findings emerged that not only demonstrate the role of disrupted VMAT2 in nigral degeneration, but also support its role in disrupting the noradrenergic and serotonergic systems of PD patients. The translational relevance of the VMAT2 LO mouse model to nigral pathology was most recently called into attention by the work of Christian Pifl and Oleh Hornykiewicz (2014). Fifty-three years after Hornykiewicz convinced Walther Birkmayer to inject levodopa into PD patients, Pifl and colleagues resurrected functional synaptic vesicles from striata of post mortem cases and demonstrated that VMAT2 is functionally impaired in PD. While it was known that reduced VMAT2 expression may be associated with neuronal susceptibility in PD (Miller et al., 1999), this work demonstrated there is indeed a functional impairment in human PD. Meanwhile, research by David Goldstein and Irwin Kopin (described in Chapter 4) would reveal that vesicular uptake of norepinephrine contributes to dysautonomia in the peripheral nervous system. While Hornykiewicz' team demonstrated a correlation between VMAT2 function and PD pathology, a clinical case report from Saudi Arabia demonstrated that loss-of-function

mutation in *SLC18A2* actually caused infant-onset Parkinsonism, orthostatic hypotension, and psychiatric disturbances in a consanguineous familial cohort.

In my study of the consequences of reduced vesicular function in the noradrenergic and serotonergic systems of VMAT2 LO mice, I found several findings to be particularly intriguing. As described in Chapters 2 and 3, VMAT2 LO mice undergo accelerated, age-related degeneration of the locus ceruleus preceding the SNpc. This staging, coupled with the complete sparing of the dopaminergic ventral tegmental area (a region less preferentially affected in PD) challenged my initial assumptions about the causal relationship between cytosolic monoamine breakdown and neuronal vulnerability. In my serotonin aim, I observed that despite reductions in transmitter and increased turnover, the dorsal raphe and its efferent innervation are unaffected in VMAT2 LO mice. However, the consequent disruptions in the neurophysiology have implications applicable to the study of PD and comorbid depression.

**On the staging of LC and SN loss and the relative toxicities of cytosolic DA and NE**

The progressive staging of LC and then SNpc cell loss in VMAT2 LO mice follows the progression of Lewy pathology (LP) described by Braak and colleagues (Braak et al., 2003). Thus, the comparison of VMAT2 catecholamine pathology to Braak staging was met favorably in peer review and professional presentations. However, Lewy pathology does not predict cell death, nor do our mice exhibit Lewy pathology. Moreover, in humans, degeneration of the LC does not correspond with disease progression. VMAT2 LO pathology also contrasts with the staging and susceptibility to degeneration in the LC and SNpc of MPTP models, in which the SNpc is much more

vulnerable. This clear and consistent contrast in VMAT2 LO mice has thus prompted discussion of the relative toxicities of DA and NE, and the relative susceptibility of the LC and SNpc to degeneration.

The relative toxicities of cytosolic DA and NE breakdown may at first seem germane to this topic. With respect to enzymatic metabolism (Figure 5-1), DA and NE are both oxidatively deaminated by MAO, yielding reactive aldehyde intermediates and $H_20_2$. While DOPAL is reactive and correlates with PD pathology in humans, DOPEGAL is even more unstable, a characteristic which has precluded reproducible attempts to assay its presence in tissue or test its toxicity *in vitro* (personal communication, David Goldstein). On the other hand, the autoxidation pathways of DA and NE are similar, with the DA and NE quinone species following parallel oxidation and cyclization pathways in the formation of dihydroxyindole, the monomeric unit of neuromelanin. A means by which to test the relative toxicities of enzymatic versus autoxidative breakdown would be to perform a study in which VMAT2 LO mice were chronically treated with an MAO-A inhibitor, which would hypothetically increase autoxidative breakdown and reduce enzymatic metabolism of the monoamine. If toxicity can be ascribed to either breakdown pathway, one would expect MAO-A inhibition to alter the extent of catecholaminergic degeneration in VMAT2 LO mice.

The relative toxicities of DA and NE become a moot point when we consider the overall cytosolic burden faced by noradrenergic neurons, in contrast to dopaminergic neurons. Canonically, DA neurons synthesize, uptake, and metabolize DA. By virtue of biological parsimony, NE neurons synthesize and uptake DA as a precursor for NE. Moreover, the NET has greater affinity for DA than it does NE, and its affinity for DA

exceeds that of DAT. So regardless of the relative toxicities of DA and NE, noradrenergic neurons are subject to the cytosolic toxicity of both transmitters. The observations that human LC neurons exhibit neuromelanin pigmentation earlier than SNpc neurons (Foley and Baxter, 1958) suggest that noradrenergic neurons are subject to greater oxidative burden.

From an evolutionary perspective, an adaptive mechanism for dealing with increased cytosolic catecholamine burden in noradrenergic neurons would be to increase vesicular sequestration capabilities. Indeed, such capability has been demonstrated in tracking the uptake and toxicity of radiolabeled MPP+ (Speciale et al., 1998). In both mice and monkeys, the LC is less preferentially affected by MPTP, despite demonstrating greater uptake of MPP+. Pharmacological interrogation has revealed that the increased uptake corresponds with increased sequestration of MPP+ into VMAT2-containing organelles.

The staging of catecholaminergic cell loss in VMAT2 LO mice is a reversal of what has been observed in MPTP models. This is a direct consequence of the VMAT2 LO phenotype. While wild-type mice have significantly greater VMAT2 expression in LC neurons versus SNpc neurons, VMAT2 LO mice have comparably low expression of VMAT2 in both nuclei. In retrospect, these contrasts are evident in the relative fluorescence of VMAT2 labeling in Figure 2-1. Thus, the SNpc and LC of VMAT2 LO mice are both equally unprotected against their respective cytosolic catecholamine burdens; under the concomitant burden of cytosolic DA and NE, the VMAT2 LO LC is the first to fall.

**A challenge to the cytosolic catecholamine hypothesis: the invincible VTA**

Sparing of VTA in VMAT2 LO mice challenges the hypothesis that the ratio of DAT to VMAT2 expression dictates neuronal vulnerability in Parkinsonian degeneration. This hypothesis is well supported by the relative DAT and VMAT2 expression levels in the putamen and nucleus accumbens of MPTP monkeys and PD patients. However, the VTA of VMAT2 LO mice show absolutely no age-related degeneration, despite a drastically increased ratio of DAT to VMAT2, suggesting another mechanism of neurotoxicity.

A key finding that reconciles these disparities was Mosharov and colleagues' demonstration that cytosolic calcium, α-synuclein, and cytosolic dopamine collectively drive oxidative stress and neuronal death in midbrain dopamine neurons (Pifl et al., 2014). Mechanistically, Mosharov showed that increased cytosolic calcium influx caused an increase in cytosolic DA. VTA neurons differ drastically from SNpc neurons in their cytosolic calcium dynamics. SNpc neurons utilize calcium channels to drive autonomous pacemaking. In contrast, VTA neurons rely on sodium channels for pacemaking and richly express the calcium-buffering protein calbindin. Mosharov demonstrated that VTA neurons are protected from this toxicity, and that VMAT2+/- SNpc neurons are more susceptible than wild-type neurons to these three challenges.

A key factor that differentiates the VTA from the SNpc (as well as the LC), is that it relies on calcium influx through voltage-gated calcium channels to drive its autonomous pacemaking (Surmeier et al., 2005). Calcium may thus be a required component of neurotoxicity in VMAT2 LO mice. There is strong support for increased Ca++ in age-related neurodegeneration. A reconciled view of these hypotheses could

hold that excessive cytosolic calcium drives neurotoxicity by its own accord, while insufficient vesicular function results in increased cytosolic burden, resulting in amplified or accelerated neurodegeneration. Why is the VTA so comparatively robust? From an evolutionary perspective, it could be posited that natural selection strongly favors preservation of a brain region that reinforces our drive to mate, whereas degeneration of fine motor skills only affected our forebearers long after they become evolutionarily irrelevant.

Given the proposed toxic interplay between cytosolic catecholamines and calcium in the LC and SNpc, a potential neuroprotective strategy would be to attenuate calcium-influx. Metabotropic glutamate receptors (mGLUR4/5) have emerged as therapeutic targets in PD, due to their role in mediating hyperexcitability and their selective expression in catecholamine neurons and the basal ganglia (Smith et al., 2012). The mGLUR5 antagonist MTEP has been demonstrated to provide robust neuroprotection to the SNpc and LC of MPTP-treated monkeys (Masilamoni et al., 2011). An experiment to test the hypothesis that calcium-catecholamine interplay drives the VMAT2 LO degenerative phenotype would be to chronically treat VMAT2 LO mice in an aging study to determine if MTEP can protect against age-related catecholaminergic degeneration. MGLUR5 negative allosteric modulators (NAM) have also shown promise in treating levodopa-induced dyskinesia. Addex Therapeutics recently launched a Phase III trial to evaluate the efficacy of the mGLUR5 NAM dipraglurant in treating dyskinesia in Parkinson's disease. It will be interesting to see if post-hoc analyses reveal evidence of neuroprotection in PD patients. Interestingly, dipraglurant has also shown preclinical

efficacy in animal models of depression; at the time of this writing, Addex is also initiating Phase I clinical trials for dipraglurant in treatment-resistant depression.

Shifting to another pipeline therapeutic, Newron's safinamide has passed Phase III clinical trials as an add-on therapeutic in managing the symptoms of late-stage Parkinson's disease (Schapira et al., 2013), and is poised to launch in 2015. Safinimide is a multi-mechanism PD therapeutic that selectively inhibits MAO-B (over MAO-A), inhibits DA reuptake, and inhibits glutamatergic release. Thus, safinamide would hypothetically raise concentrations of total DA (by blocking glial DA metabolism) preferentially in the synapse (DAT blockade), and attenuate cytosolic calcium-influx. Safinamide would thus block multiple routes of cytosolic DAergic toxicity discussed in this dissertation. Currently, Teva's selective MAO-B inhibitor rasagiline is the front-running PD monotherapy for early Parkinson's disease. A delayed-start clinical trial assessing UPDRS scores of PD patients has produced data that suggests (inconclusively) that rasagiline is neuroprotective. It will be interesting to see if safinimide shows this effect, and if it will supplant rasagiline as a front line PD monotherapy.

**Serotonergic resilience**

The lack of serotonergic neurodegeneration did not support the hypothesis that increased cytosolic serotonin would cause neurotoxicity. However, pathology within the raphe nuclei is a variable and inconsistent feature of PD. I did observe neurochemical depletion and alterations in serotonergic signaling that correlate to depression in humans, which supports a link between reduced vesicular function and the nonmotor symptoms of PD. PD features highly comorbid depression, at rates that are significantly greater than

in patients with chronic illness. PD and depression both feature reductions in extracellular serotonin; VMAT2 LO mice have reductions in synaptic serotonin release and tissue content.

While degeneration of the serotonergic raphe occurs in PD, the most saliently affected nuclei are the median raphe and raphe obscurus, with the latter providing descending serotonergic innervation (Halliday, et al., 1990). A recent investigation (co-authored by Glenda Halliday) specifically examined the number of serotonergic neurons in the dorsal of raphe of post mortem PD cases, as well as striatal SERT abundance and 5-HT content (Cheshire et al., 2015), effectively providing the same measures I reported in my investigation in VMAT2 LO mice. Cheshire and colleagues reported that PD patients exhibited a significant reduction in striatal 5-HT (approximately 70% of caudate 5-HT), but exhibited no loss in SERT abundance in the striatum nor quantity of serotonergic neurons within the dorsal raphe, compared to control cases. Thus, to the measures I have explored, reduced vesicular function in mice faithfully capitulates serotonergic pathology in PD. Examination of the median raphe and raphe obscurus will provide further insight as to whether reduced vesicular function can cause serotonergic Parkinsonian degeneration.

My hypothesis that serotonergic neurons would also degenerate was based on the fact that 5-HT undergoes parallel synthetic and breakdown pathways to the catecholamines, and that all three monoamine systems typically degenerate to some extent in humans (Figure 5-1). However, there has been little investigation into the toxicity of cytosolic 5-HT breakdown. A recent report indicated that 5-HIAL can stabilize alpha-synuclein *in vitro*, which could conceivably contribute to Lewy Pathology

in PD. However, no reports have sufficiently demonstrated that a physiologically relevant excess of (enzymatic or autoxidative) 5-HT breakdown can exert neurotoxicity. If neurotoxicity could occur from cytosolic 5-HT, a possible source of protection may be in the raphe's expression of serotonin binding protein (SBP), which covalently binds iron-oxidized serotonin (Vauquelin et al., 1994); however, there has been no investigation into this protein's neuroprotective role.

The preservation of serotonergic innervation in the VMAT2 LO striatum provoked my brief exploration of L-DOPA induced dyskinesia in VMAT2 LO mice. In PD, striatal SERT abundance and SERT/DAT ratios have been shown to correlate with levodopa-induced dyskinesia severity (Politis, 2012). The preservation of serotonergic innervation against a setting of dopaminergic degeneration in the striatum led me to hypothesize that VMAT2 LO mice might express L-DOPA induced dyskinesia. Interestingly Pitx3-deficient *Aphakia* mouse exhibits similar striatal innervation pattern, (though this occurs from a developmental rather than degenerative defect) and expresses levodopa-induced dyskinesia in the absence of any chemical lesion. I reproduced this study but observed no AIMS behavior in VMAT2 LO mice. I ascribe the lack of AIMS in VMAT2 LO mice to the inability of their 5-HT neurons to sufficiently transport dopamine into synaptic vesicles, even if they are synthesizing it from exogenous levodopa. Conditional genetic suppression of VMAT2 in dopamine neurons would provide a means by which to test this hypothesis. One group has generated conditional knockouts of VMAT2 in 5-HT neurons using a *cre-lox* system, placing *cre* expression under control of the *Slc6a4* (SERT) promoter (Narboux-Neme et al., 2011). However, attempts to knockout VMAT2 selectively in DA neurons have resulted in postnatal

lethality, just as in global knockout animals. By selectively knocking-in the VMAT2 LO transgene in dopaminergic neuron, one could explore the effects of noradrenergic and serotonergic compensation in a setting of striatal dopaminergic degeneration.

Another observation that bears relevance to levodopa-induced dyskinesia is that VMAT2 LO mice exhibit abolished response to the 5-HT1A agonist 8-OH-DPAT and increased 5-HT2 receptor response (discussed in chapter 4 as a features of human depression). This is interesting from a therapeutic perspective, as 5-HT1A agonists and 5-HT2 antagonists have been explored as targets in levodopa-induced dyskinesia. 5-HT2 antagonists have not fared well in clinical trials. On the other hand, the 5-HT1A agonist piclozotan has shown promise as an anti-dyskinetic therapy in one multi-center Phase II clinical trial, however these results have not been replicated and clinical development of piclozotan has since been terminated. A potential reason for the lack of clinical efficacy may lie in the fact that patients with Parkinson's disease have reduced levels of serotonin (inferred from 5-HIAA in CSF), and those with depression have been shown to have even less (Kostic et al., 1987). Thus it is conceivable that 5-HT1A sensitivity is reduced in all of Parkinson's disease, and that a depressive state or CSF 5-HIAA levels may be predictive of a dyskinetic patient's therapeutic response to a 5HT1A agonist. This idea can be tested in mice by assessing the anti-dyskinetic effects of piclozotan in 6-OHDA-lesioned TPH2 LOF (which also feature 5-HT1A desensitization) and wild-type mice. This hypothesis would be supported if the TPH2 LOF mice required a greater dose (than their wild-type littermates) of piclozotan in order to suppress dyskinesia.

## Concluding Remarks

This dissertation supports a role for reduced vesicular function in the extranigral pathology and nonmotor symptoms of PD. In light of recent clinical data demonstrating reduced vesicular function in the nigral DA neurons and noradrenergic nerves of the sympathetic nervous system, impaired vesicular function is in all likelihood a pathological event contributing to neurodegeneration in human PD. These data support the rationale of increasing vesicular function as a means by which to achieve neuroprotection in PD.

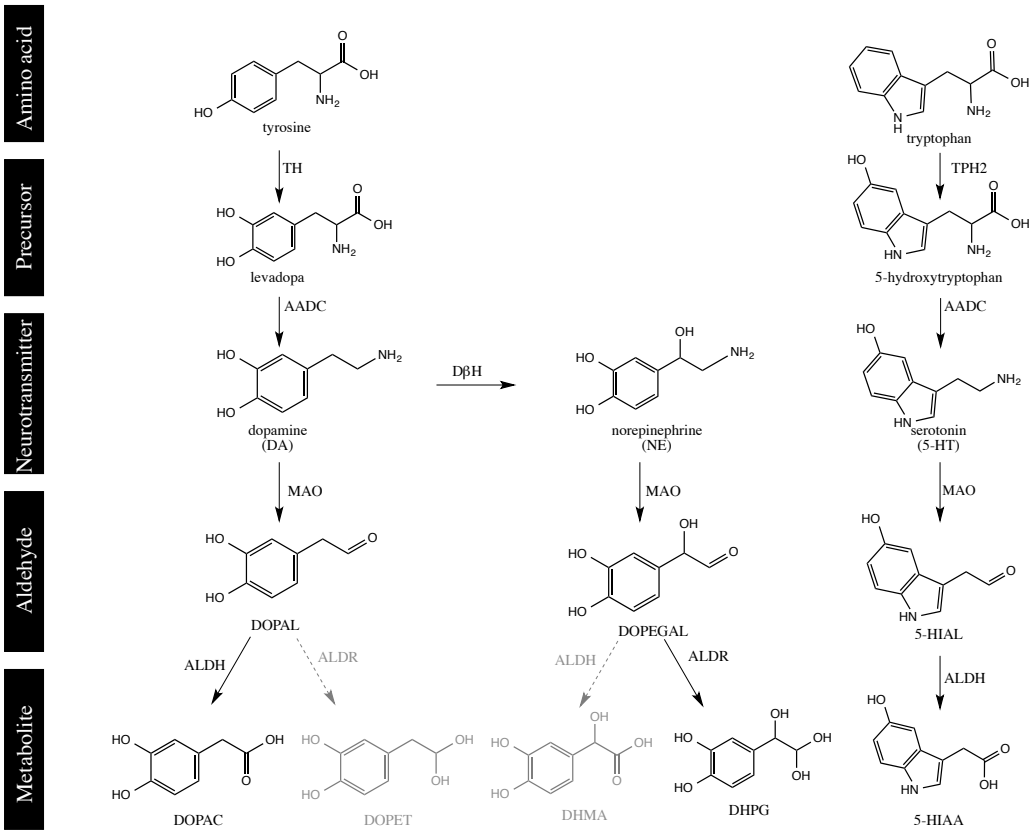
Amino acid
Precursor
Neurotransmitter
Aldehyde
Metabolite
tyrosine
TH
levadopa
AADC
dopamine
(DA)
MAO
DOPAL
ALDH
ALDR
DOPAC
DOPET
DβH
norepinephrine
(NE)
MAO
DOPEGAL
ALDH
ALDR
DHMA
DHPG
tryptophan
TPH2
5-hydroxytryptophan
AADC
serotonin
(5-HT)
MAO
5-HIAL
ALDH
5-HIAA

Figure 5-1. Neuronal pathways for the biosynthesis and metabolic breakdown of monoamines. Dopamine, norepinephrine, and serotonin neurons utilize amino acids to produce their cognate neurotransmitters. **Left.** In dopamine neurons tyrosine hydroxylase (TH) converts l-tyrosine (TYR) to levadopa (L-DOPA). L-amino acid decarboxylase converts L-DOPA to dopamine (DA), which is then sequestered into synaptic vesicles by VMAT2. In noradrenergic neurons, dopamine-β-hydroxylase converts DA to norepinephrine (NE). Monoamines are enzymatically deaminated by monoamine oxidase (MAO) to form reactive aldehyde intermediates: DA is deaminated to DOPAL, NE is deaminated to DOPEGAL. DOPAL and DOPEGAL are detoxified by aldehyde dehydrogenase and aldose reductase, respectively to form didydroxyphenylacetic acid (DOPAC) and dihydroxyphenylglycol (DHPG). Serotonin metabolism occurs similarly, with several key distinctions. The amino acid tryptophan is hydroxylated by tryptophan hydroxylase (TPH2, which bears high homology to TH) to form 5-hydroxytrypotphan (5-HTP). Like L-DOPA, 5-HTP is decarboxylated by AADC, yielding serotonin (5-hydroxytryptamine, 5-HT). MAO metabolizes 5-HT to 5-hydroxyindolealdehyde (5-HIAL), which ALDH in turn converts to hydroxyindoleacetic acid (5-HIAA).

**References**


Braak H, Del Tredici K, Rub U, de Vos RA, Jansen Steur EN, and Braak E (2003) Staging of brain pathology related to sporadic Parkinson's disease. *Neurobiol Aging* **24**:197–211.

Kostic VS, Djuricic BM, Covickovic-Sternic N, Bumbasirevic L, Nikolic M and Mrsulja BB (1987) Depression and Parkinson's disease: possible role of serotonergic mechanisms. *Journal of Neurology* **234**(2): 94-96.

Masilamoni GJ, Bogenpohl JW, Alagille D, Delevich K, Tamagnan G, Votaw JR, Wichmann T, and Smith Y (2011) Metabotropic glutamate receptor 5 antagonist protects dopaminergic and noradrenergic neurons from degeneration in MPTP-treated monkeys. *Brain* **134**:2057–2073.

Miller GW, Gainetdinov RR, Levey AI and Caron MG (1999) Dopamine transporters and neuronal injury. *Trends in Pharmacological Sciences* **20**(10): 424-429.

Mosharov EV, Larsen KE, Kanter E, Phillips KA, Wilson K, Schmitz Y, Krantz DE, Kobayashi K, Edwards RH and Sulzer D (2009) Interplay between Cytosolic Dopamine, Calcium, and α-Synuclein Causes Selective Death of Substantia Nigra Neurons. *Neuron* **62**(2): 218-229.

Pifl C, Rajput A, Reither H, Blesa J, Cavada C, Obeso JA, Rajput AH, and Hornykiewicz O (2014) Is Parkinson's Disease a Vesicular Dopamine Storage Disorder? Evidence from a Study in Isolated Synaptic Vesicles of Human and Nonhuman Primate Striatum. J Neurosci 34:8210–8218.

Rilstone JJ, Alkhater RA, and Minassian BA (2013) Brain Dopamine-Serotonin Vesicular Transport Disease and Its Treatment. N Engl J Med. 368(6): 543-550.

Schapira AH, Stocchi F, Borgohain R, Onofrj M, Bhatt M, Lorenzana P, Lucini V, Giuliani R and Anand R (2013) Long-term efficacy and safety of safinamide as add-on therapy in early Parkinson's disease. *European Journal of Neurology : the Official Journal of the European Federation of Neurological Societies* **20**(2): 271-280.

Smith Y, Wichmann T, Factor SA, and DeLong MR (2012) Parkinson's disease therapeutics: new developments and challenges since the introduction of levodopa. *Neuropsychopharmacology* **37**:213–246.

Speciale SG, Liang CL, Sonsalla PK, Edwards RH and German DC (1998) The neurotoxin 1-methyl-4-phenylpyridinium is sequestered within neurons that contain the vesicular monoamine transporter. *Neuroscience* **84**(4): 1177-1185.

Surmeier DJ, Mercer JN and Chan CS (2005) Autonomous pacemakers in the basal ganglia: who needs excitatory synapses anyway? *Current Opinion in Neurobiology* **15**(3): 312-318.

Vauquelin G, Del Rio MJ and Pardo CV (1994) Serotonin Binding Proteins: An In Vitro Model System for Monoamine-related Neurotoxicitya. *Annals of the New York Academy of Sciences* **738**(1): 408-418.

# APPENDIX:

# Adaptation of CLARITY: Hydrogel Tissue Clearing on a Shoestring

## Introduction

Through the course of this dissertation, I had the pleasure of exploring a few side projects that ultimately did not weave into the body of my dissertation aims. For me, the most interesting of these was my adaptation of the CLARITY tissue clearing protocol.

In spring of 2013, CLARITY emerged as a tissue clearing technique that allowed the structural and molecular interrogation of intact, transparent, biological tissues. CLARITY was developed by Kwanghun Chung in the laboratory of Karl Deisseroth at Stanford University (Chung et al., 2013). Tissue clearing is a means by which one removes lipids from tissue while maintaining its structural integrity. In effect, this process renders tissues permeable to light and antibody penetration, while maintaining the structural integrity and presence of molecules with linkable amide-groups (i.e. proteins). CLARITY permits the ability to study spatial and quantitative interrogation of intact biological tissues. Alternative approaches to this goal carry disadvantages of requiring time-intensive sectioning and reconstruction, loss of native molecules after permeabilization, and limited potential for tissue re-use. CLARITY surmounts of these challenges (Kim et al., 2013).

The "CLARITY" moniker was retrofitted as an acronym for "**C**lear **L**ipid-exchanged **A**crylamide-hyridized **R**igid **I**maging/**I**mmunostaiing/***In situ*** hybridization-compatible **T**issue-h**Y**drogel". In principle, the technique involves perfusing biological tissue in a liquid hydrogel monomer composed of acrylamides and formaldehyde, embedding the tissue by polymerizing the hydrogel, and extracting the lipids via electrophoresis or passive lipid diffusion. Because the hydrogel forms cross-links with the amide groups of amino acids, all structural and functional proteins remain in the

clarified hydrogel matrix. The resulting hydrogel-tissue hybrid is completely transparent and permeable to antibodies. Following imaging, clarified hydrogel tissue can be re-cleared of IHC antibodies and used in multiple subsequent rounds of immunohistochemical labeling.

At the time of CLARITY's initial report, I was tasked with performing stereology of the dorsal raphe in mice to determine if the VMAT2 LO genotype resulted in age-related serotonergic cell loss. In contrast to the SNpc and LC, several characteristics of the dorsal raphe make it particularly challenging to assess by stereology. It is a narrow midline structure, whereas the others are broad and bilateral; this means that in a given coronal slice, there is less ROI area, and fewer neurons to count. Between the different subregions of the dorsal raphe, neuronal density is variable, thus requiring differentiation of the ROIs to avoid distorting stereological estimate. Lastly, the coronal shape of the DR varies abruptly while progressing in the rostral-caudal direction, thus requiring flawless sectioning, sampling, and ordering in tissue arrangement and precluding the use of the stereology's software to account for missing sections or allow ordering error.

During a meeting with Gary in which I lamented the challenges of dorsal raphe topography, he suggested I consider CLARITY. Thus began a summer-long creative break of improvisation, salvage, and chemical spills. I later traveled to Palo Alto to train in the Deisseroth Laboratory's CLARITY Workshop at Stanford. I was successful in adapting the CLARITY clearing technique and applying immunolabeling protocols. At the same time, I gradually improved my sectioning and immunolabeling techniques for traditional stereology. As I worked on both techniques in concert, I would learn that computational and imaging resources required to image and analyze neuronal populations

in thick tissue were more costly than the technique was advantageous for this particular research question. However, by this time I successfully performed stereology of the dorsal raphe in mice. We found CLARITY to be useful in other applications in our laboratory and are continuing to improve and adapt the technique to other applications. These applications include phenotyping brain slices following electrophysiology experiments, and use in formalin-fixed human spinal cord tissue.

Our initial goal of using CLARITY for counting neuronal populations will be feasible in the near future. At the time of this writing, Emory's imaging core is adapting a new microscope technology: selective-plane illumination microscopy (SPIM). SPIM is superior to confocal microscopy in terms of both time- and cost- efficiency in imaging thick immunolabeled specimens; thus the goal of imaging and counting neuronal populations in clarified tissue will be feasible in the not-so-distant future. SPIM has been lauded by *Nature Methods* as the 2014 Method of the Year. In collaboration with Zeiss, the Deisseroth Lab has developed a SPIM chamber and optics to optimize this technique for CLARITY specimens (Tomer et al., 2014). We are indeed at a new frontier in immunohistochemical imaging.

As described in the protocol published in *Nature*, CLARITY employs the use of costly materials that are not readily available for exploratory research in most laboratories. As with cat skinning, there are many ways in which most protocols can be improvised and optimized for adaptation; CLARITY is no exception. This appendix describes my efforts to adopt the protocol in our laboratory, different approaches to tissue clearing, examples of immunolabeling, and the varied applications in which we applied CLARITY.

**Method**

Our protocol for CLARITY is built around the framework of the original method described in (*Chung, 2013*). Thus, this protocol follows many of the same steps, but I will indicate where and how we have deviated, optimized, or improvised from the original protocol through the course of this document.

**Solution preparation**

The hydrogel solution was prepared as described Chung, 2013. Please observe all safety precautions listed on the MSDS forms for each product. For 400 mL of hydrogel monomer, combine the hydrogel components (Table 1) at 4°. Note: Exclude bis-acrylamide for thin tissue slices (300 μm). Note that the hydrogel *outside* of the tissue will not polymerize. The hydrogel monomer was then divided into 40 mL aliquots, for perfusion into individual mice. Clearing solution was prepared by combining the ingredients listed in Table 2.

**Transcardial Perfusion with hydrogel solution**

Mice were anesthetized with isoflurane, and their thoracic cavities were opened with fine scissors. 60 mL of ice cold PBS was transcardially perfused into the left ventricle, using a peristaltic pump; 20 mL of ice cold hydrogel monomer were subsequently perfused. Brains were rapidly dissected and dropped into the remaining 20 ml of hydrogel monomer (on ice). Brains were stored at 4° for 2-3 days.

**Drop-fixing of 300 μm thick brain slices used in electrophysiology experiments**

To perform CLARITY on 300 μm slices used in electrophysiology experiments, slices can be drop-fixed into hydrogel. Because of the thinness of the tissue, it is best to use

hydrogel without bis-acrylamide so that the surrounding hydrogel does not polymerize with the tissue, making it easier to remove the tissue after polymerizaing. Drop-fixed tissue should be stored for 3-7days before polymerization.

**Hydrogel polymerization**

Because oxygen interferes with the polymerization process, it is necessary to remove oxygen from the solution and conical prior to polymerization. As described in the Chung protocol, this requires the use of an airtight desiccation changer with inlet ports. This was undesirable for two reasons: 1) using a desiccation chamber, one must break the vacuum in order to secure the conical vial, and 2) I did not have a desiccation chamber. Thus, I constructed a glovebox to serve as our de-gassing chamber (Figure A-1).

**Homemade Glove Box Construction**

**Materials**

1 Hefty 27.4 L storage container

2 4" Dryer Dock tube couplings

2 Large Rubbermaid gloves

2 large zip-ties

2 barbed quick release inlet ports

Tygon tubing (1/4" ID) for vacuum and gas flow

Silicone caulk

Epoxy resin

1 Pressure-release valve (Parker, N2008)

**Tools needed**

Caulk gun

Dremel saw, or other cutting tool

**Arm holes.** Using the Dremel saw, cut 2 9 cm (4") circular holes into the Hefty container. Hooked, male ends of the Dryer Dock quick connect coupling were placed into the holes and secured with silicone caulk. Gloves were then secured by inverting the cuffs around the edges of the female port and securing with zip ties. Note: The male and female Dryer Dock couplings should not be combined until after the caulk has dried; they will allow uncoupling to permit the transfer of materials into and out of the glove box.

**Inlet ports.** Inlet ports were placed on the sides of the container, as indicated in Figure A-1. Each port was constructed by: using the soldering iron to create a hole smaller than the barbed fitting of the female quick-connect port. While the plastic was still melted, the barbed end was firmly inserted into the new hole. After cooling, epoxy resin was placed at the juncture between the barbs and the plastic on the inside of the container, and at the juncture of the port and the exterior of the container.

**Chamber seal**

The container lid was placed on a flat surface with closure side facing upward. A test tube rack was placed on top of the container lid. A liberal amount of silicone caulk was applied around the perimeter, at the juncture of the lid and box, and then clamped shut for 24 hours.

**Connections**

Tygon tubing (0.25” ID; 0.5” OD) was used to connect the quick release valves to vacuum and nitrogen sources. A release valve was connected to the third port to relieve excess positive pressure within the box.

**De-gassing**

Sample tubes were placed in the glove box via an uncoupled glove port and placed in a tube rack within the glove box, with lids removed. N2 was turned on; positive pressure was evident when gloves blew outward. Vaccuum was applied to remove oxygen, at a rate that equilibrated glove position. After 1 minute, vacuum was removed to allow nitrogen flow to create positive pressure for 2 minutes. The interior nitrogen hose was directed toward the conical tubes containing the samples to ensure oxygen displacement prior to closure. The conical vials were then reclosed. **Note:** these times were not empirically optimized; they just work well.

**Polymerization and removal**

To polymerize, hydrogel samples were transferred from 4° storage to a 37° water bath for 3 hours. When the hydrogel solidified, brains were removed from conical vials using a metal spatula. Embedded tissue was separated from excess hydrogel with gloved fingers. Brain samples were then placed in 50 mL clearing solution and rocked on an orbital shaker for 24 hours at room temperature. Samples were then rocked for in 50 mL of

clearing solution at 37 for 24 hours to further dialyze out residual excess PFA, initiator, and monomer.

If one wishes to clear sliced sections of tissue from a whole hydrogel-embedded brain, it is easiest to section the brain prior to clearing, using a brain matrix to slice at 1 mm intervals. At this point, samples can be cleared by either **electrophoretic** or **passive** tissue clearing.

**Electrophoretic tissue clearing**

Electrophoretic tissue clearing (ETC) was the first proscribed method for removing lipids from CLARITY tissue (passive clearing would later emerge as an alternative). The process involves placing the brain sample in an electrophoretic tissue clearing chamber (Figure A-2), and applying constant current in circulating clearing solution. Under electrophoresis, all phospholipids migrate in the direction of the electric field while all amide-cross-linked molecules remain in complex with the hydrogel matrix.

**ETC Chamber construction**

Holes were soldered into the lid and bottom of the side of a 60 ml nalgene container. While plastic was melted, barbed tube fittings were screwed into the holes. Epoxy resin was used to seal the inside and outside of the fittings. Opposite of the inlet port, two holes were soldered into the side of the container for the electrode fittings, 20 mm apart. These were sealed in place with epoxy and dried overnight. 0.5 mm platinum wire was fashioned into electrodes as depicted in Figure A-2, and sealed into the electrode fittings with epoxy.

Note: The Chung protocol calls for 10 cm of 99.99% platinum from Sigma-Aldrich, which cost $700 at the time of this writing. We instead ordered 95% platinum from Rio Grande Jewelry for $70, with no observable problems with electrophoresis.

**Electrophoretic Tissue Clearing Setup**

**Circulator**. Our circulator setup (Figure A-3) consisted of a large waterbath, 5 L Nalgene carboy, peristaltic pump (Masterflex L/S, Cole-Parmer) peristaltic pump, the ETC chamber, and an aquarium filter (McMaster-Carr 7562A17). As indicated in Figure A-3, Tygon tubing (0.25" ID; 0.5" OD) connected the components so that clearing solution flowed in the following cycle:

carboy → pump → ETC chamber → aquarium filter → carboy(repeat)

Note: peristaltic pumps are designed for short interval use. Friction and pressure from extended use can eventually crack tubing. Thus, it is important to regularly check the integrity of the tubing in the pump by dissembling the tube and roller housing. Replace tubing (Tygon, OD: 0.25"; ID: 0.125") if there are any signs of brittleness or collapse (in my experience, this occurred every 2-3d). On a related note, it is prudent to have some means of retaining spilled liquid from breakages or leaks. It should also be noted that the clearing solution efficiently dissolves and penetrates Styrofoam. Finally, SDS is a very good detergent; combined with boric acid, it is very good floor stripper.

**Sample placement.** Samples were placed in a BD 40 um cell strainer. The bottom of a second strainer was used as a lid to prevent sample contact with electrodes. The sample holder with tissue was then placed between the electrodes.

**Electrophoresis.** The power supply was connected to the electrodes and set at a constant current of 450 mA, based off of the collective experience of the CLARITY Forum. Flow was set on the peristaltic pump to be just sufficient to prevent accumulation of bubbles; however, excessive flow rate may cause tumbling of the sample. The Deisseroth Laborotory recommends 1-2 L/min. In our setup with fresh platinum electrodes, setting #8 on the Masterflex pump fell within this range and worked well.

**Daily monitoring and maintenance**.

By this protocol, electrophoretic tissue clearing of a whole brain will take between one and two weeks. Daily examination is important for tracking clearing (Figure A-4). It is common for the ETC process to cause a yellowing ("cooking") of the hydrogel tissue. Yellowing can be mitigated by reducing the electrophoresis current or by increasing the circulator flow rate.

Tissue clearing occurs most efficiently at pH=8.5. Electophoretic oxidation generates acidic byproducts that will gradually lower the pH of the clearing solution. The easiest way to monitor to this is to dip pH strips into the carboy or ETC chamber when checking the clearing progress of the brain.

**Passive Clearing**

Tissue may also be cleared passively, without electrophoresis. This can be applied to whole brains, or sliced sections of brains. To perform passive clearing, place tissue in appropriately sized volume of clearing buffer. For whole brains, a 50 ml conical tube works well. Because hydrogels (and tissue-hydrogel hybrids) swell over time, a 15 ml conical will be too small. For individual 300 μm sections (e.g. from electrophysiology experiments) of tissue, a 2 ml Eppendorf tube is sufficient. We performed our passive clearing at 37° in a rocking incubator. One can accelerate this process by increasing the temperature up to 50°.

**Duration**. For a whole brain at 37°, this passive clearing took approximately 30 days, with semi-regular solution changes. (Figure A-5). For sections of tissue (300 – 1000 μm), this process takes approximately 3-7 days.

**Choosing between electrophoretic vs. passive clearing**

There are advantages and disadvantages to either clearing method (electrophoretic or passive).

- Electrophoretic clearing is significantly faster, but frequently (if not consistently) causes hydrogel discoloration.
- Passive clearing creates flawlessly transparent tissue, but requires substantially more time for clearing thick tissue. For thin tissue, this method is especially advantageous.

A means by which to expedite the clearing of thick tissue clearing is to run the tissue through electrophoresis for several days to accelerate the initial migration of lipids, and

then switch to passive clearing. When tissue has reached transparency (Figure A-5), it can be prepared for immunohistochemistry. Remove samples from clearing solution and wash in PBS-Tx for 1 day at room temperature, then in fresh PBS-Tx for 1 day at 55°.

**Immunohistochemistry Trials**

The prototypical CLARITY immunohistochemistry protocol is described in (Chung, 2013) and on the CLARITY Resource Center. Below I describe the methods we employed, which feature only minor deviation.

**Buffer**

For all immunohistochemistry trials, washes and incubations were performed in phosphate-buffered saline containing 1% Triton-X100 (PBS-Tx).

**Antibodies**

The following antibodies were used at 1:50.

- Rabbit α-TH (Millipore AB152)
- Rabbit α-TPH2 (Novus NB100-74555)
- Rat α-DAT, Alexafluor 488 (Millipore MAB369)
- Goat α-rabbit-488 (Invitrogen A11006)

**Immunohistochemistry in 300 µm and 1 mm thick tissue**

Hydrogel-embedded brains were sliced in a brain matrix at 1 mm intervals. Sections were passively cleared in a 50 ml conical in a stationary 50° water bath, with daily solution changes. Clearing was first evident at day 3, and complete transparency was

reached at day 8. Brain sections were incubated in 750 µl PBS-Tx with primary antibodies at concentrations of 1:50 at 37° for 2 days. Sections were than washed in PBS-Tx, shaking at 37° for one day, then incubated in secondary antibody at concentrations of 1:50 at 37° for 2 days. Sections were then washed in PBS-Tx for 1 day, with shaking.

**Preparation for imaging**

In order to eliminate light scattering during imaging, samples must be immersed in an imaging media with the same refractive indes. The Chung protocol employs the FocusClear clearing agent for this purpose. However, at $30 / ml, it is prohibitively expensive to use in protocol adaptation. An economical alternative is 80% glycerol in PBS, which has the same refractive index as FocusClear.

Sections were transferred to 80% glycerol and stored overnight. 80% glycerol matches the refractive index of the tissue (minimizing light scattering) and reverses osmotic swelling that occurs in clearing buffer and PBS.

**Imaging Chamber**

For 1 mm slices, an imaging chamber was constructed from 1 microscope slide, poster tack, and a coverslip [Figure A-6]. Poster tack was rolled to a cylinder with a uniform diameter and placed on the microscope slide to form a frame for the tissue section. The tissue was then placed within the poster tack frame. The side of a razor blade was used to flatten the poster tack to a height of approximately 1 mm. A cover slip was then placed on top, and gently pressed until it made contact with the tissue. 80% glycerol was added

to the chamber by carefully inserting a pipette tip at the juncture of the cover slip and poster tack. The hole was closed after filling. For 300 μm sections, tissue, glycerol and a coverslip were placed directly onto the slide.

**Widefield imaging**

Widefield fluorescent images of TPH2, TH, and DAT are shown in Figures A-7, A-8, and A-9. Low magnification imaging of CLARITY tissue can be accomplished with confocal or simple widefield fluorescent microscopy. With widefield imaging, one can observe fluorescent structures and cell bodies at low magnification (25-100X). A second advantage of using widefield light microscopy, is that light scattering through the depth of the tissue allows one to discern structural features of the tissue, as shown in Figure A-9.

Because optics for higher magnification have an inherently shallower depth of field, it is necessary to use confocal microscopy for high-magnification imaging. Because of the thickness of sample tissue, high magnification imaging requires a means by which to limit the depth of the z-plane to avoid out-of-focus noise. At this time, single- and two-photon confocal microscopy are the most readily available methods by which to accomplish this. The drawbacks to this approach are that, even with a high-end two-photon microscopy setup, it is a time-intensive technique that carries the considerable tradeoff of photobleaching and expenisve hourly core rates. If adapted to CLARITY, light sheet microscopy will allow more rapid and economical imaging with limited risk of photobleaching (Tomer et al., 2014).

**Subsequent rounds of immunohistochemical labeling**

Following imaging, brains can be re-cleared of antibodies for subsequent immunolabeling. Transfer the sample from the imaging media to 50 ml of PBS-Tx, and incubate at room temperature or 37° overnight with shaking. Then transfer the sample to clearing solution, and incubate at 60° overnight with shaking. Transfer to 50 ml PBS-Tx and incubate overnight with shaking. The sample is now ready for the next round of antibody incubations.

**Storage.** Following imaging, hydrogel tissue can be stored at room temperature in PBS-Tx. Cleared brains appear to store well in clearing buffer as well. I have stored brains over 12 months in clearing buffer at room temperature, without any apparent structural degradation; however, I have not compared immunoreactivity between storage conditions. It is not advised to store brains in glycerol or FocusClear for more than 48 hours (imaging time window), as CLARITY forum users have observed this to cause the irreversible formation of cloudy precipitates in the hydrogel-tissue matrix (observations on the Clarity Forum).

**Notes on temperature**

The incubation temperatures recommended in this protocol are based off trials run by the Deisseroth Laboratory and the CLARITY Forum community. These can be adjusted for further optimization. In general, increasing temperature increases the kinetics of clearing and washes, and the hydrogel tissue appears to tolerate temperatures up to 60°, at least for time intervals less than one week (I have not tested beyond one week). Anecdotally,

increasing the temperature from 37° to 50° has been reported to enhance antibody binding and penetration for several forum users. However, this does not necessarily mean that increasing the temperature will improve immunolabeling for all antibodies.

**Acknowledgements**

There are many people who were instrumental in my adaptation of CLARITY for use in the Miller Laboratory at Emory. In an effort to share the technique with the scientific community and employ crowd-sourcing to improve CLARITY, the Deisseroth Labororatory hosted an online forum (*clarityresourcecenter.org*), in which they and other researchers exchanged ideas for making the protocol more time- and cost-efficient. With Gary's support, I attended the CLARITY workshop at the Deisseroth Laboratory at Stanford, where I had the pleasure of training under hydrogel engineer Kristin Engberg and the opportunity to present my own CLARITY progress to Karl Deisseroth. My labmate and fellow pharmacologist Kristen Stout optimized CLARITY for tissue-phenotyping following FSCV experiments. Miller Lab Alum Thomas Guillot provided technical consult during the construction phases of this project. Lastly, Gary granted me the artistic license, trust, and purchasing power necessary to undertake this exciting endeavor.

| Hydrogel Component | Add | Final Concentration |
|---|---|---|
| Acrylamide (40%) | 40 mL | 4% |
| Bis-acrylamide (2%)* | 10 mL | 0.05% |
| VA-044 Initiator | 1 g | 0.25% |
| 10X PBS | 40 mL | 1x |
| 16% liquid PFA | 100 mL | 4% |
| $dH_2O$ | 210 mL | - |

**Table A-1. CLARITY hydrogel ingredients**. Note that bis-acrylamide should be omitted when fixing tissue slices.

| Clearing Solution Ingredient | Add | Final Concentration |
|---|---|---|
| Boric acid | 123.66 g | 200 mM |
| Sodium Dodecyl Sulfate | 400 g | 4% |
| $dH_2O$ | Fill to 10 L | - |
| NaOH | To pH=8.5 | - |

**Table A-2. CLARITY tissue clearing solution.**

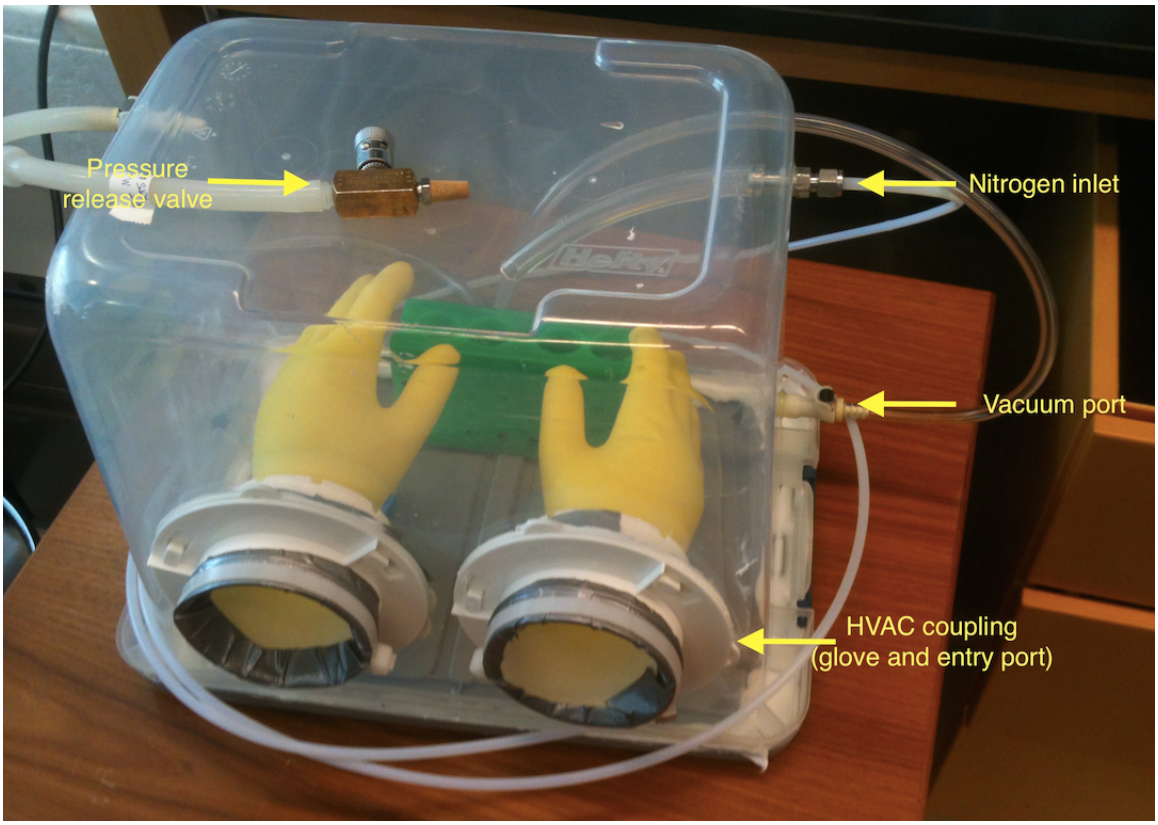
Pressure
release valve
Nitrogen inlet
Vacuum port
HVAC coupling
(glove and entry port)

**Figure A-1. Glove box constructed for de-gassing CLARITY hydrogel.**

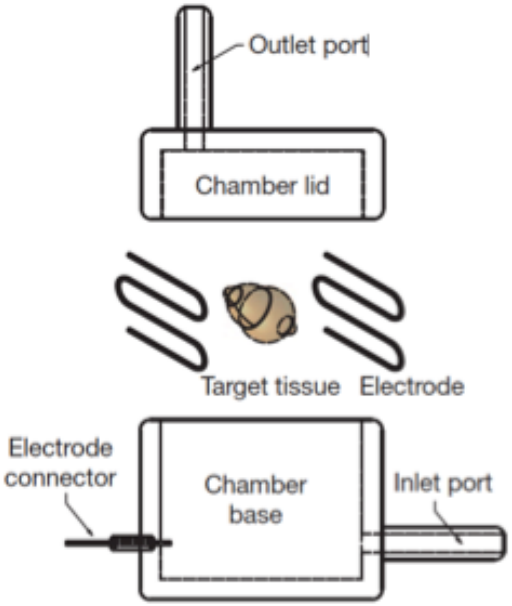
Outlet port
Chamber lid
Target tissue
Electrode
Electrode connector
Chamber base
Inlet port


National Brand

**Figure A-2: Electrophoretic tissue clearing chamber.** Left, CAD drawing of ETC chamber (as adapted from Chung, 2013). ETC chamber as constructed in the Miller Laboratory at Emory University.

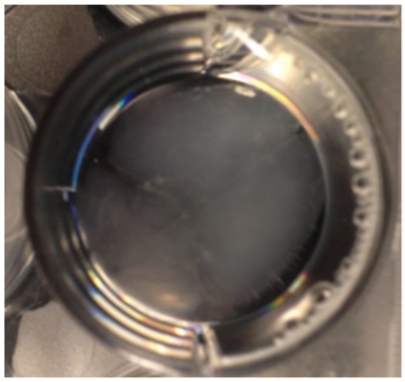

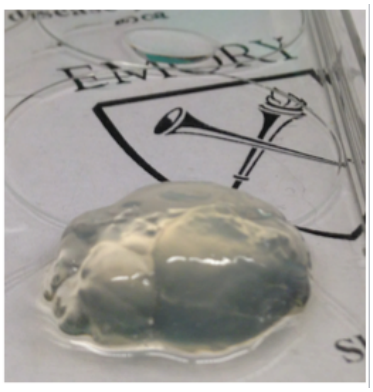
EMORY

**Figure A-3. Clarified hydrogel mouse brain.** Left: dorsal view, in clearing buffer. Center, Ventral view, clearing buffer. Right, view of hydrogel brain outside of buffer.

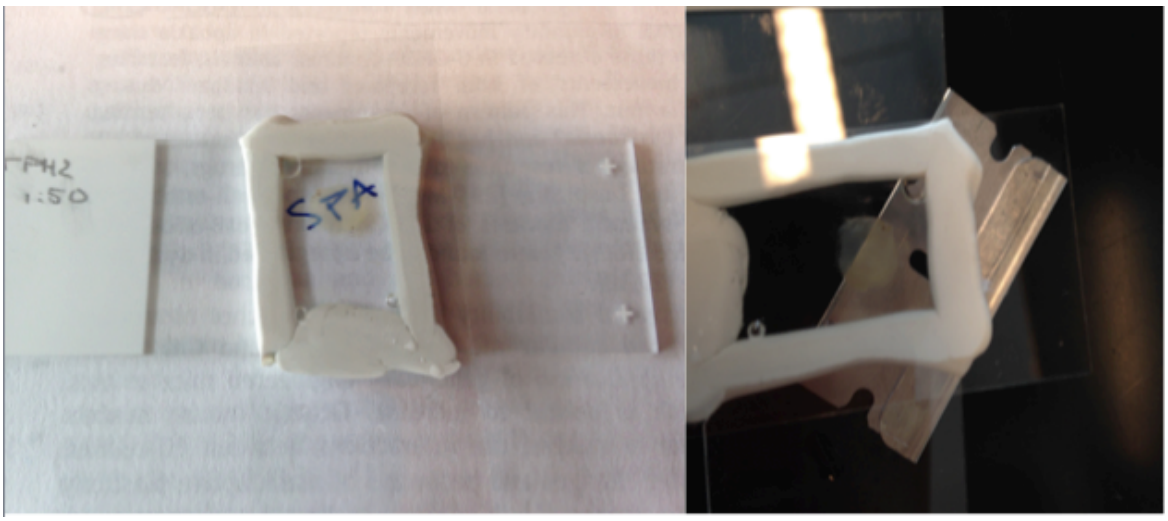
FPH2
1:50
SPA

**Figure A-4. Imaging chamber for 1 mm slice of clarified tissue.**

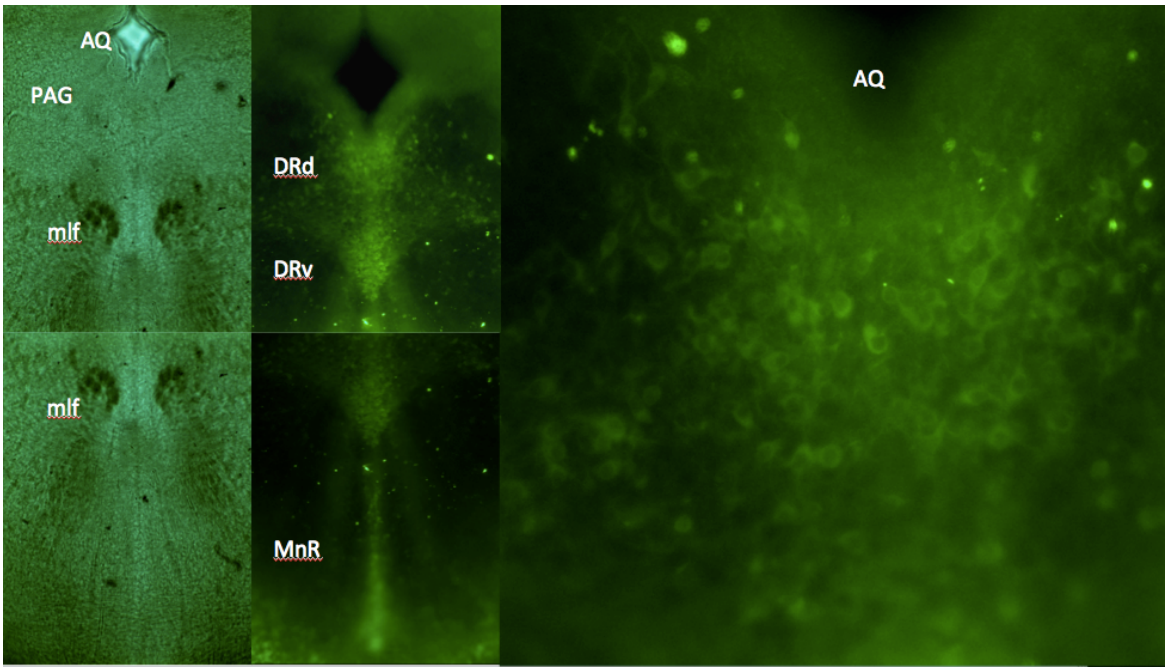
AQ
PAG
mlf
DRd
DRv
mlf
MnR
AQ

**Figure A-5. TPH2 immunolabeling of the dorsal and median raphe in 1 mm thick hydrogel tissue.** Left panels, transmitted light widefield micrographs of the midbrain (50X magnification). Center panels, immunofluorescence revealing TPH2 immnoreactivity in the dorsal and ventral DR (50X magnification). Right panel, 200X magnification of the dorsal DR. mlf=medial longitudinal fasciculus, PAG=periaqueductal gray, AQ=cerebral aqueduct.

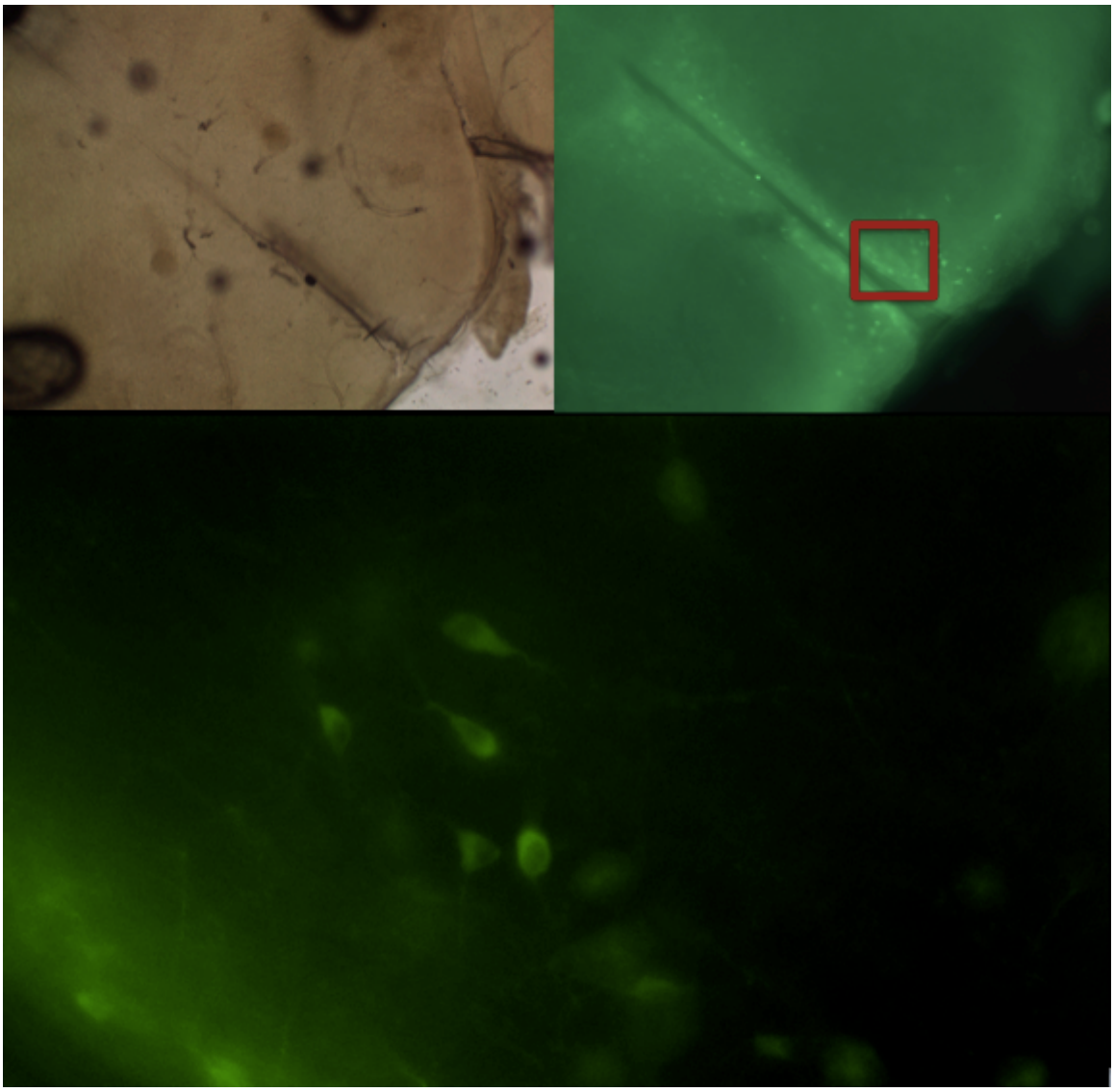

**Figure A-6. TH+ neurons in the arcuate hypothalamic nucleus.** TH immunolabeling of 1mm slice of clarified brain tissue. Images captured at 50X (top) and 200X (bottom) magnification.

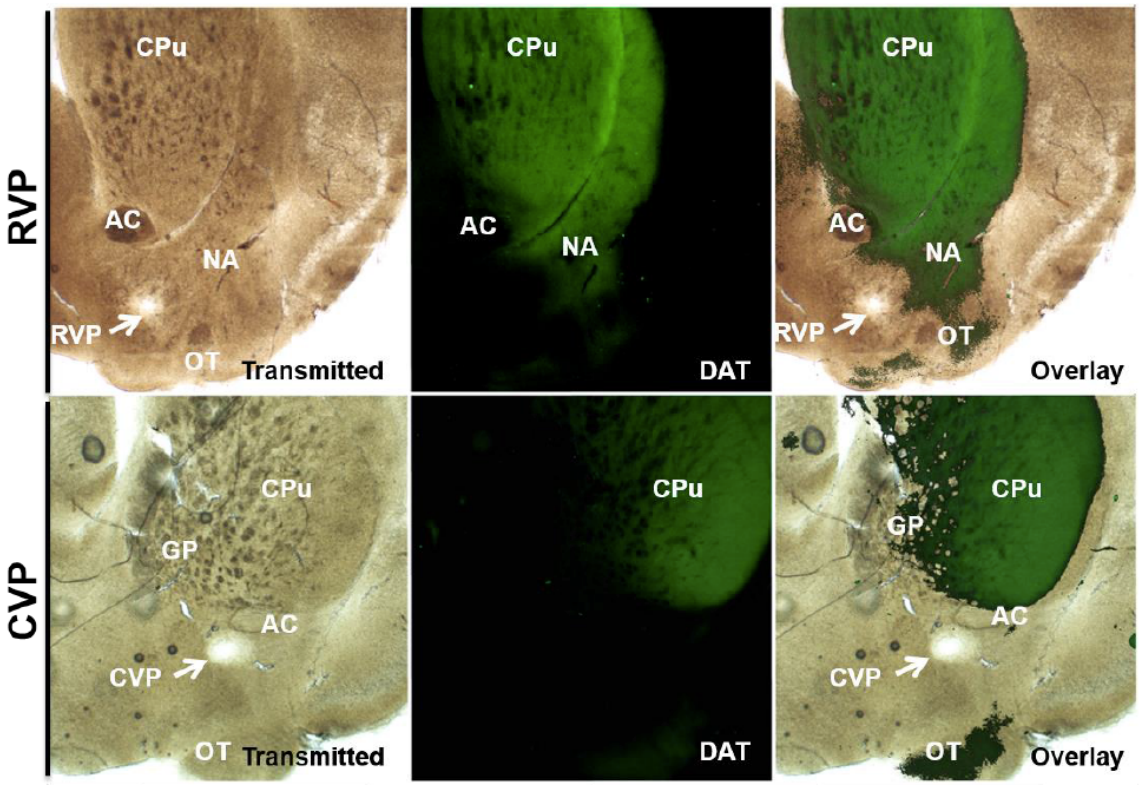
RVP
CVP
CPu
AC
NA
RVP
OT
Transmitted
CPu
AC
NA
DAT
CPu
AC
NA
RVP
OT
Overlay
CPu
GP
AC
CVP
OT
Transmitted
CPu
DAT
CPu
GP
AC
CVP
OT
Overlay

**Figre A-7. IHC of dopamine transporter in clarified FSCV tissue.** Following fast scan cyclic voltammetry experiments, slices were electrolytically lesioned at the recording site in the caudal and rostral ventral pallidum (white arrow). Images captured at 50X magnification. CPu=Caudate putamen, AC=anterior commisure; NA=nucleus accumbens; GP=Globus pallidus.

**References**

Chung K, Wallace J, Kim S-Y, Kalyanasundaram S, Andalman AS, Davidson TJ, Mirzabekov JJ, Zalocusky K a, Mattis J, Denisin AK, Pak S, Bernstein H, Ramakrishnan C, Grosenick L, Gradinaru V, and Deisseroth K (2013) Structural and molecular interrogation of intact biological systems. Nature 497:332–7.

Kim SY, Chung K, and Deisseroth K (2013) Light microscopy mapping of connections in the intact brain. Trends Cogn Sci 17:596–599.

Tomer R, Ye L, Hsueh B, and Deisseroth K (2014) Advanced CLARITY for rapid and high-resolution imaging of intact tissues. Nat Protoc 9:1682–97.

CLARITY Resource Center. Deisseroth Laboratory, Stanford University. Web. <http://clarityresourcecenter.org>.